Contract A5-149-32

Sampling and Analysis of Organic Aerosol

CARBONACEOUS SPECIES METHODS COMPARISON STUDY

Barbara J. Turpin and James J. Huntzicker

Oregon Graduate Center

Prepared for California Air Resources Board

Oregon Graduate Center
Department of Environmental Science and Engineering
19600 N.W. Von Neumann Drive
Beaverton, Oregon 97006

March 14, 1988

ABSTRACT

Field testing and implementation of a time-resolved in situ carbon analyzer, examination of organic aerosol sampling artifacts, and the investigation of organic aerosol speciation took place during the Carbonaceous Species Methods Comparison Study (CSMCS) in Glendora, California, during August, 1986. Uncertainties due to sample handling and loss of organic carbon during storage were eliminated in the in situ carbon analyzer by combining the sampling and analysis functions into a single instrument. Comparison of the diurnal profiles of organic carbon with those of elemental carbon, a tracer for primary combustion aerosol, and ozone, an indicator of photochemical activity, provided evidence for the secondary formation of organic aerosol in the atmosphere. From the study of organic sampling artifacts organic carbon concentrations on quartz fiber backup filters behind Teflon front filters (TQ) were found to be about 1.4 times greater than concentrations on quartz fiber backup filters behind quartz fiber front filters (QQ). Organic carbon concentrations on quartz fiber front filters showed a strong face velocity dependence which was virtually eliminated when apparent organic carbon concentrations from TQ backups are subtracted from QQ front filter concentrations. In an additional experiment samples were collected with different combinations of three unknowns: adsorbed organic vapor, volatilized organic particulate material, and organic aerosol. Both experiments indicated that adsorption is the dominant artifact in the collection of organic aerosol on quartz fiber filters. Saturation of adsorbed vapor was observed in a laboratory experiment but was not observed for the loadings obtained in the Carbonaceous Species Methods Comparison Study data. Samples were also analyzed by direct thermal desorption/gas chromatography/mass spectroscopy (TD/GC/MS). Carboxylic acid, polycyclic aromatic hydrocarbon, and alkane concentrations were examined for diurnal variations and differences in front and backup filters.

ACKNOWLEDGMENT

The assistance of Dr. Mary Ligocki, Dr. James F. Pankow, Mr. Ken Hart, Mr. Robert Cary, Dr. John Rau, and Mr. Lorne Isabelle is gratefully acknowledged.

This report was submitted in fulfillment of California Air Resources Board Contract A5-149-32, "Sampling and Analysis of Organic Aerosol", under the sponsorship of the California Air Resources Board. Work was completed as of March 14, 1988.

DISCLAIMER

The statements and conclusions is this report are those of the contractor and not necessarily those of the California Air Resources Board. The mention of commercial products, their source or their use in connection with material reported herein is not to be construed as either an actual or implied endorsement of such products.

TABLE OF CONTENTS

LIST OF FIGURES

LIST OF TABLES

SUMMARY AND CONCLUSIONS

The Carbonaceous Species Methods Comparison Study conducted in Glendora, California, during August, 1986 was designed (1) to quantify the overall uncertainty of carbonaceous aerosol monitoring which results both from differences in sampling and differences in analytical techniques, and (2) to investigate the problem of vapor sampling artifacts which inhibit the accurate assessment of organic aerosol concentrations. The Oregon Graduate Center (OGC) contributions to this study consisted of the field testing and implementation of a time-resolved in situ carbon analyzer, examination of organic aerosol sampling artifacts, and the investigation of organic aerosol composition.

Interlaboratory Comparison

The certainty with which carbonaceous aerosol is measured was evaluated through (1) blind interlaboratory analysis of 20 aliquots of "reference" aerosol samples and (2) nine days of simultaneous sampling using the range of sampling and analysis methods applied by eight different research groups. Twelve of the aliquots in the blind analysis were triplicates from each of four ambient samples and provided a blind measure of analytical precision for each laboratory. The blind measures of precision for the OGC results agreed well with our own reported uncertainties. The interlaboratory agreement for total carbon measurements was reasonably good with a coefficient of variation ranging from 4% for ambient samples to 14% for the unleaded automotive exhaust sample (Countess, 1988). However, agreement among the various laboratories regarding the appropriate division of total carbon into organic and elemental fractions was quite poor. The interlaboratory precision for elemental carbon ranged from 24% to 85% with an uncertainty of 34% for ambient samples. These results suggest that total aerosol carbon can at present be monitored with a fair amount of confidence, but further research will be required to assure correct division of total carbon into organic and elemental fractions in the absence of an absolute standard.

In Situ Carbon Analysis

The field sampling portion of the study was conducted in Glendora, California, during August, 1986. OGC sampling and analysis was performed by an *in situ* sampling and analysis system and by manual samplers, the filters from which were analyzed with the OGC laboratory thermal-optical analysis system (Huntzicker et al., 1982; Johnson et al., 1981).

The *in situ* carbon analyzer was developed to investigate the time-dependent aerosol chemistry of organic carbon. Uncertainties due to sample handling and loss of organic carbon during storage were eliminated by combining the sampling and analysis functions into a single instrument which could operate on a time cycle as short as 90 minutes. Carbon analysis was accomplished with a thermal-optical method in which organic carbon is thermally desorbed in an oxygen-free atmosphere, and elemental carbon is oxidized in a 2% oxygen in 98% helium atmosphere. Correction is made for pyrolytic conversion of organic to elemental carbon during the carbon analysis by monitoring the optical transmittance of helium-neon laser light through the filter. A second independent filter sampler collects particle-free ambient air and thus provides an estimate of the adsorption of organic vapors on the particulate sampling filter.

Total carbon uncertainties are 3.1% with detection limits of 0.2 μg carbon. The *in situ* carbon analyzer was operated on a cycle ranging from 90 to 180 minutes. Concentrations of total, organic, and elemental carbon showed strong diurnal variations with peaks occurring during the daylight hours. Comparison of the diurnal profile of organic carbon with those of elemental carbon, a tracer for primary combustion aerosol, and ozone, an indicator of photochemical activity, provided evidence for the secondary formation of organic aerosol in the atmosphere.

Vapor Artifact Studies

Filter sampling for organic aerosol is complicated by two artifact errors. Adsorption of organic vapors on the sampling filter comprises a positive artifact, and volatilization, which removes material from the filter, is a negative artifact (Cadle et al., 1983; McDow, 1986). These sampling artifacts are not well understood and therefore inhibit attempts

to accurately assess aerosol concentrations. In experiments performed by our laboratory in Portland, Oregon, organic carbon was found on backup filters behind Teflon and quartz fiber front filters, which are essentially 100% efficient in removing particles. This could only occur if organic vapor adsorbs on quartz fiber filters. (Quartz —or less preferably glass—fiber filters are necessary substrates for thermal-optical carbon analysis.)

Organic aerosol was collected as a function of filter face velocity (i.e., the velocity of air flow through the filter) in the Carbonaceous Species Methods Comparison Study to investigate the importance of organic sampling artifacts under Los Angeles conditions. Apparent organic carbon concentrations on quartz fiber backup filters behind Teflon front filters (TQ) are about 1.4 times greater than concentrations on quartz fiber backup filters behind quartz fiber front filters (QQ). Lower concentrations on QQ backups can be explained by the difference in adsorption capacities for Teflon and quartz fiber filters. The Teflon filter adsorbs little because of its low surface area. The quartz fiber filter, however, has a large surface area and adsorbs a significant amount of organic vapors, reducing the concentration of adsorbable vapors which reaches the QQ backup filter. This result suggests that the TQ backup filter provides a better estimate of the vapor adsorption artifact present on the QQ front filter.

Organic carbon concentrations on quartz fiber backup filters behind both quartz fiber and Teflon front filters show a strong face velocity dependence as do apparent organic carbon concentrations on quartz front filters. When apparent organic carbon concentrations from TQ backups are subtracted from QQ front filter concentrations, the face velocity dependence is virtually eliminated. A face velocity dependence of organic carbon concentrations is evidence of the presence of a sampling artifact. If the adsorbed vapor on the TQ backup filter was originally volatilized particulate material from the front filter, the face velocity dependence would be removed by adding the TQ backup to the QQ front filter. However, if the adsorbed vapor on the TQ backup filter was originally organic vapor, the artifact correction would be made by subtraction. Thus, these results suggest that adsorption is the dominant

sampling artifact in the collection of organic aerosol on quartz fiber filters. Similar results were obtained in the Portland experiments (McDow, 1986).

An additional experiment was performed in which three sampling ports sampled with different combinations of three unknowns: adsorbed organic vapor, volatilized organic particulate material, and organic aerosol. This was accomplished by removing all, part, and none of the particulate material in the ambient air sampled by ports 1, 2, and 3. Thus, adsorbed organic vapor remained the same, but the organic aerosol concentration observed by each port was different as was the potential for volatilization of that particulate material. This experiment indicated that adsorption of organic vapors rather than volatilization of collected particulate matter was the dominant artifact in the sampling of organic aerosol.

A laboratory experiment was conducted to further the understanding of the process of vapor adsorption. A relatively constant concentration of organic vapor in air with a low aerosol content was sampled by the in situ carbon analyzer with varying sampling times. Aerosol loading doubles with doubling of collection time while the marginal increase in vapor loading diminishes with increased sampling duration. Vapor loading reaches a steady state after about 200 minutes of collection. This result suggests that longer sampling durations will reduce the percentage of collected organic material which is adsorbed vapor and that with long enough collection time vapor adsorption will approach filter site saturation. Saturation phenomena were not observed in the Carbonaceous Species Methods Comparison Study data.

Gas Chromatography/Mass Spectroscopy

Front and backup filter samples collected in a two-port sampler were analyzed by direct thermal desorption/gas chromatography/mass spectroscopy (TD/GC/MS). Large concentrations of carboxylic acids were found on both front and backup filters. The lower vapor pressure acids showed a substantial difference between day and night concentrations with elevated concentrations occurring during the day. Polycyclic aromatic hydrocarbons were found almost entirely on the front filter, and most of

the material appears to be in particulate form. The dominant alkanes identified were C_{24} through C_{29} which also appear to be predominantly in the particulate phase. The ratio of particulate material to adsorbed vapor increased with increasing carbon number (decreasing vapor pressure) for the alkanes C_{22} through C_{27}. Further examination of these data will provide additional insight into both sampling artifacts and the distribution of organic material between the gaseous and particulate phases.

Conclusions

1. Disagreement among the various investigators persists as to the proper method for separating carbonaceous aerosol into its organic and elemental fractions. However, there is an acceptable level of agreement for the analysis of total carbon.
2. The apparent concentration of organic aerosol is dependent on the velocity of air flow through the sampling filter. This is a consequence of the adsorption of organic vapors on the filter. This velocity dependence can be removed by an appropriate correction.
3. Adsorption of organic vapors rather than volatilization of collected particulate matter is the dominant artifact in the sampling of organic aerosol. The role of volatilization appeared to be small, but further study is require to gain a better understanding of this process.
4. Correction for the adsorption of organic vapors on the filter medium is essential if an accurate assessment of the role of organic aerosol is to be obtained. The best method for correction appears to be the measurement of organic carbon on a quartz fiber backup filter behind a Teflon front filter, which is sampling the aerosol in parallel with a regular quartz fiber particulate filter. This provides an estimate of the amount of adsorbed organic vapor on a quartz fiber particulate filter. (Quartz fiber is the preferred medium for carbon analysis.)
5. The Oregon Graduate Center *in situ*, thermal-optical carbon analyzer provides adequate sensitivity and temporal resolution for the study of carbonaceous aerosol in California and the Los Angeles Basin, in particular.

6. Organic aerosol showed strong diurnal patterns on all days, and comparison of the diurnal patterns of organic aerosol, elemental carbon, and ozone, which is a measure of the photochemical reactivity of the atmosphere, provided strong evidence for the secondary formation of organic aerosol.

7. The analysis of specific organic compounds on both aerosol and backup filters showed that all but the most non-volatile compounds were subject to sampling artifacts.

RECOMMENDATIONS

1. Further research is necessary on the analytical speciation between organic and elemental carbon.
2. To obtain an accurate measure of the organic carbon component of the aerosol, it is necessary to correct for the adsorption of organic vapors on the filter sampling medium.
3. The use of a quartz fiber backup filter behind a quartz fiber particulate filter underestimates the amount of adsorbed vapor on the quartz particulate filter. To obtain a more accurate correction, the amount of adsorbed vapor on the quartz fiber particulate filter should be obtained from a measurement of the organic carbon concentration on a quartz fiber backup filter behind a Teflon particulate filter.
4. In situations where a time resolution as short as two hours is necessary in the measurement of organic and elemental carbon aerosol, the Oregon Graduate Center thermal-optical, in situ carbon analyzer is appropriate.

CHAPTER 1: INTRODUCTION

The Oregon Graduate Center (OGC) contributions to the Carbonaceous Species Methods Comparison Study (CSMCS), conducted in Glendora, California, during August, 1986 consisted of the field testing and implementation of a time-resolved in situ carbon analyzer, examination of organic aerosol sampling artifacts, and the investigation of organic aerosol speciation. Diurnal profiles of organic carbon (OC) and elemental carbon (EC) obtained from the in situ carbon analyzer were used to identify periods when gas-to-particle formation of organic aerosol was occurring. In addition, several sampling and analytical methods were compared in the "round-robin" interlaboratory study in which OGC was a participant.

This report discusses each of the experiments. Because of the central importance of the OGC thermal-optical carbon analyzer to this work, a detailed discussion of the analytical sequence and quality assurance procedures is included.

CHAPTER 2: SAMPLE HANDLING AND THERMAL-OPTICAL CARBON ANALYSIS

Prior to sampling all quartz fiber filters were heat-cleaned at 500 C in air for at least two hours and stored in petri dishes lined with aluminum foil. The aluminum foil was cleaned at 380 C. At the end of the sampling period the filters were returned to the petri dishes and immediately stored at -10 C until analysis. A blank filter was assigned to each sampling day and was treated in exactly the same manner with respect to filter preparation, handling, and analysis as the analytical filters collected on that day. Flow readings and pressure drops were recorded at the beginning and end of each sampling period. A dry test meter was used to calibrate all filter sampler flow rotameters, and a counter in line with each pump monitored collection time.

The Thermal-Optical Carbon Analysis Method

The OGC thermal-optical laboratory carbon analyzer is described in detail by Huntzicker et al. (1982) and Johnson et al. (1981). Briefly, it is a thermal volatilization-combustion technique in which the reflectance of 633 nm He-Ne laser light from the filter sample is used to distinguish between OC and EC during the analysis. Because the analysis procedure has changed somewhat since the original publications, a description of the current analytical sequence follows.

Organic carbon is volatilized by heating the sample in two steps to 470 C and 610 C in pure helium. The volatilized organic carbon is oxidized to CO_2, reduced to CH_4, and measured by a flame ionization detector (FID). The oven temperature is then reduced to 420 C and oxygen is added to achieve a composition of approximately 2% O_2 in 98% He. Elemental carbon is then combusted by stepping the temperature to 750 C (through 510, 550, 590, and 670 C). When elemental carbon combustion is complete, the oven temperature is reduced to 280 C. Two calibrations follow, both accomplished by automatic injection of a known amount of methane. The first is performed in a O_2-He atmosphere and the second in pure He. FID response is somewhat sensitive to carrier gas composition, and dual calibrations improve the accuracy of the analysis.

During the organic phase of the analysis some organic carbon is pyrolytically converted to elemental carbon causing the filter to darken. Unless a correction is made for this effect, the elemental carbon fraction can be seriously over-estimated. This correction is accomplished by measuring the optical reflectance of the filter continuously throughout the analysis. After the addition of oxygen, the reflectance begins to increase because of the oxidation of elemental carbon. The point at which the filter reflectance reaches its pre-pyrolysis value is taken to be the split point between OC and EC. All carbon measured before this point (as represented by the FID signal) is considered organic and after, elemental. A complicating factor in making this correction is that the FID signal lags the reflectance signal by the transit time of the carrier gas from the volatilization-oxidation oven to the FID. To achieve an accurate pyrolysis correction, it was necessary to align the FID and reflectance signals by measuring the transit time. This was accomplished by measuring the time between sample insertion and FID response for clean filter punches doped with sucrose.

The time sequence for valve switching and temperature control is given in Table 1, and a typical output is shown in Figure 1. In this figure the FID and reflectance signals have been aligned. The procedure of Table 1 describes the regular analysis program which distinguishes between organic and elemental fractions. Backup filters, upon verification that they contain no elemental carbon, can be run on a short analysis program for total carbon alone. In this program the oven is held at 800 C in a 2% O_2-98% He atmosphere. All material is removed in a single step when the filter punches are inserted. An internal CH_4 calibration is run as above.

Analysis Procedure

For each day of operation of the laboratory carbon analyzer at least one instrument blank and punches from one field blank were run. The instrument blank measurement was used to ensure that the system was working properly and was not contaminated. Blank corrections used an average of all field blanks run during the analysis of that sample set. Blank subtraction was done by dividing the analysis into eight sections

Table 1. LABORATORY CARBON ANALYSIS TIME SEQUENCE

ELAPSED TIME (SEC.)	OVEN TEMP. (C)	VALVE CHANGES
0	280	system has been purged with He; FID on line; atmosphere is pure He
200	470	organic carbon removal begins
400	610	organic carbon removal continues
680	420	organic carbon removal complete; oven temp. reduced
1000	420	oxygen introduced
1140	510	elemental carbon oxidation begins
1240	550	elemental carbon oxidation continues
1340	590	elemental carbon oxidation continues
1440	670	elemental carbon oxidation continues
1540	750	elemental carbon oxidation continues
1840	280	elemental carbon oxidation complete; oven temperature reduced
1880	280	CH_4 calibration loop switched on line; calibration in O_2-He
1920	280	CH_4 calibration loop switched off line;
2120	280	carrier gas switched to pure He
2140	280	CH_4 calibration loop switched on line; calibration in He
2180	280	CH_4 calibration loop switched off line
2410	280	FID switched off line
2414	280	analysis complete

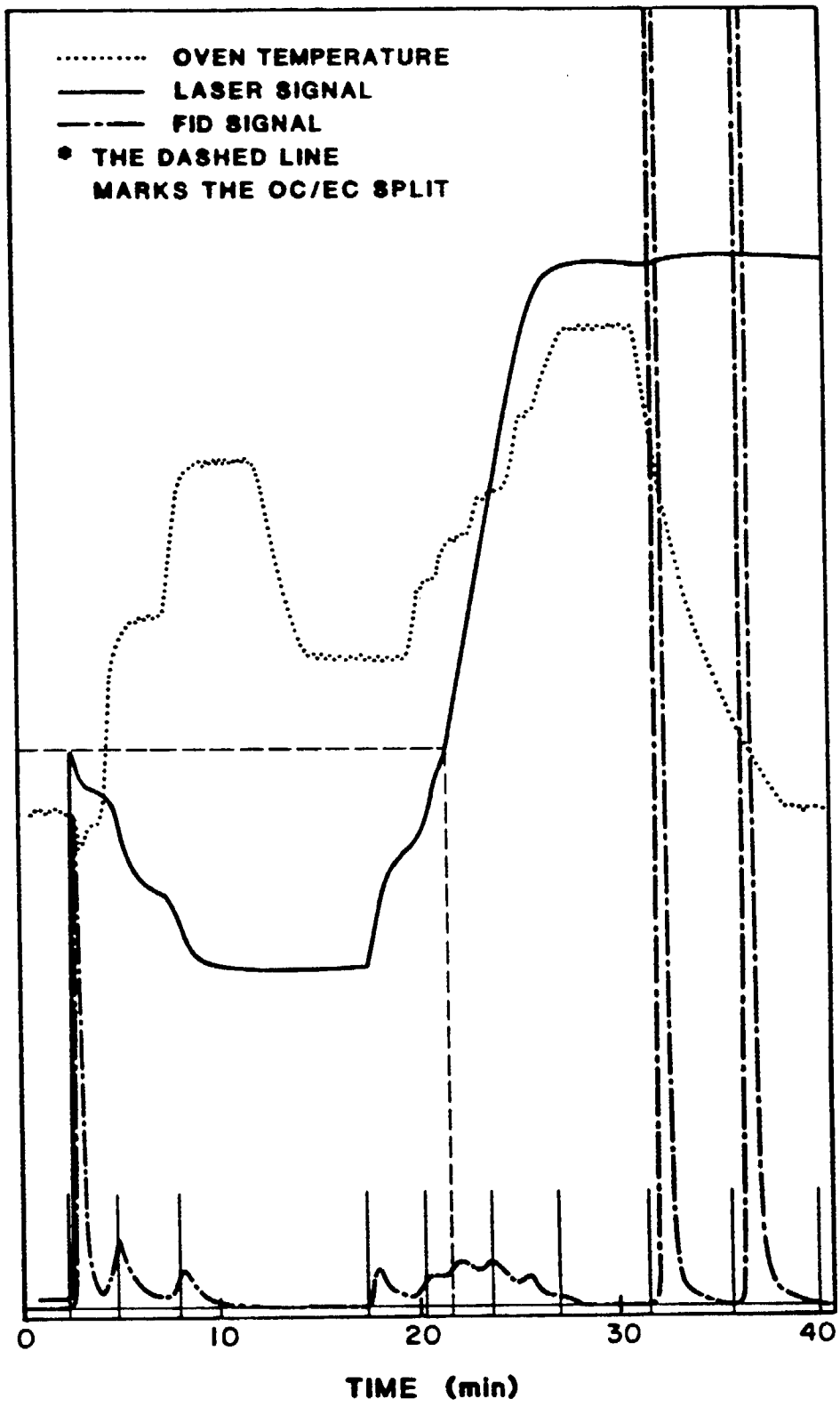

Figure 1. Typical output for laboratory thermal-optical carbon analyzer. Oven temperature, optical reflectance, and flame ionization detector. The dashed line at about 21.3 minutes is the split point between organic and elemental carbon.

plus the division established by the organic-elemental carbon split and subtracting the blank value from the sample value on a section by section basis.

External standards were prepared from a sucrose solution containing 5 g of carbon/liter deionized water. Filter punches were heat-cleaned in the carbon analyzer oven, then cooled in place, and doped with enough solution to give 20 to 35 μg of carbon. Replicate analysis of at least 10% of all samples in each data set was performed, providing a data set for statistical evaluation. In addition, selected filters were reanalyzed periodically over the course of the seven months required to analyze all samples. These were used to investigate aerosol aging losses resulting from volatilization during storage. Aging measurements were made on 8 filters on April 15 and 17 filters on May 19, 1987. These filters were all initially run in November, 1986. A mean loss of 1.1 $\pm$ 0.5 $\mu gC/cm^2$ and 1.3 $\pm$ 0.3 $\mu gC/cm^2$ (uncertainty is the standard error of the mean) were observed for April and May results respectively despite cold storage at -10 C in Gelman petri dishes. Loss was independent of loading. The average OC loading was 14.6 $\mu gC/cm^2$ and experienced a 9% loss as a result of 6 months of cold storage.

Field blanks

Blank subtraction could be accomplished in one of two ways. If the instrument blank dominates, the mass of carbon measured in the field blank analysis would be independent of the number of punches used (or the mass of carbon on the blank per cm^2 would be inversely proportional to the number of punches used), and the blank should be subtracted on a mass basis. Alternatively, if the filter blank dominates, the blank value expressed in $\mu gC/cm^2$ will be independent of the number of punches used. Thirty-two blank runs from the long and short analysis programs using 1 to 3 punches were examined by paired t-test to determine whether the 1, 2, and 3 punch samples could be from the same population when expressed as μgC and as $\mu gC/cm^2$. The results were consistent with the dominance of the filter blank, indicating that subtraction on a mass per surface area basis is optimal. When summed over all sections of the long analysis program, the mean blank value was 0.5 $\mu gC/cm^2$ with a standard error of

the mean of 0.2 $\mu gC/cm^2$.

External standards

During analysis of the first set of samples (round robin) a 9% difference was observed between external and internal standards. This prompted us to check the accuracy of the sucrose solution approach with a second external standard. Ten CH_4 samples containing between 2 and 25 μg of carbon were injected into the laboratory carbon analyzer. The ratio of methane to sucrose responses was 1.01 ± 0.05. Thus, there was no difference in the results at the 95% confidence level, validating our external calibration method, and an appropriate correction was made in the internal calibration. The linearity of instrument response was verified by the good fit (R^2 = 99.3%) between mass of carbon injected and instrument response over the range studied in the CH_4 experiment.

Uncertainties

The accuracy of total carbon measurements was ±2%, as determined by the uncertainty in instrument response to external sucrose standards. Measures of precision were based on replicate filter analyses and were determined by one-way analysis of variance. They represent combined instrument uncertainties and variations in aerosol deposition over the filter area. They are presented in Table 2.

Table 2. LABORATORY CARBON ANALYZER UNCERTAINTIES

	ROUND ROBIN SAMPLES	TWO PORT & FACE VEL. SAMPLES
ORGANIC CARBON (OC)	8.4%	4.3%
ELEMENTAL CARBON (EC)	6.9%	7.5%
TOTAL CARBON (TC)	7.0%	4.6%
TOTAL CARBON FROM BACKUP FILTERS		6.7%
NUMBER OF REPLICATES	16	14
NUMBER OF REPLICATES FOR BACKUP FILTERS		38

CHAPTER 3: ROUND ROBIN STUDY

The Carbonaceous Species Methods Comparison Study evaluated the overall uncertainty of carbonaceous aerosol monitoring through (1) nine days of simultaneous sampling using the range of sampling and analysis methods applied by eight different research groups and (2) interlaboratory analysis of aliquots of "reference" aerosol samples. The second study is described in detail by Countess (1988), and the OGC participation will be discussed here. Twenty aliquots of samples collected on 8" x 10" Pallflex QAST quartz-fiber Hi-Vol filters were distributed to 13 laboratories by Environmental Monitoring and Services, Inc. (EMSI) for blind analysis. The sample sets included ambient CSMCS samples, automotive exhaust samples, ambient Medford, Oregon, samples dominated by wood smoke emissions, an ambient sample treated to significantly reduce the organic fraction, an organic aerosol sample generated in a smog chamber, and a sample blank. Three aliquots from each of four ambient samples were provided to all participants, to provide a blind measure of precision.

The results from the OGC analysis of the round robin samples are presented in Appendix I. Uncertainties are discussed in the previous section. These uncertainties apply to all samples except Y11-06 and the powdered samples. For Y11-06 the extreme blackness of the sample prevented an accurate determination of the correction for the pyrolytic conversion of organic to elemental carbon which occurs during the organic analysis. (The correction procedure relies on continuous measurement of the filter reflectance during the analysis. If the filter is overly black, the method becomes insensitive.) Thus for Y11-06 the uncertainties for OC and EC were determined from replicate measurements of that sample only.

Three powder samples were also distributed by EMSI. We deposited material from these samples on pre-weighed, pre-baked quartz fiber filters. The deposition system consisted of a 47 mm in-line filter holder which had a 5 ft section of 0.25 in copper tubing attached as an inlet line. A small amount of powder which had been placed in the bottom

of a beaker was sucked onto the filter by connecting a pump behind the filter. This method resulted in a somewhat non-uniform deposit on the filter with the heaviest deposit at the edge and the lightest deposit at the center. The filters were re-weighed after the deposition procedure. Punches taken from these filters were analyzed for OC, EC, and TC by the usual thermal-optical method. All three samples showed significant residual color after analysis. Y21 was reddish-brown suggesting soil dust, and Y22 and Y23 were grayish-black. The latter color could have resulted from incomplete removal of EC during the analysis, but a re-analysis of a previously run set of punches from sample Y23 yielded no further carbon. If residual color was due to EC, it was EC that was not removable at 750 C in a 2% oxygen-98% helium atmosphere. Because of these problems (i.e., non-uniform deposition and residual color) the uncertainties cited above must be regarded as minimum uncertainties for the powder samples. We very rarely analyze powder samples and do not have a reservoir of historical confidence in the procedure used. Thus, we have chosen not to assign uncertainties to these results. Our level of confidence in the powder results is not high.

Because of the blind nature of this comparison, interpretation of these results has been left to EMSI. The measures of precision for the OGC results, based on blind analysis of four ambient samples submitted in triplicate are: organic carbon, 7.4%; elemental carbon, 6.2%; and total carbon, 7.4% (Countess, 1988). These are consistent with our estimates determined by replicate analysis of sample aliquots. The lack of an absolute standard for organic and elemental carbon makes it impossible to evaluate the accuracy of the participants' performance. However, the spread in the values reported indicates the uncertainty with which carbonaceous aerosol is measured. The coefficient of variation for total carbon ranged from 4.2% for the ambient CSMCS sample to 14.1% for the unleaded automotive exhaust sample (Countess, 1988). Countess expressed the uncertainty in the split between organic and elemental carbon as the variation in the EC to TC ratio. Excluding the organic aerosol sample, the coefficient of variation of this ratio ranged from 10% for the diesel sample to 83% for the heavily loaded wood smoke sample. The precision for elemental carbon, calculated from his numbers, ranges from 24% to 85%

for the diesel and wood smoke samples respectively with an uncertainty of 34% for the ambient samples.

CHAPTER 4: THE IN SITU CARBON ANALYZER

Introduction

Carbonaceous aerosol is recognized as a major component of both urban and rural aerosols (Shah et al., 1986; Gray et al., 1984). It can originate from both primary and secondary processes. The former are associated with direct emission of carbon-containing particles into the atmosphere and include incomplete combustion, industrial processes, and biological emissions (e.g. pollens and plant waxes). Elemental carbon (i.e., soot) is predominantly a product of combustion processes and is therefore a good tracer for combustion-generated organic aerosol. Secondary carbonaceous aerosol is formed in the atmosphere by condensation of products of photochemical reactions. Secondary formation of sulfur and nitrogen containing aerosols in the atmosphere and formation of organic aerosols by sunlight irradiation of specific gaseous organic compounds in smog chambers are well documented (Hidy et al., 1975; McMurry and Grosjean, 1985; Heisler and Friedlander, 1977). However, there is considerable uncertainty concerning the importance of secondary processes in the formation of organic aerosols in the ambient atmosphere.

Progress in the understanding of this problem has been hampered by lack of adequate time resolution in conventional filter sampling methods for organic aerosol. These methods involve the collection of aerosol by drawing ambient air through filters which are
then transported to the laboratory for analysis at a later time. Sample handling, aerosol aging uncertainties (e.g., volatilization loss during storage), and limitations in the analytical method contribute to high detection limits. To overcome these problems, long sampling periods are usually required, and consequently, most of the concentration data for carbonaceous aerosol is in the form of 12 or 24 hour averages. Because atmospheric chemistry is dynamic on the time scale of minutes to hours, a great deal of information is lost in these long averaging periods. In particular, diurnal cycles which could be associated with secondary formation processes, have been difficult to resolve.

Because of the need to obtain improved time resolution, low

detection limits, and minimal influence from sampling artifacts, an *in situ* carbon analyzer was developed. This instrument combines the sampling function of a conventional filter sampler with the analytical function of a thermal-optical carbon analyzer (Huntzicker et al., 1982; Johnson et al., 1981).

Instrument Description

The sampling section of the instrument shown in Figure 2 consists of two independent filter samplers which provide for the collection of aerosol and the determination of the vapor adsorption artifact (see Chapter 5). In each sampler two back-to-back, circular disks (1.5 cm diameter) of a quartz fiber filter (Pallflex QAOT) are mounted inside the carbon analyzer as shown in Figure 3. (Two filter disks are necessary to prevent rupture during sampling.) In the aerosol-side sampler ambient air is drawn through a 2.5 μm cut-point Marple (1974) impactor, and the fine fraction of the aerosol is collected on the quartz fiber filters along with whatever organic vapor adsorbs on the filters. Between the impactor and the filters is a ball valve (BV) which is used to isolate the system from the atmosphere during the analytical part of the cycle. A ball valve is used for this application to permit the unimpeded flow of aerosol into the instrument during the sampling part of the cycle. On the vapor side a Teflon filter (Gelman Teflon ringed, 47 mm diameter, 2 μm pore size filter) is mounted upstream of the quartz fiber filters to remove particles from the sample air. As a result, any organic carbon on the vapor-side sampling filters is adsorbed organic vapor. A Teflon solenoid valve (SV2) isolates the vapor side from the atmosphere during analysis. Both sampling lines draw from a common manifold, and the flow in both sides is maintained at 8.5 l/min. This sampling rate corresponds to a filter face velocity of 80 cm/s.

Ambient air is drawn through the filters with a pump for a preset period of time. At the end of the sampling period the aerosol ball valve (BV), the vapor-side solenoid valve (SV2), and the pump solenoid valves (SV3, SV4) close, and the instrument is converted to a carbon analyzer similar in design to the Oregon Graduate Center laboratory carbon analyzer (Huntzicker et al., 1982; Johnson et al., 1981). After purging

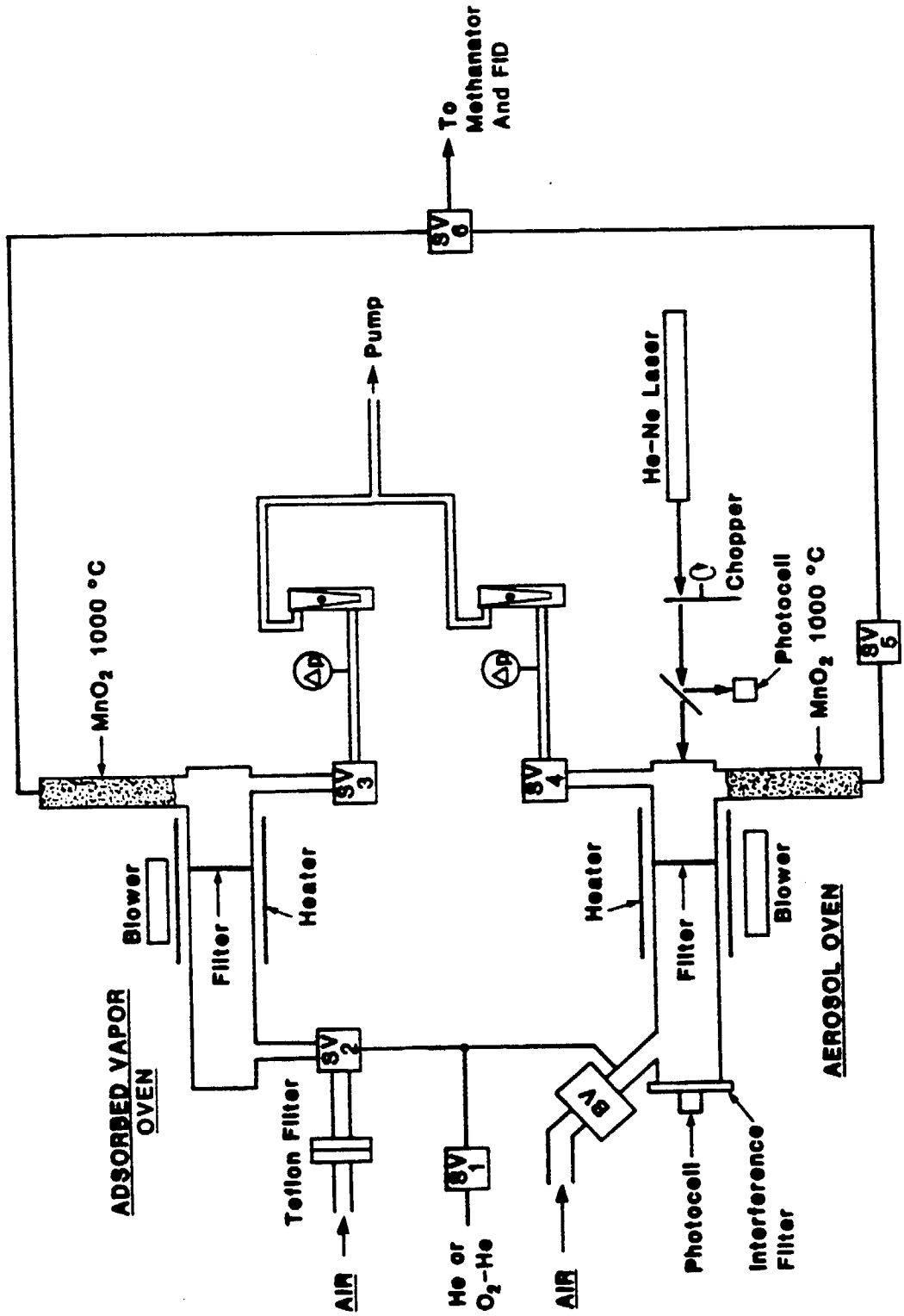

Figure 2. Schematic of in situ carbon analyzer. BV: ball valve; SV1-SV6 solenoid valves.

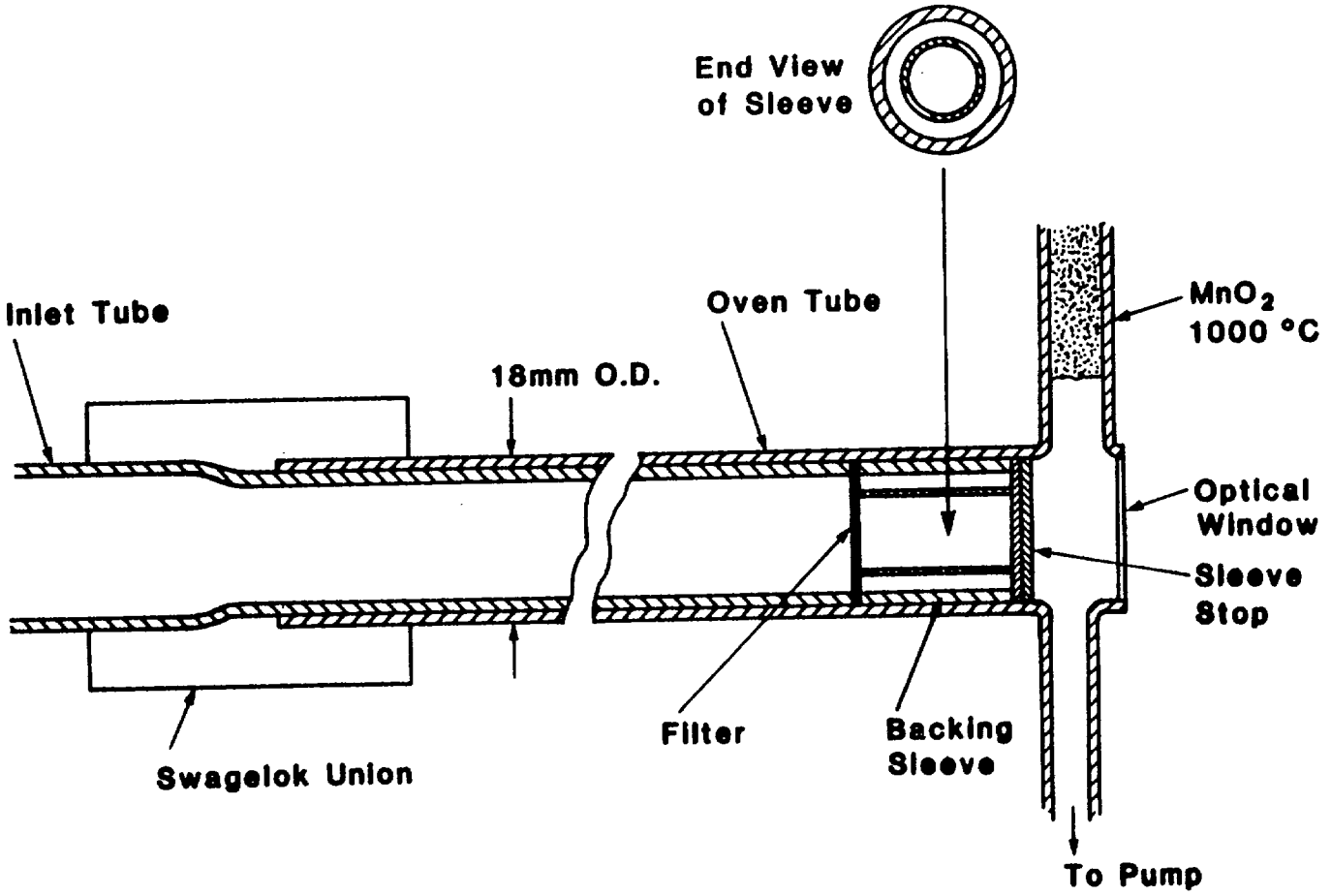

Figure 3. Filter mounting system for <u>in situ</u> carbon analyzer. The backing sleeve provides a support on which the two back-to-back quartz fiber filter disks are mounted.

the system with helium, the vapor side is analyzed by rapid heating to 650 C. Adsorbed organic vapors are volatilized and oxidized to CO_2 in a 1000 C MnO_2 bed. The CO_2 is reduced to CH_4 in a 500 C nickel-firebrick methanator and measured in a flame ionization detector (FID). At the completion of the adsorbed vapor measurement solenoid valve (SV6) switches, and the filters from the aerosol side of the instrument are analyzed. The first step in this process involves heating to 650 C in a helium atmosphere to volatilize adsorbed organic vapors and particulate organic carbon. At the completion of this process the temperature is reduced to about 350 C, and the atmosphere is changed to 2% O_2-98% He to oxidize elemental carbon. The temperature is increased in steps to 750 C, ensuring complete removal of elemental carbon. In the final step of the analysis, a known amount of methane is introduced for calibration purposes.

During organic carbon volatilization some organic carbon is pyrolytically converted to elemental carbon (i.e., charring). Correction for pyrolytic conversion is accomplished by monitoring the transmittance of a chopped 633 nm He-Ne laser light through the aerosol-side filter during the analysis. Figure 4a shows the laser transmittance for a typical analysis. At the beginning of the analysis the transmittance through the loaded filter is sampled. As the aerosol-side temperature is raised and organic material is removed, pyrolysis occurs; this results in a darkening of the filter and a decrease in transmittance. When oxygen is added, both the pyrolytically-produced elemental carbon and the original carbon begin to oxidize, and the transmittance increases until the filter is clean. The point at which the transmittance regains its initial value is considered to be the split between organic and elemental carbon. This split is shown in Figure 4 by the long line extending upwards from the time axis. All material prior to the split is considered organic and after, elemental. Some temperature dependence has been observed in the laser system as seen by the increase in transmittance when the temperature of the aerosol-side oven is reduced at the end of the analysis. The influence of this effect on the results is small and can be minimized experimentally or corrected in the computations.

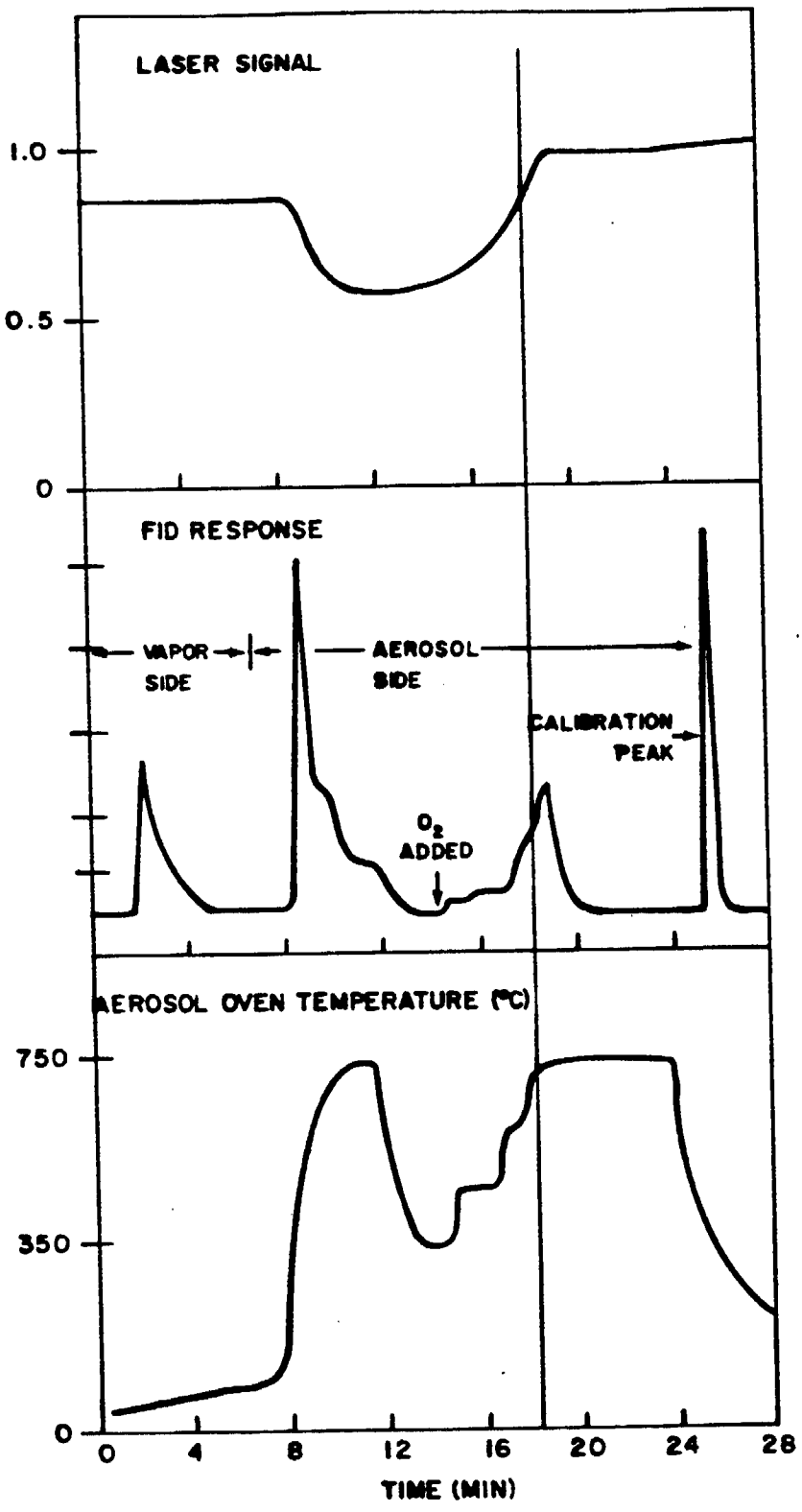

Figure 4. Typical output for in situ carbon analyzer. (a) Optical transmittance; (b) flame ionization detector; (c) temperature of aerosol-side oven. The vertical line occurring at about 18.5 minutes is the split point between organic and elemental carbon.

Figure 4b shows the time behavior of the FID during the carbon analysis. The first peak corresponds to adsorbed organic vapor on the vapor-side quartz fiber filter. The second and third peaks represent material removed from the aerosol filter before and after the addition of oxygen. The final peak is the calibration. The temperature profile of the aerosol-side oven is shown in Figure 4c; the vapor-side oven temperature is not shown.

System control, analysis, and data acquisition are all accomplished by an Apple II-Plus computer. At the end of each analysis the computer performs the pyrolysis correction, integrates the peaks, corrects for the vapor adsorption artifact, and presents the results in $\mu gC/m^3$. Any volatilization artifact is minimized because the repeated removal of the major aerosol components (including sulfates and nitrates) during the analytical part of the operating cycle prevents the buildup of a pressure drop resulting from the accumulation of particulate material on the filter.

Instrument Characterization

The analytical precision for total carbon (i.e., particulate + adsorbed vapor) was estimated by multiple injections of a known amount of CH_4 into the aerosol oven and measurement of the instrument response using the standard analysis program of the in situ analyzer. Ten injections of 180 μl of 5.39% CH_4 in He were made, and the resultant coefficient of variation was 1.3%. The corresponding detection limit (3σ) was 0.2 μg.

The accuracy of the CH_4 injection approach was checked by cross-calibrating against the laboratory thermal-optical carbon analyzer. In this experiment the response of the laboratory analyzer to known amounts of sucrose deposited on quartz fiber filter disks and to CH_4 injections was measured. The latter involved 10 injections ranging between 2 and 25 μgC. The ratio of the methane to sucrose responses was 1.01 ± 0.05. Thus, there is no difference between the two approaches at a 95% level of confidence, and it can be concluded that the methane injection method is a valid calibration for the in situ analyzer. The methane injection experiment also demonstrated the linearity of the in situ analyzer

response over the range studied. A linear regression between the mass of carbon injected and the instrument response gave a very good fit (R^2=99.5%).

To check for consistency between the aerosol and vapor sides of the instrument, a set of experiments in which both sides were pre-filtered with a Teflon filter was run. In this configuration the analytical filters in both sides collect adsorbable organic vapor and should be equivalent. Eight runs involving the sampling of ambient air for periods of either three or eight hours were made at the Oregon Graduate Center in Beaverton, Oregon. The pooled standard deviation of the difference between the two sides was 0.068 $\mu gC/m^3$, which was equivalent to a coefficient of variation of 2.2%. Because total aerosol carbon is determined by the difference between the two sides, the compounded analytical precision for the measurement of total aerosol carbon with the in situ analyzer was 3.1%.

Since each in situ analysis uses the whole sample, it is not possible to determine separate analytical precisions for organic and elemental carbon. However, results from replicate analysis of 16 ambient filter samples using the laboratory carbon analyzer should provide some insight into this question. One-way analysis of variance on the results gave the following standard deviations: total carbon, 7.0%; organic carbon, 8.4%; and elemental carbon 6.9%. (The total carbon uncertainty is larger than that obtained in the sucrose (4%) and methane injection (1%) experiments for the laboratory analyzer. This is probably because of variability in the distribution of particulate matter on the filter and error introduced during sample handling.) Because in situ analyzer uncertainties for both total carbon (1.3%) and total particulate carbon (3.1%) are less than the total carbon uncertainty for the laboratory analyzer (7%), it is likely that the precision uncertainties for organic and elemental carbon in the in situ analyzer are also less than for the laboratory analyzer.

The FID baseline can be evaluated at several points during the analysis. Because the FID response varies with carrier gas composition, slight shifts in the baseline can occur. The optimal baseline subtraction procedure minimizes the difference between the analytical

blank and the estimated baseline continuously. This, however, was not practical. The procedure which was adopted samples the baseline for the vapor side material prior to its removal, and samples the baseline separately for the He and O_2-He sections of the aerosol side analysis and for the CH_4 calibration.

The transit time between the sampling filter and the FID was determined experimentally by aligning the initial increase in optical transmission, which results from EC removal, with the arrival of CO_2 from the oxidation of elemental carbon at the FID. Good agreement was found between the experimentally determined transit time and the expected transit time calculated from flow conditions. The laser signal responds immediately to the removal of material from the filter whereas the FID signal is delayed by the transit time. Proper correction for the pyrolytic conversion of organic to elemental carbon requires that these signals be aligned.

The split between organic and elemental carbon is considered to be the point at which the transmittance regains its initial value. This determination is based on the assumption that elemental carbon is the only component of the sample which affects the optical transmittance. The analysis of 9 laboratory generated sucrose aerosol samples containing 15 to 90 μgC supported this assumption. The transmittance through the loaded filter (initial laser signal) was almost identical to the transmittance through the clean filter (final laser signal) and although a large fraction of the organic material underwent pyrolysis, the sample was properly reported as entirely organic. Sampling and analysis of sucrose aerosol used only the aerosol side sampler and a typical analysis is shown in Figure 5.

The response of optical transmittance to filter loading was investigated by sampling a black ink aerosol generated in the laboratory. A solution of 2.9 g/l of Staedtler mars 745 black drawing ink (Hogan, 1985) was nebulized, deionized in an ^{85}Kr charge neutralizer, aged in continuous flow chambers and sampled at 9 l/min through the *in situ* carbon analyzer. Twelve samples containing between 1 and 100 μg of elemental carbon were collected. Beer's law adapted for particles on

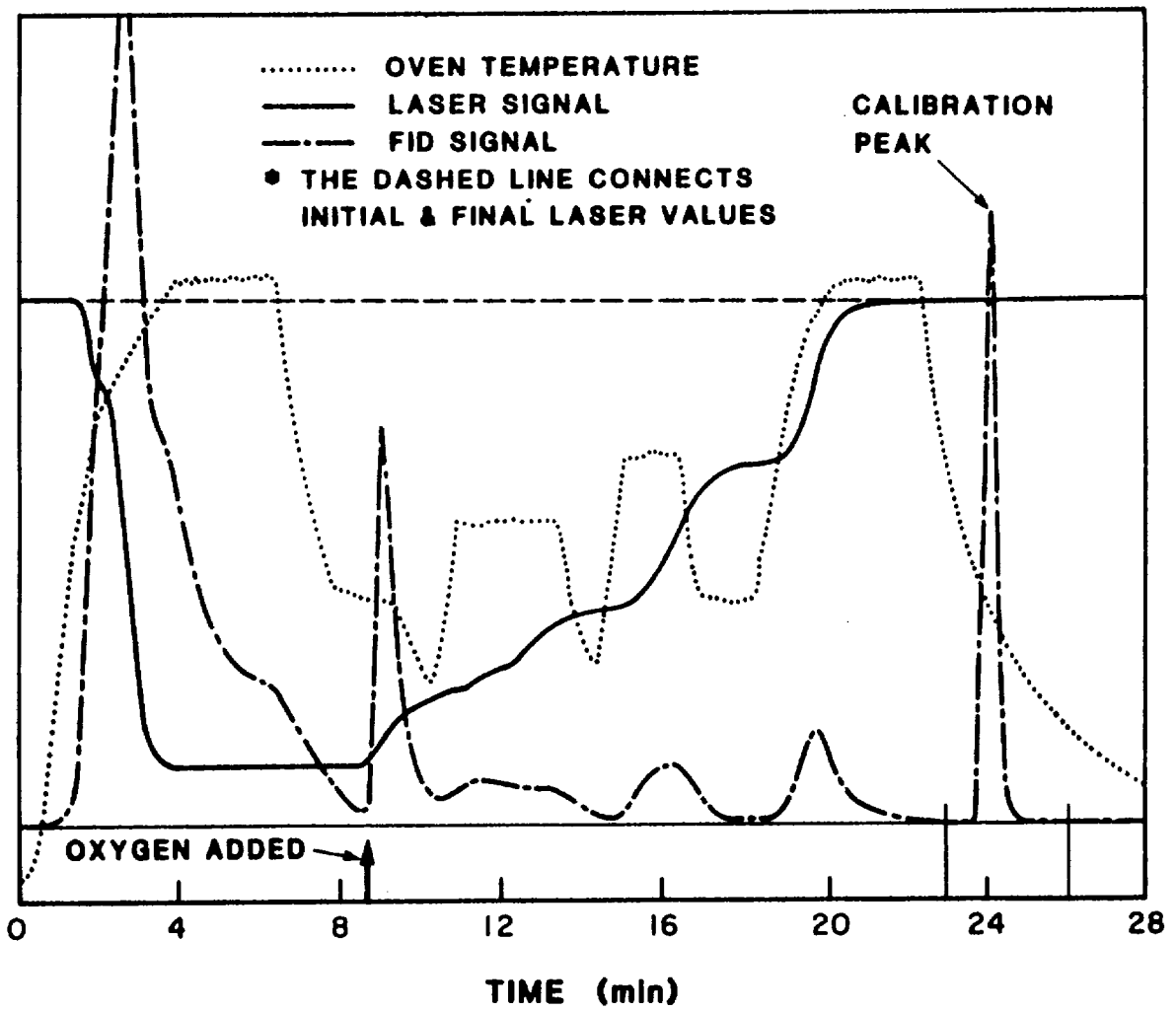

Figure 5. Typical <u>in situ</u> carbon analyzer output for a sucrose aerosol collection. Optical transmittance, flame ionization detector, and oven temperature. Adsorbed vapor was not measured in this experiment. The dashed line is drawn horizontally from the initial laser transmittance signal.

filters is $I=I_0\exp(-bC)$ where I and I_0 are the intensities of transmitted light for the sample and blank, C is the concentration ($\mu gC/cm^2$) and b is the extinction coefficient ($cm^2/\mu g$). Optical absorbance ($ABS = -\ln I/I_0$) varies linearly with elemental carbon loading to about 25 μgC as shown in Figure 6. Beyond this point Beer's law breaks down, and increases in filter loading have a diminishing affect on the absorbance.

In a complimentary experiment, aerosol was collected until no further change in the transmittance was observed. The transmittance through a perfectly black filter is greater than zero. This was also observed by Gundel et al. (1984) and attributed to a "light pipe" effect which they observed through an optical microscope. The in situ carbon analyzer transmittance has been adjusted to read zero through a perfectly black filter. The breakdown of Beer's law occurs at a high enough loading that it will not affect the sensitivity of the pyrolysis correction in the range in which the instrument is operated.

Comparison With The Conventional Sampling And Analysis Method

Organic and elemental carbon concentrations were measured by the in situ carbon analyzer and by manual sampling during the Carbonaceous Species Methods Comparison Study in Glendora, California, in August, 1986. The in situ carbon analyzer was assembled in an Air Resources Board trailer. Ambient air was sampled at 8.5 l/min through a 1 in. diameter manifold extending 3 ft above the roof and capped with a rain shield and bug screen. It operated on a cycle ranging from 90 to 180 minutes. Analysis time accounted for 40 minutes of that cycle. Instrument blanks were measured every evening by setting the program to collect for 0 minutes followed by carbon analysis. A three-peak internal calibration program was also run daily. This program was identical to the normal analysis program except that the methane calibration loop was switched on-line during the vapor-side analysis, again during the He segment of the aerosol-side analysis, and during the final stages of the O_2-He segment (i.e., the elemental carbon part of the cycle). Because the instrument response differed by as much as 10% between these three conditions, appropriate response factors were incorporated into the data output.

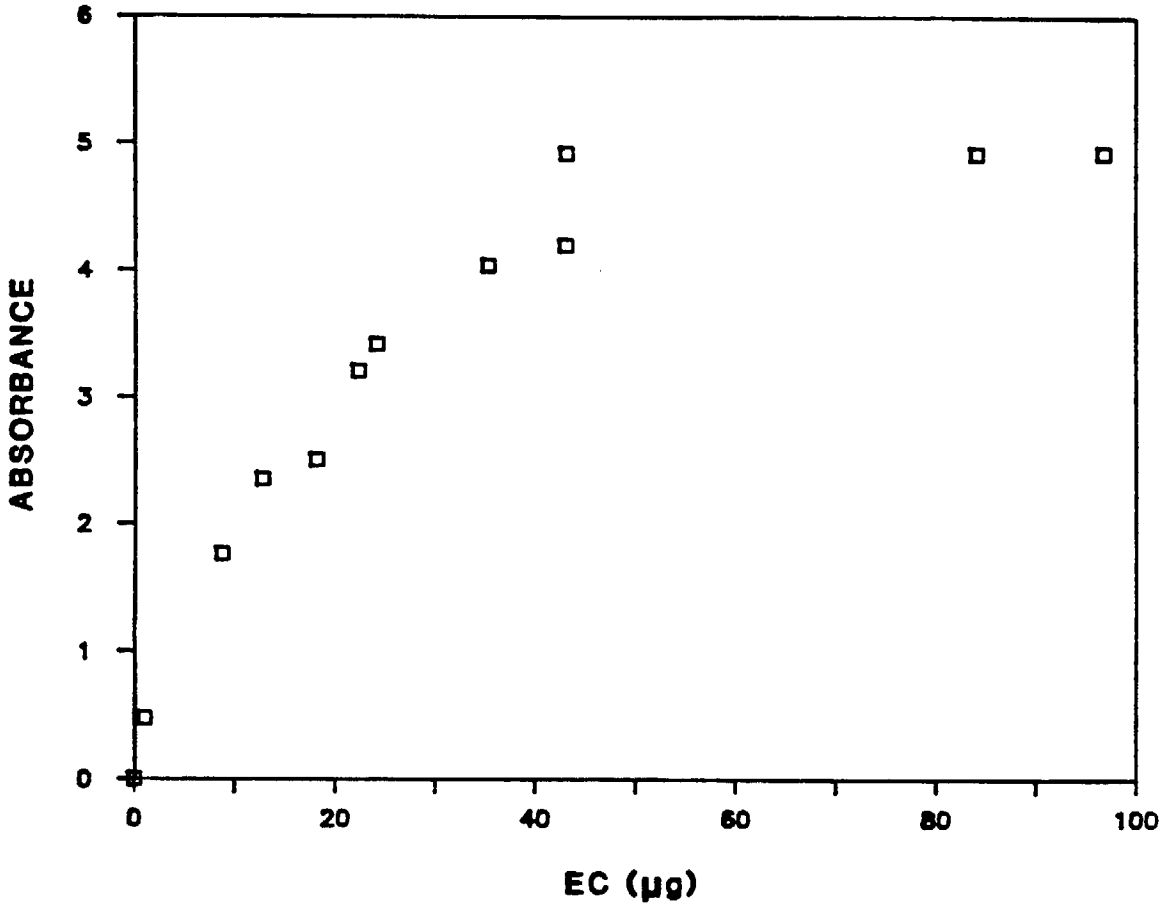

Figure 6. Comparison of optical absorbance ($-LnI/I_o$) and elemental carbon loading (µg) for the in situ carbon analyzer. The filter area is 1.77 cm^2.

Manual samples were collected with a two-port sampler. A laminar flow field was developed in each sampling port by attaching a 25 cm long, 3.7 cm i.d. aluminum tube to the filter holder inlet. This was capped with a rain shield and bug screen and shaded from the sun. One port contained a 2.5 μm cut-point Marple (1974) impactor with a jet Reynolds number of 7400 (Marple and Liu, 1975; the Reynolds number for a round jet impactor is uw/v where u is the fluid velocity through the jet (cm/s), w is the jet diameter, and v is the kinematic viscosity of the fluid (cm^2/s)). The impactor was situated about half way down the tube and the filter holder contained a 47 mm quartz fiber filter (Pallflex QAOT) for aerosol collection. The second port held a 47 mm Teflon filter (Zefluor, 2 μm pore size) followed by a quartz fiber filter for the vapor adsorption estimate. Both ports sampled ambient air at a flow rate of 25 l/min which was equivalent to a filter face velocity of about 43 cm/s. The impactor surface was cleaned and coated daily with Apiezon N vacuum grease to reduce bounce (Cheng and Yeh, 1979; Esmen et al., 1978). For the first two days of the study 4-hour samples were collected during the day and an 8-hour sample at night. For the remaining 7 days 12 hour samples were collected. The samples were analyzed for OC, EC and TC using the laboratory thermal-optical carbon analyzer described in Chapter 2. They were also analyzed by direct thermal desorption GC/MS (see Chapter 7). Midway through the sampling program a third port was added to this sampler to accommodate a dilution experiment of Susanne Hering's design (see Chapter 6). The manual sampler carbon data are listed in Appendix B.

Figures 7 - 9 compare in situ concentrations for total, organic and elemental particulate carbon with manual sampler concentrations. In situ results are composites of measured values, averaged over the collection period of the manual sampler. Linear regression fits with 95 percent confidence intervals are given in Table 3. The fits are quite good for total and elemental carbon (R^2=92% and 98% respectively). For organic carbon, however, the regression was not significant at the 5% level despite the fact that R^2=85%. This resulted from the small number of samples available for comparison and the inherent variability in the measurement. (Unfortunately, less samples were available for the organic

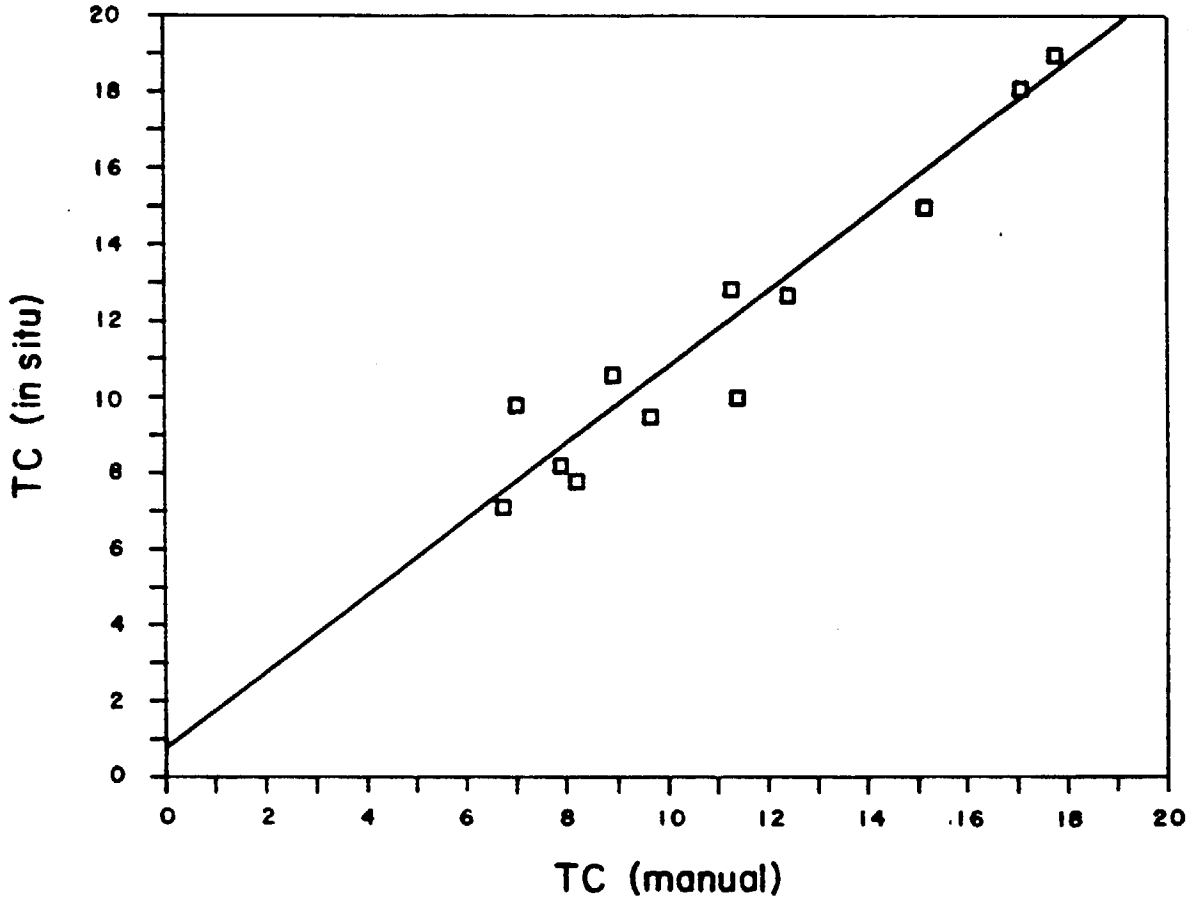

Figure 7. Comparison of in situ and manual sampler results ($\mu gC/m^3$) for total particulate carbon. The solid line is the linear least squares fit of Table 3.

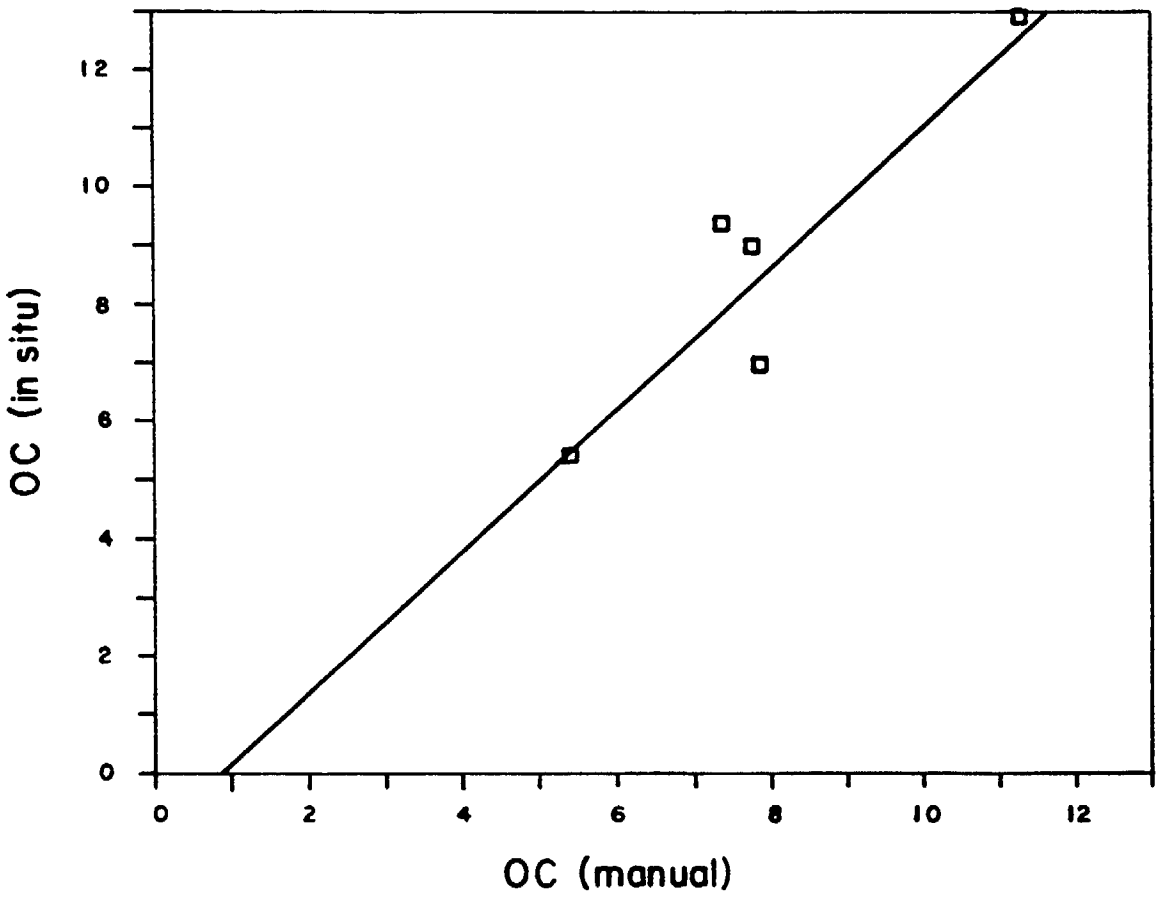

Figure 8. Comparison of in situ and manual sampler results ($\mu gC/m^3$) for particulate organic carbon. The solid line is the linear least squares fit of Table 3.

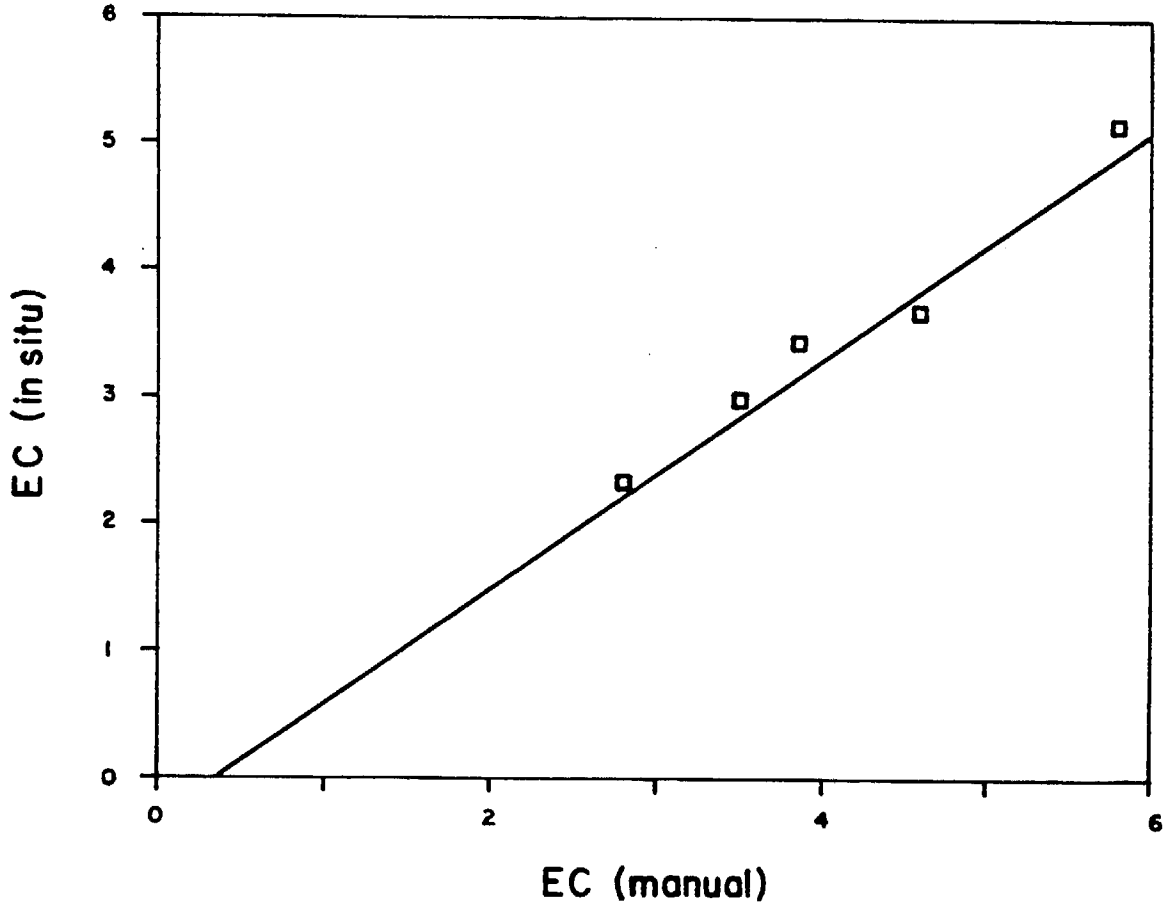

Figure 9. Comparison of in situ and manual sampler results ($\mu gC/m^3$) for elemental carbon. The solid line is the linear least squares fit of Table 3.

TABLE 3. REGRESSION RESULTS FOR COMPARISON OF IN SITU AND MANUAL METHODS.

Uncertainties are 95% confidence intervals. The number of samples comprising the regression is indicated by n, and R^2 is the percentage of the variance explained by the regression.

	In Situ = a + b (Manual)			
	a	b	R^2	n
Total Carbon	0.8 ± 2	1.0 ± 0.2	92%	12
Organic Carbon*	−1.0 ± 8	1.2 ± 1	85%	5
Elemental Carbon	−0.3 ± 1	0.9 ± 0.2	98%	5

*An F-test showed that the organic carbon regression was not significant at the 5% level.

and elemental carbon comparisons because of a malfunction in the optical transmittance system during the first week of the study.)

A paired, two-sided t-test showed no significant difference between in situ and manual sampler results for either total or elemental carbon at the five percent level. However, for elemental carbon a single-sided t-test indicated that the in situ values were significantly less than the manual sampler values. The magnitude of that difference was about 14 percent. The most likely cause of this discrepancy relates to the different optical systems used in the in situ and laboratory analyzers for the pyrolysis correction. The former uses optical transmittance, but the latter uses optical reflectance. The observed difference is probably a fundamental one resulting from the different types of optical measurements and is still under investigation. Because of the good agreement for particulate total and elemental carbon (apart from the 14% systematic deviation for the latter), it is reasonable to conclude that the in situ analyzer also provides reliable results for aerosol organic carbon.

Ambient Measurements

The in situ carbon analyzer CSMCS data are presented in Appendix C. Total aerosol carbon data are plotted in Figure 10. Figure 11 shows the twelve hour average particulate OC, EC, and TC data from the two-port sampler. Despite the gaps in the data which occurred during calibration and service periods, strong diurnal variations are seen for total, organic, and elemental carbon with peak concentrations occurring during the daylight hours. The vapor artifact comprised 20 to 50% of the organic material on the manual samples and 30 to 60% of the organic material on the in situ samples. The larger in situ artifact is probably a result of the double filter arrangement and short sampling periods employed by the instrument (see Chapter 5). In addition, 30 to 50% of the material removed after the addition of oxygen during in situ carbon analysis was pyrolyzed organic material. Thus, both corrections were significant.

Concentrations of particulate organic and elemental carbon and ozone, an indicator of atmospheric photochemical activity, are plotted

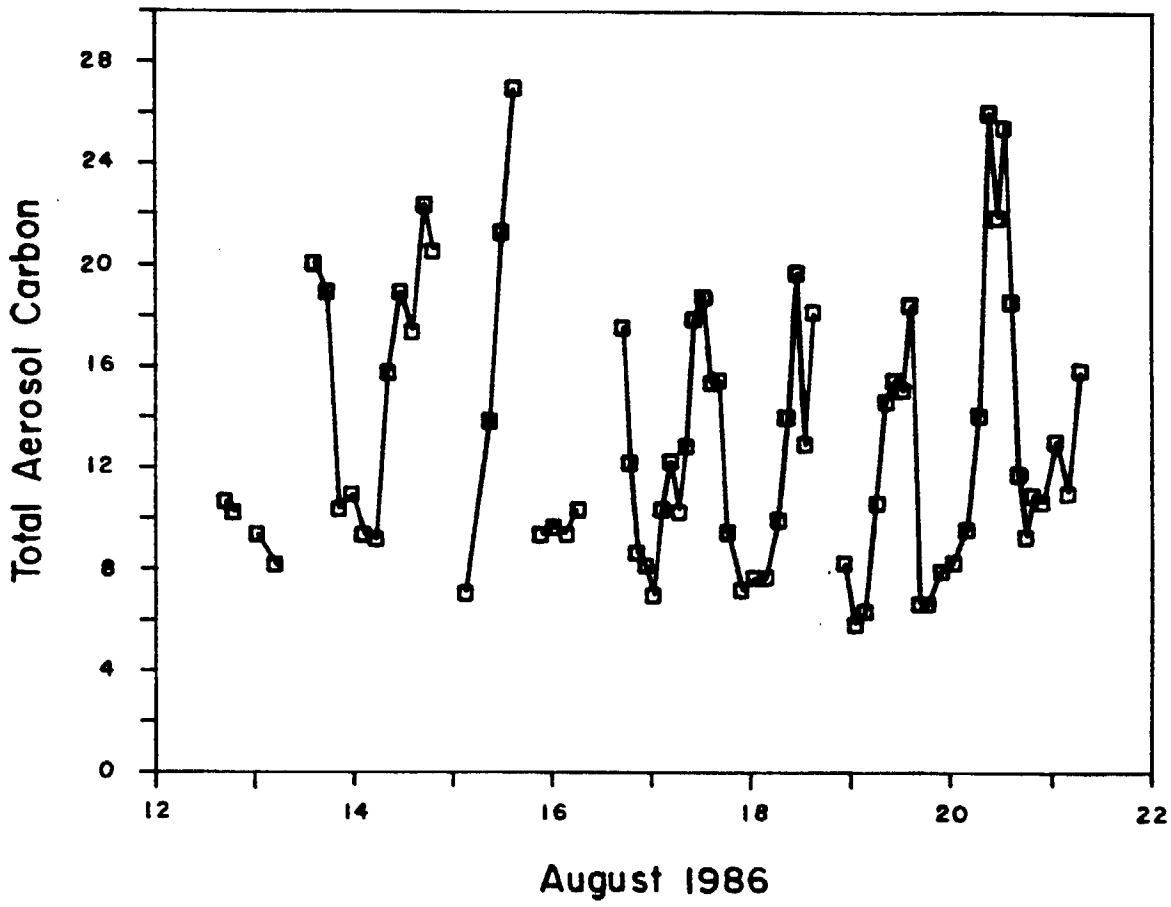

Figure 10. Total particulate carbon concentrations ($\mu gC/m^3$) for particles under 2.5 μm in diameter at Glendora, California, August 12-21, 1986.

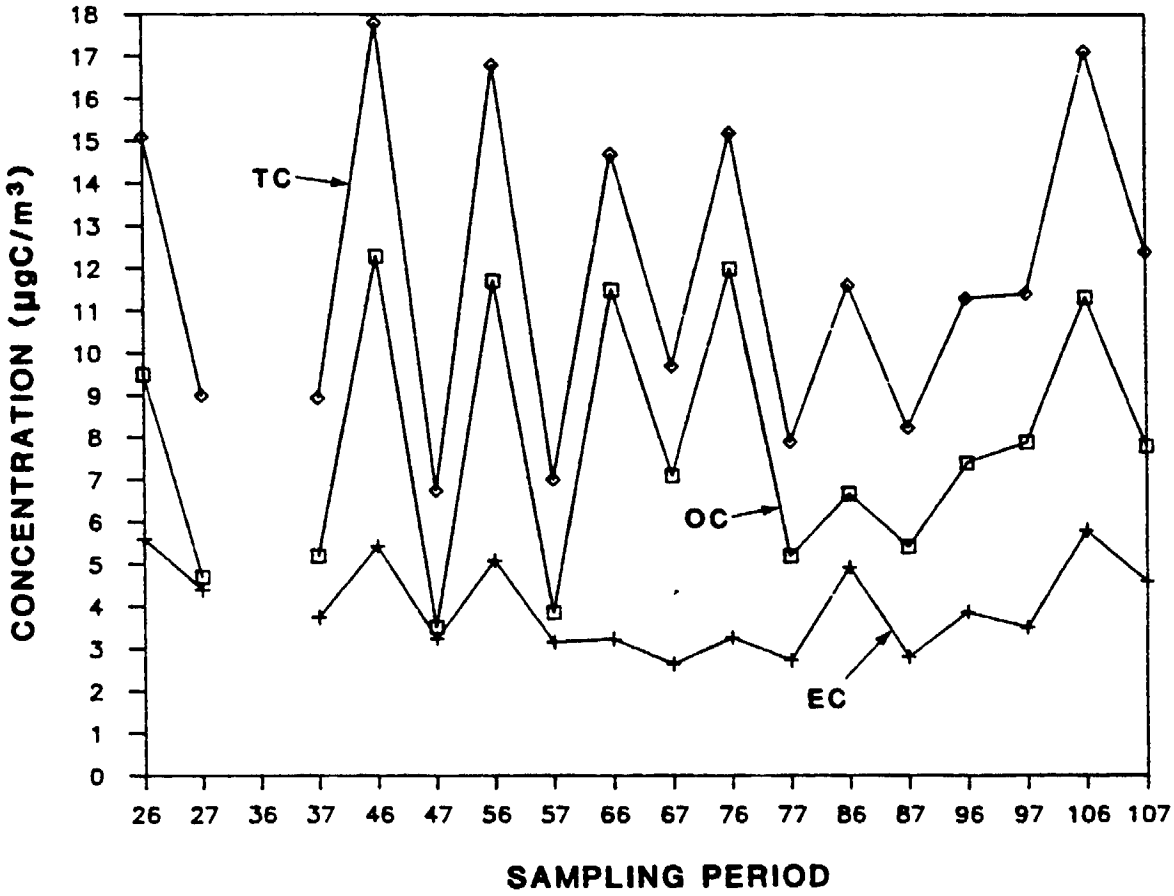

Figure 11. Twelve hour average concentrations (µgC/m^3) of particulate organic (OC), elemental (EC), and total carbon (TC) for particles under 2.5 µm in diameter at Glendora, California, August 12-21, 1986. The sampling period is identified by a three digit code. The right most digit indicates day (6) or night (7), and the left one or two digits (2-10) indicate the sampling day. Thus sampling period 106 corresponds to the daytime (08:00-20:00) sample for day 10 of the study.

for August 19 and 20 in Figures 12 and 13. Ozone data are from the California Air Resources Board, Haagen-Smit Laboratory. Each data point represents the midpoint of the sampling period. For both days mid-day temperatures exceeded 32 C, and there was a strong ground-based inversion on the morning of August 20.

On August 19 ozone peaked at about 2 pm (1400 PDT) at a concentration of about 23 pphm, indicating "moderate" photochemical smog. Both organic and elemental carbon exhibited similar diurnal patterns with their peaks broadly distributed over much of the mid-day. Because elemental carbon is a tracer for primary, combustion-generated aerosol, it is likely that the organic aerosol on this day was principally primary. However, the ratio of organic to elemental carbon increases steadily from 2.3 in the 0530 to 0730 (PDT) sample to a maximum of 4.2 in the 1400 to 1530 (PDT) sample. This maximum corresponds to the ozone maximum. The "additional" organic carbon (beyond that explained by a correlation with elemental carbon) probably results from some photochemical aerosol formation.

The situation of August 20, however, is much more dramatic. Elemental carbon showed a distinct maximum at about 0900 (PDT) which corresponded with the highest CO concentrations recorded during the study, 4 ppm as a 1 hour average. These pollutant levels are probably a result of the accumulation of local emissions during the morning inversion. Organic carbon experienced a secondary maximum at this time which was probably also the result of primary emissions. However, as the elemental carbon concentration fell sharply, the concentrations of organic carbon and ozone rose sharply and reached their maxima in early afternoon. The times of the ozone and organic aerosol maxima are not significantly different with respect to the range of uncertainty created by the averaging process. At the time of the ozone and organic carbon maxima, the ratio of organic to elemental carbon also reached its maximum (6.8). These observations strongly suggest a secondary origin for the afternoon peak in organic carbon.

Further investigation of the roles of primary and secondary processes in the formation of organic aerosol is underway. The in situ carbon analyzer was used in the Southern California Air Quality Study

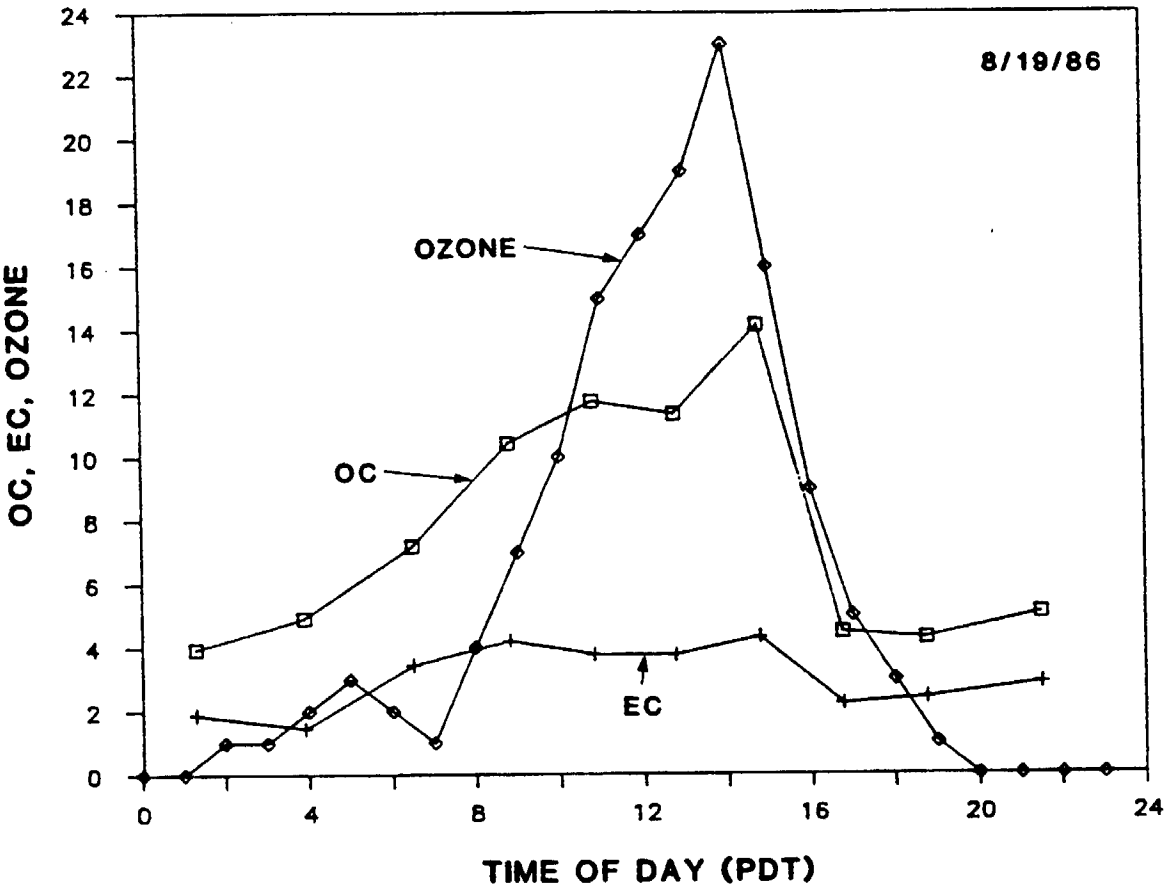

Figure 12. Concentrations of ozone (pphm), particulate organic carbon ($\mu gC/m^3$), and particulate elemental carbon ($\mu gC/m^3$) at Glendora, California, August 19, 1986.

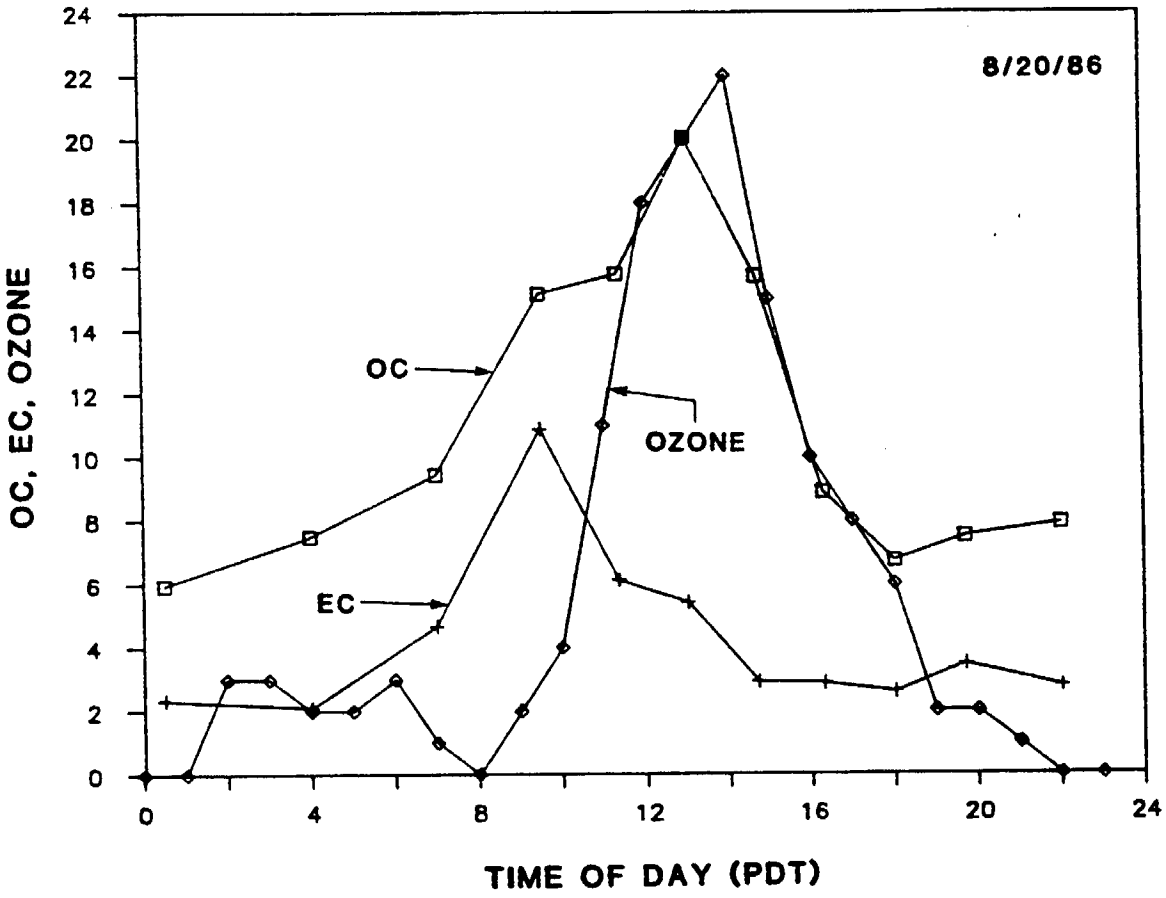

Figure 13. Concentrations of ozone (pphm), particulate organic carbon ($\mu gC/m^3$), and particulate elemental carbon ($\mu gC/m^3$) at Glendora, California, August 20, 1986.

(SCAQS) in Claremont, California (summer, 1987), and in Long Beach, California (fall, 1987), and interpretation of these data will be reported in a subsequent publication.

CHAPTER 5: VAPOR ADSORPTION ARTIFACT STUDIES

Filter sampling for organic aerosol is complicated by two artifact errors. Adsorption of organic vapors on the sampling filter comprises a positive artifact, and volatilization, which removes material from the filter, is a negative artifact (Cadle et al., 1983; McDow, 1986). The importance of adsorption is evidenced by the presence of significant concentrations of organic carbon on backup filters behind primary aerosol filters (Cadle et al., 1983). Volatilization can occur when the collected particulate material is exposed to a pressure drop during sampling. Additionally, a change in ambient air quality can cause a redistribution of material between the gas and particulate phases, resulting in a weighted average filter sample which gives more weight to ambient conditions toward the end of the sampling period. These sampling artifacts are not well understood and therefore cause considerable uncertainty in measurements of organic aerosol.

Experiments performed by our laboratory (McDow, 1986) in the Portland area have shown (1) that the apparent concentration of aerosol organic carbon as collected on quartz fiber filters decreases with increasing filter face velocity. Elemental carbon concentrations show no face velocity dependence. (2) The concentration of organic carbon on backup filters also decreases with filter face velocity. (3) At a face velocity of 40 cm/s the concentration of organic carbon on quartz fiber backup filters behind Teflon front filters was about a factor of 2 greater than on quartz fiber backup filters behind quartz fiber front filters. Finally, (4) when the concentrations of organic carbon on quartz fiber backup filters behind Teflon front filters were subtracted from the concentrations of organic carbon on quartz fiber (front) filters, the face velocity dependence of the apparent aerosol organic carbon concentration was greatly reduced. These results suggest that adsorption of organic vapors is the dominant artifact in the sampling of organic aerosol.

Face velocity experiments were performed in the Carbonaceous Species Methods Comparison Study to investigate the importance of organic

sampling artifacts under Los Angeles conditions. In addition, an extensive GC/MS study was conducted on front and backup filters collected on the two-port filter sampler.

A six-port filter sampler shown in Figure 14 permits simultaneous collection of six filter samples from a common manifold. Laminar flow is maintained in the manifold by drawing air out through the bottom of the manifold as well as through the sampling ports. Impactors installed at the delivery tube inlets remove all particles larger than 1.0 μm. A sharp particle cut-off efficiency curve is ensured by operating at a Reynolds number of 7000 (Marple and Liu, 1975). Three of the filter holders contained a quartz fiber (Pallflex QAOT) front filter followed by a quartz fiber backup filter (designated QQ), and the other three contained a Teflon (Zefluor, 2 μm pore size) filter followed by a quartz fiber filter (designated TQ). The TQ combination was used to estimate the amount of vapor adsorption artifact on the QQ front filter. All QQ and TQ combinations sampled air at 9 l/min, but three different face velocities (20, 40, and 80 cm/s) were used for the three sets of QQ and TQ filters. The face velocity is the volumetric flow rate per unit filter area. Different face velocities were achieved by reducing the filter areas with annular masks as shown in Figure 15.

It was discovered after the conclusion of the field study that the 80 cm/s QQ filters had not seated properly in the holder, invalidating all measurements from this sampling port. The face velocity sampler collected 12 hour samples on a standard CSMCS schedule, with filter changes at 0800 and 2000 PDT. Impactors were cleaned and regreased with Apiezon N vacuum grease daily. Care was taken to shade the filter holders from the sun. The samples were analyzed on the OGC laboratory thermal-optical carbon analyzer, and the data are presented in Appendix D. Concentrations of OC, EC, and TC found in particles less than 1.0 μm in diameter are plotted in Figure 16. A consistency check between this sampler and the two-port sampler was favorable (see Chapter 8).

The measured concentrations ($\mu gC/m^3$) of organic carbon collected on the backup filters are shown in Figures 17 and 18, and Figures 19-23 and Table 4 present comparisons in terms of x-y plots and regressions. A

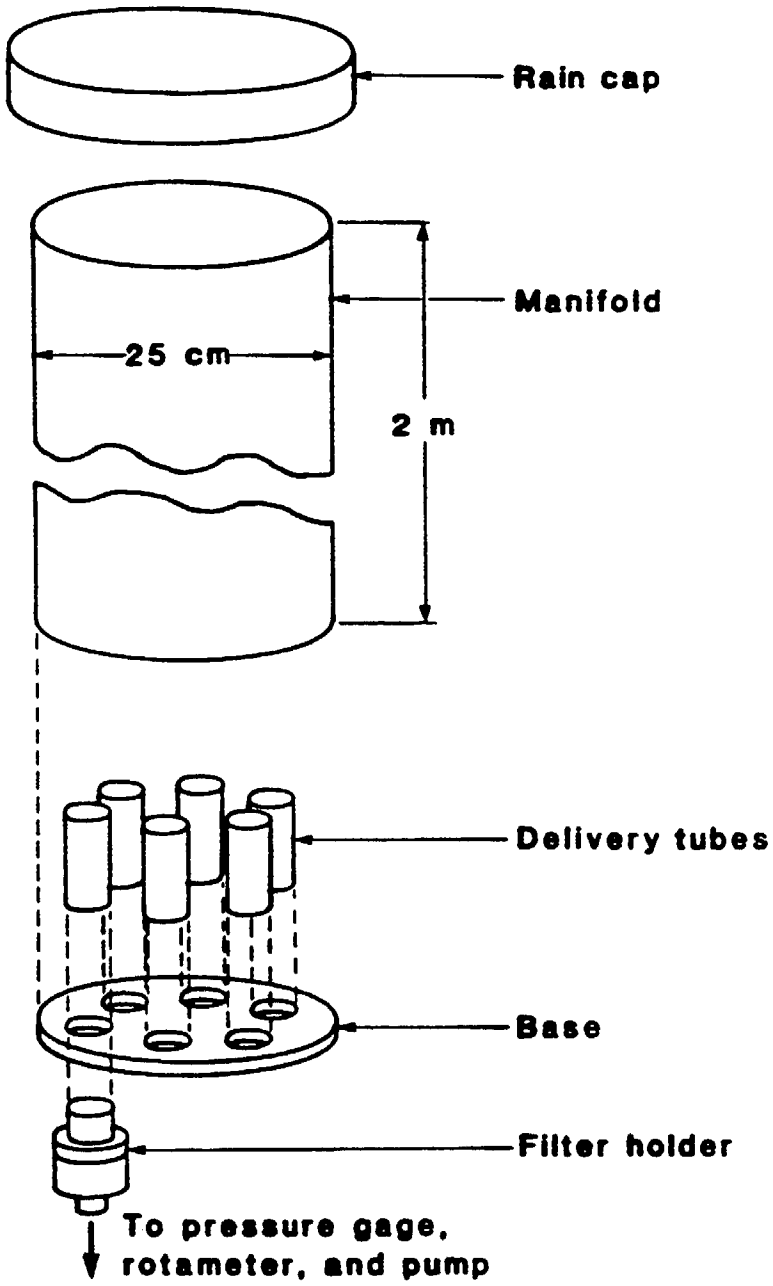

Figure 14. Six port filter sampler used in face velocity experiment.

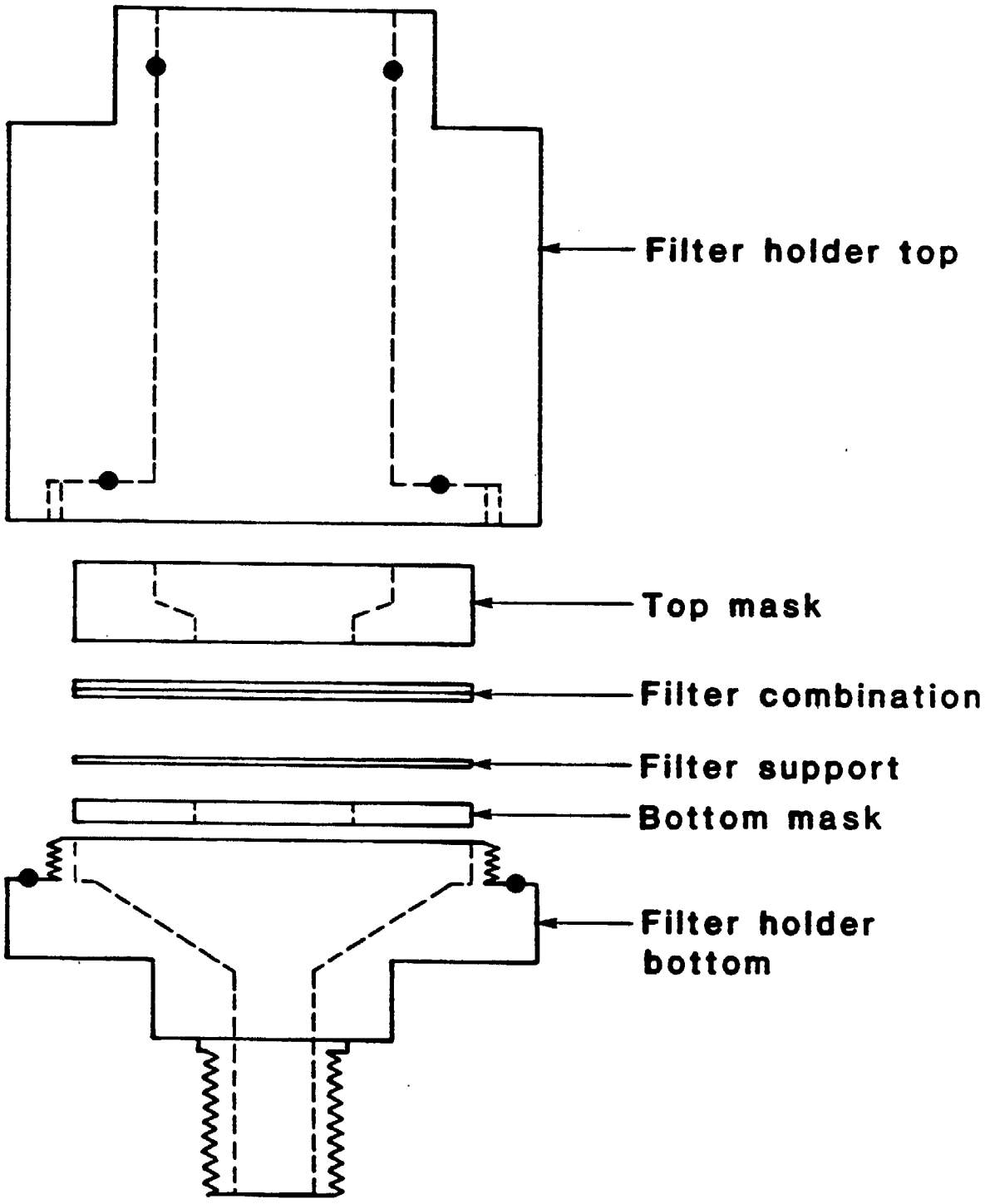

Figure 15. Aerosol filter holder with annular masks used in face velocity experiment. The solid black circles are O-rings.

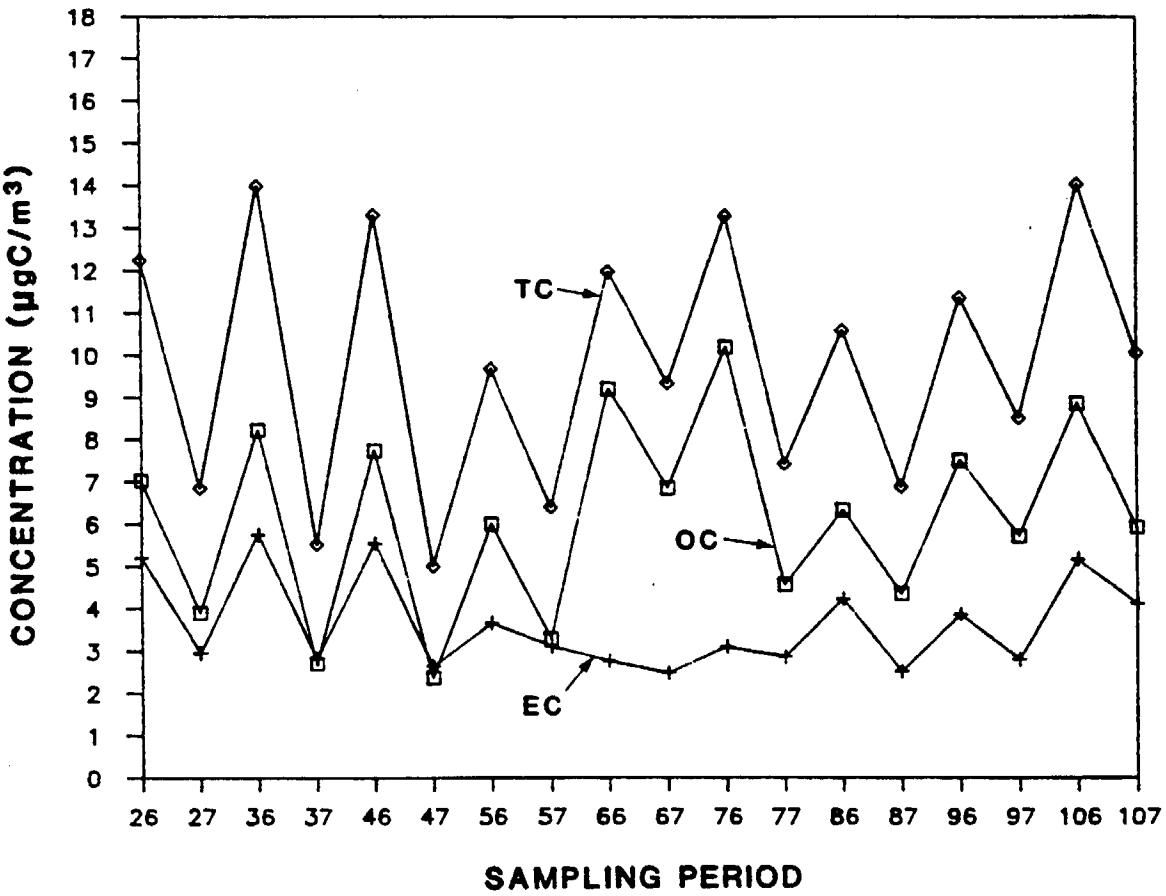

Figure 16. Twelve hour average concentrations (µgC/m^3) of particulate organic (OC), elemental (EC), and total carbon (TC) in particles under 1.0 µm in diameter. The sampling period is identified by a three digit code. The right most digit indicates day (6) or night (7), and the left one or two digits (2-10) indicate the sampling day. Thus sampling period 106 corresponds to the daytime (08:00-20:00) sample for day 10 of the study.

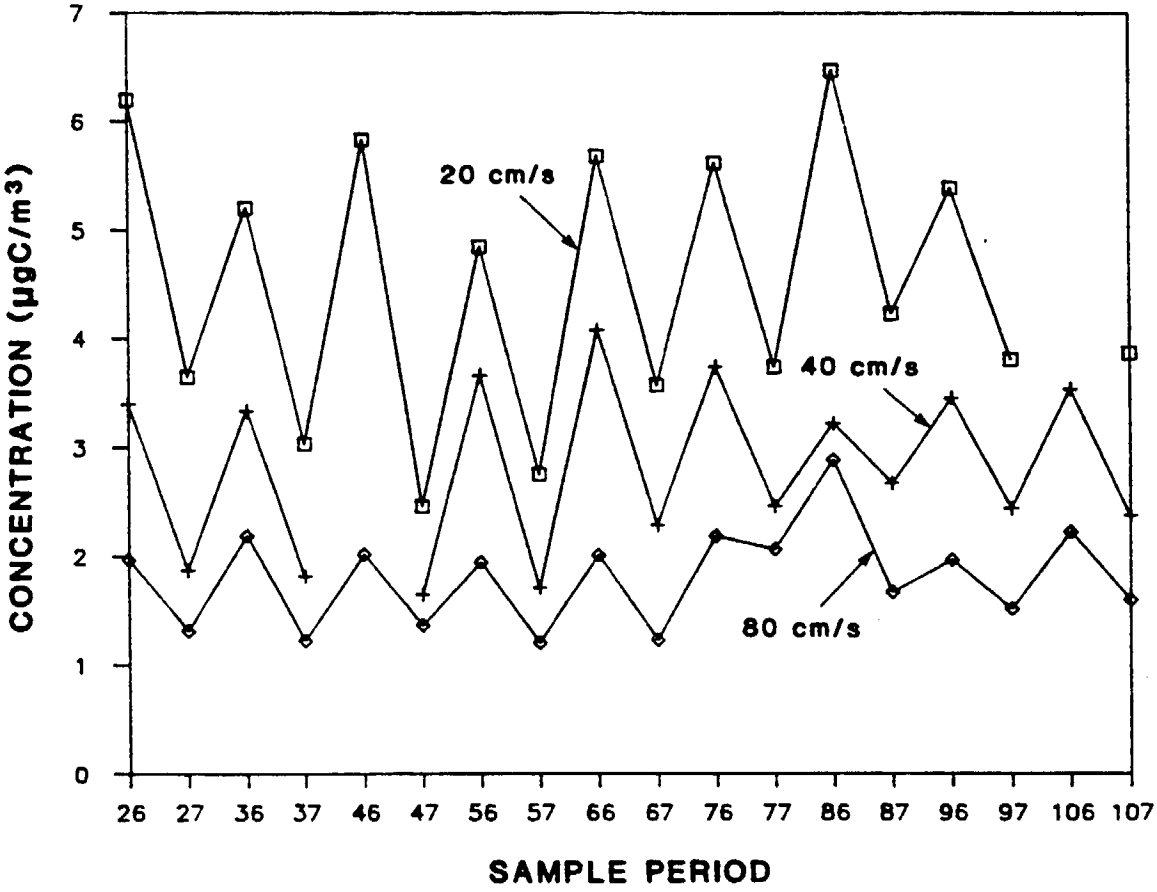

Figure 17. Organic carbon concentrations (µgC/m^3) on quartz fiber backup filters behind Teflon front filters for face velocities of 20, 40 and 80 cm/s. The sampling period is identified by a three digit code. The right most digit indicates day (6) or night (7), and the left one or two digits (2-10) indicate the sampling day. Thus sampling period 106 corresponds to the daytime (08:00-20:00) sample for day 10 of the study.

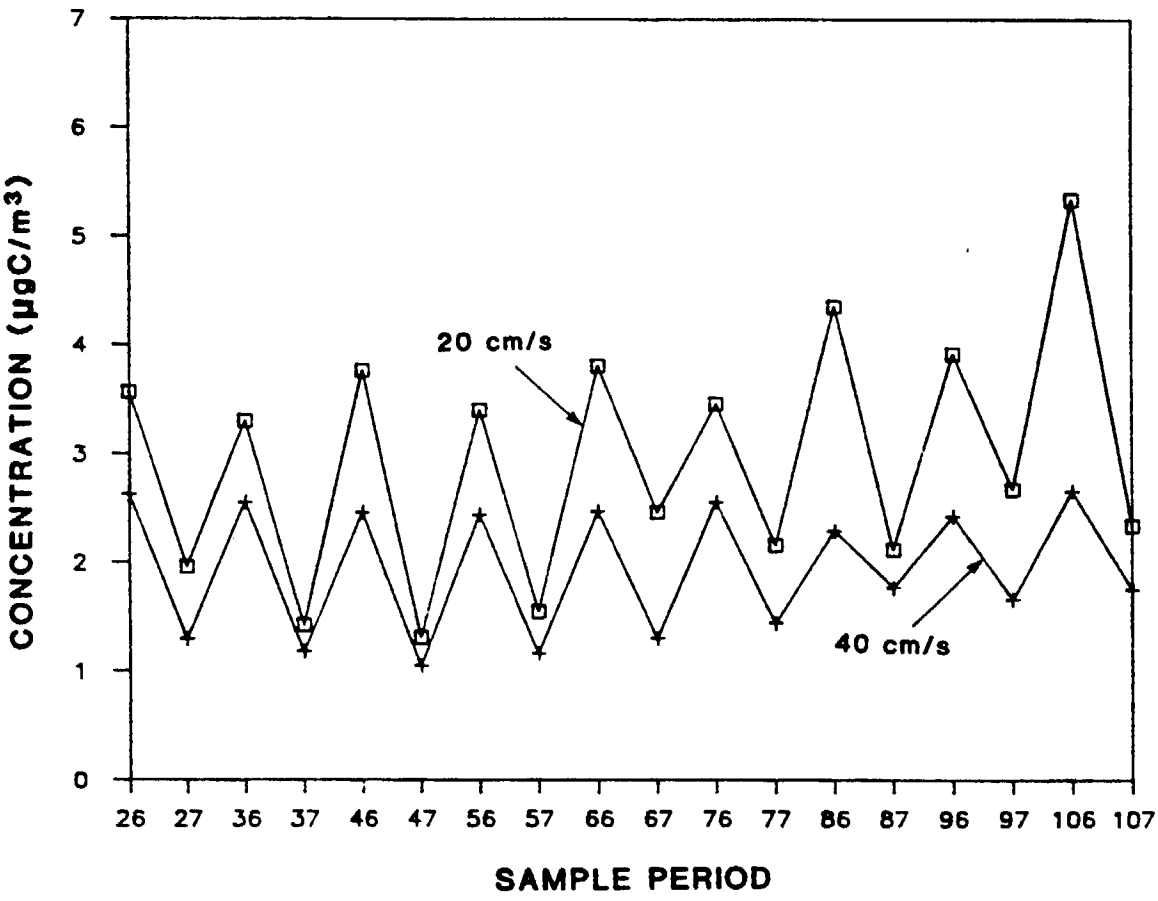

Figure 18. Organic carbon concentrations ($\mu gC/m^3$) on quartz fiber backup filters behind quartz fiber front filters for face velocities of 20 and 40 cm/s. The sampling period is identified by a three digit code. The right most digit indicates day (6) or night (7), and the left one or two digits (2-10) indicate the sampling day. Thus sampling period 106 corresponds to the daytime (08:00-20:00) sample for day 10 of the study.

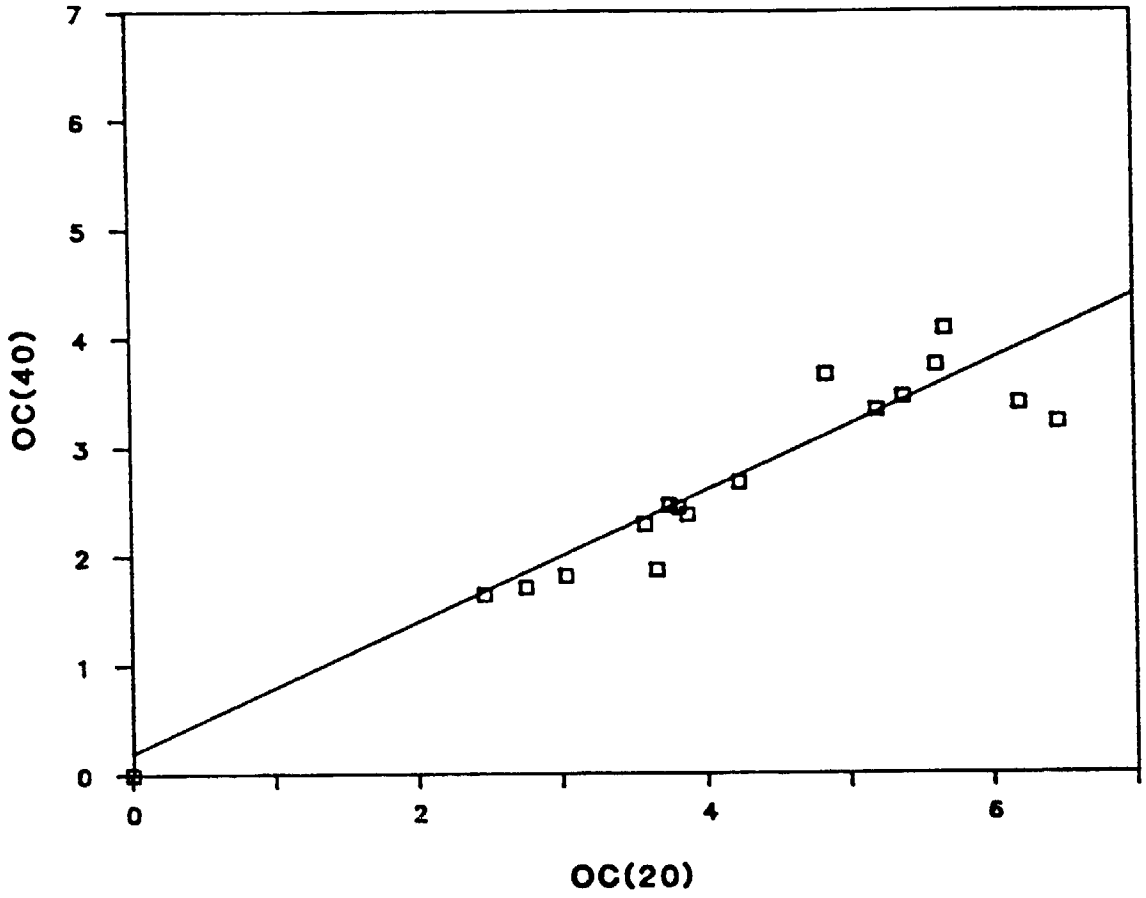

Figure 19. Comparison of organic carbon concentrations ($\mu gC/m^3$) at face velocities of 20 and 40 cm/s for quartz fiber backup filters behind Teflon front filters. The solid line is the linear least squares fit of Table 4.

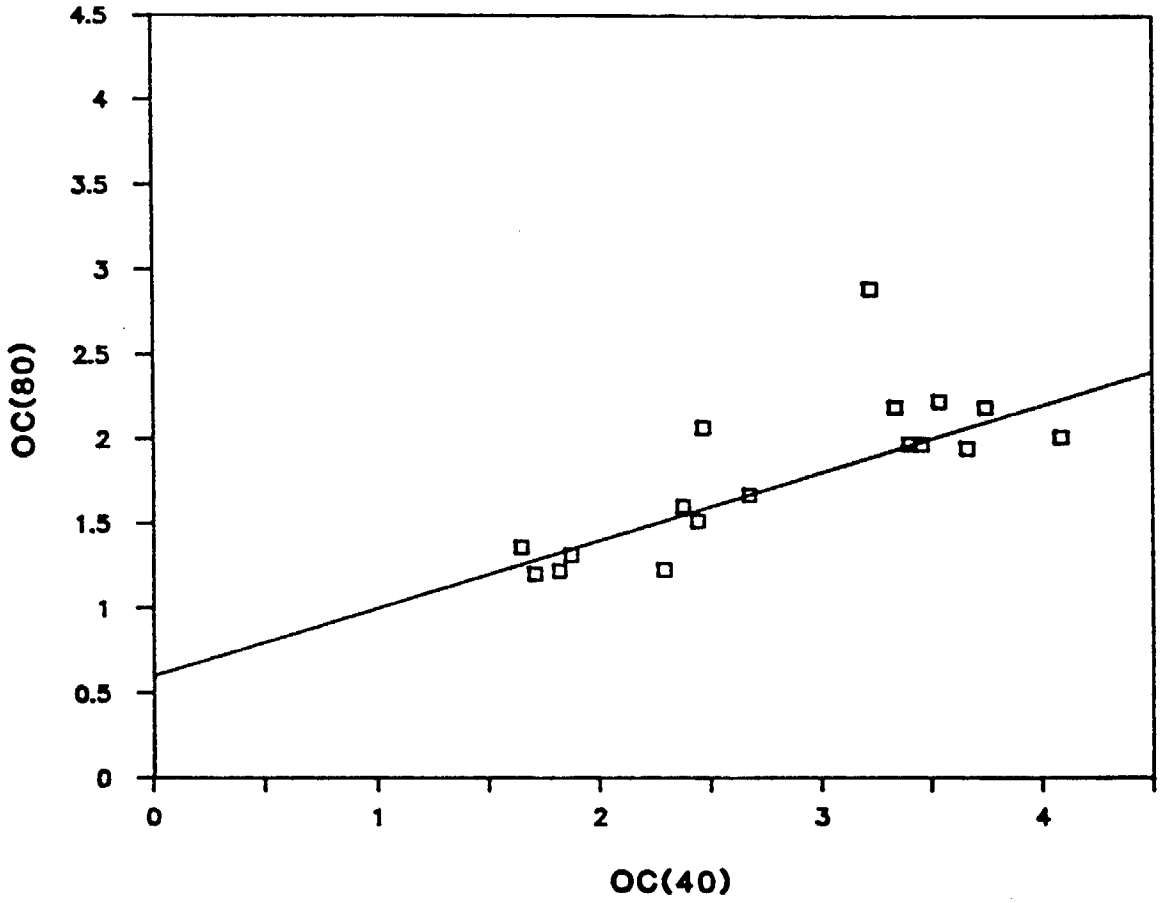

Figure 20. Comparison of organic carbon concentrations ($\mu gC/m^3$) at face velocities of 40 and 80 cm/s for quartz fiber backup filters behind Teflon front filters. The solid line is the linear least squares fit of Table 4.

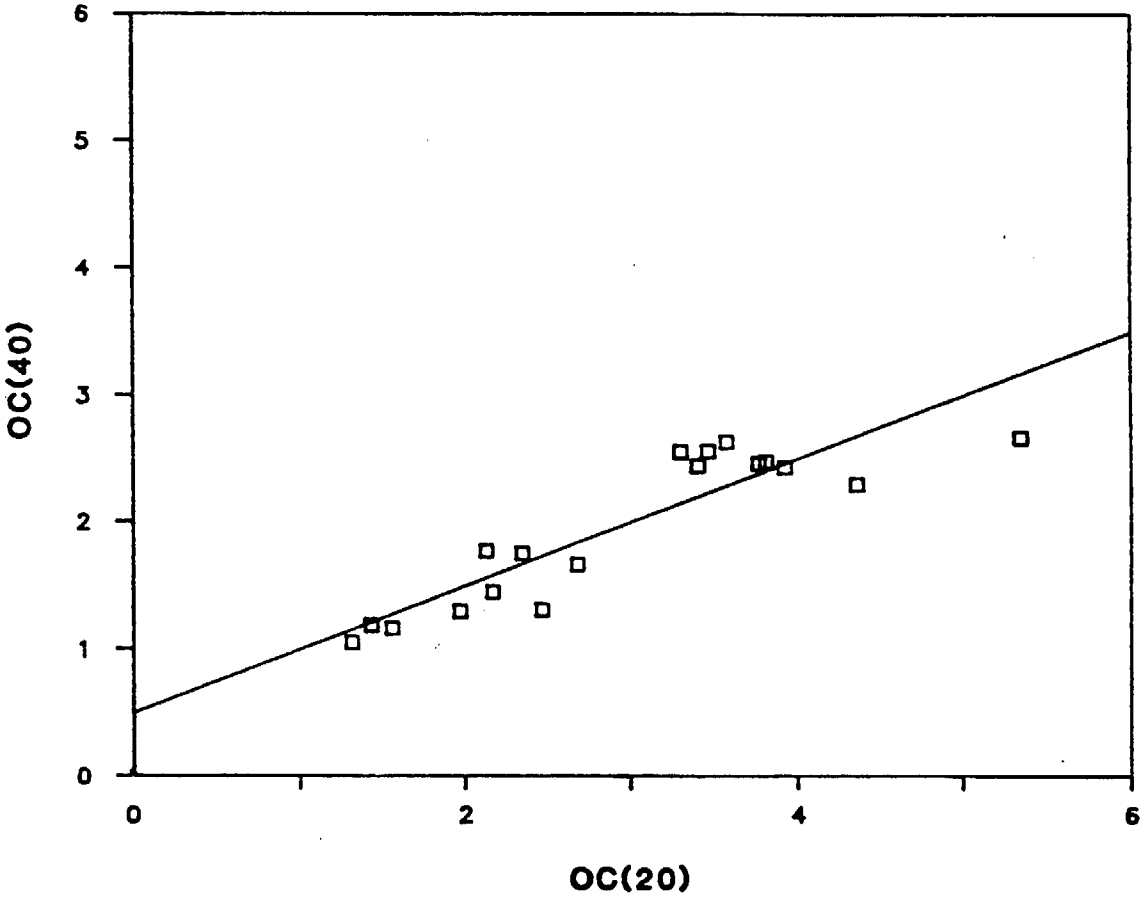

Figure 21. Comparison of organic carbon concentrations ($\mu gC/m^3$) at face velocities of 20 and 40 cm/s for quartz fiber backup filters behind quartz fiber front filters. The solid line is the linear least squares fit of Table 4.

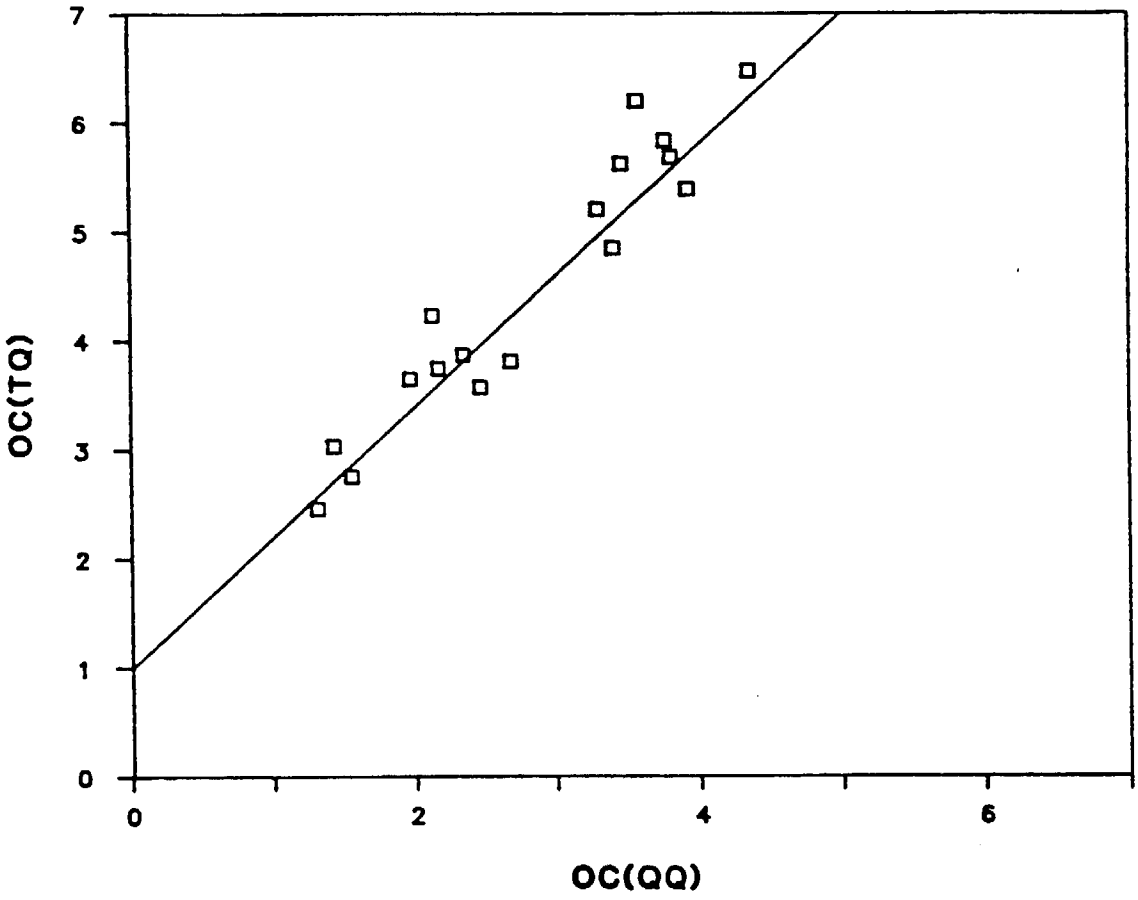

Figure 22. Comparison of organic carbon concentrations ($\mu gC/m^3$) for quartz fiber backup filters behind quartz fiber front filters and quartz fiber backup filters behind Teflon front filters at a face velocity of 20 cm/s. The solid line is the linear least squares fit of Table 4.

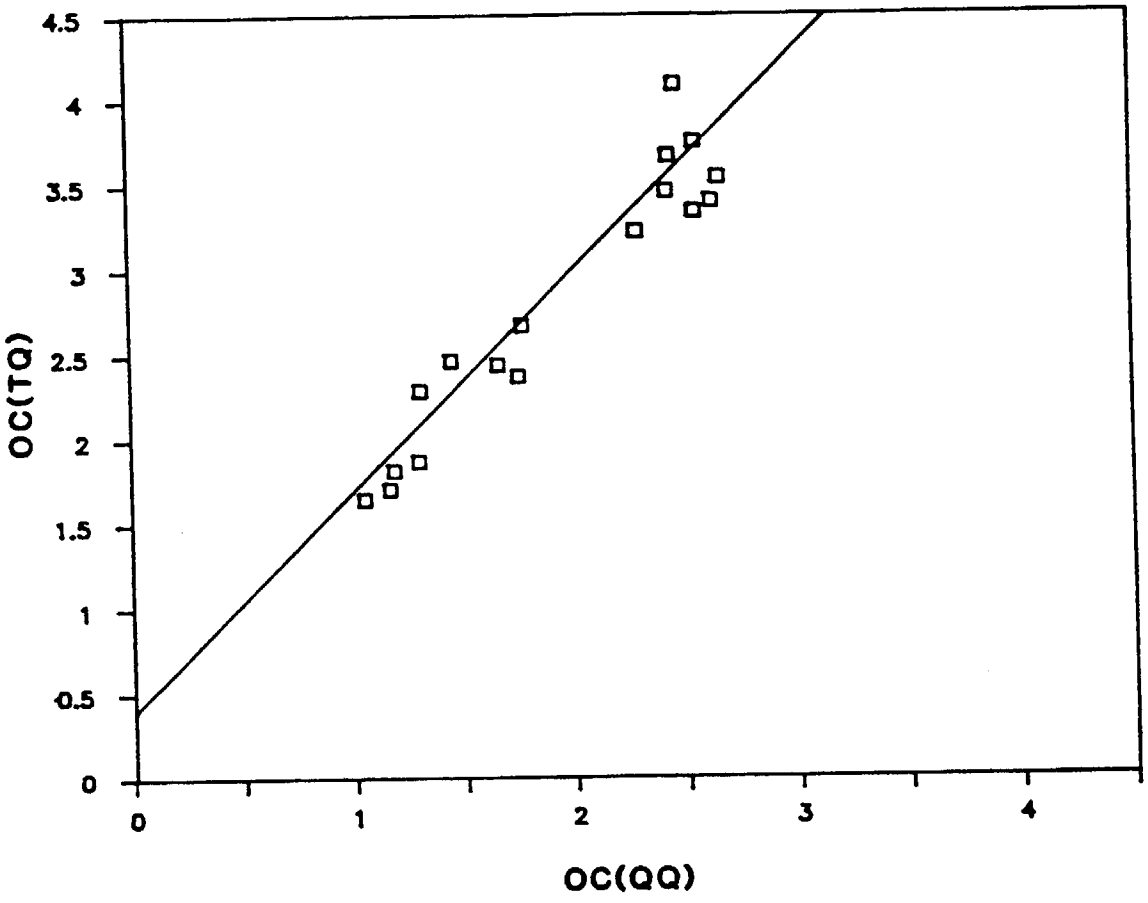

Figure 23. Comparison of organic carbon concentrations ($\mu gC/m^3$) for quartz fiber backup filters behind quartz fiber front filters and quartz fiber backup filters behind Teflon front filters at a face velocity of 40 cm/s. The solid line is the linear least squares fit of Table 4.

Table 4. REGRESSION RESULTS FOR COMPARISON OF FACE VELOCITY SAMPLER BACKUP FILTERS.

The percentage of the variance explained by the regression of Y on 1 predictor in X is given by R^2. The ratio is mean value of X/mean value of Y.

$$Y = a + bX$$

X	Y	RATIO (X/Y)	R^2
TQB(20)	TQB(40)	1.6	80%
TQB(40)	TQB(80)	1.6	54%
TQB(20)	TQB(80)	2.5	73%
QQB(20)	QQB(40)	1.5	80%
QQB(20)	TQB(20)	0.6	92%
QQB(40)	TQB(40)	0.7	90%

strong diurnal variation is apparent with the peak loadings occurring during the day. A substantial decrease in measured concentration is observed with increasing face velocity (decreasing exposed filter surface area) for both TQ and QQ backup filters. In addition, the measured concentrations of organic carbon on 40 cm/s TQ backup filters are about 1.4 times greater than the concentrations measured on QQ backup filters. QQ backup filter loading averaged 3.2 $\mu gC/cm^2$. In comparison, in McDow's (1986) Portland experiment organic carbon concentrations on TQ backup filters were a factor of 2 greater than QQ backups for an average QQ backup loading of 2.5 $\mu gC/cm^2$. This observation and the diurnal variation of backup filter concentrations are corroborated by the two-port sampler results.

Lower concentrations on QQ backups can be explained by the difference in adsorption capacities for Teflon and quartz fiber filters. The Teflon filter adsorbs little because of its low surface area. The quartz fiber filter, however, has a large surface area and adsorbs a significant amount of organic vapors, reducing the concentration of adsorbable vapors which reaches the QQ backup filter. This result suggests that the TQ backup filter provides a better estimate of the vapor adsorption artifact present on the QQ front filter. In Portland, an experiment in which one port contained a QQ and one a QTQ (Teflon filter, inserted between two quartz fiber filters) filter combination was used to determine whether contamination from the Teflon filter might be responsible for the difference between TQ and QQ backup results (McDow, 1986). Carbon loadings on the final quartz filters agreed within 0.10 $\mu gC/cm^2$, which is much lower than the differences observed on the TQ and QQ backups. An additional experiment (McDow, 1986) demonstrated that slightly more material was present on QQ backups than on TQQ final backups collected simultaneously indicating that some vapor adsorbed on the Teflon filter. Neither result can be explained by contamination from Teflon filters.

The front filter results are presented in Figures 24-26. Elemental carbon measurements are not affected by sampling artifacts and therefore provide a good quality control check. A two-sided paired t-test showed no significant difference between 20 and 40 cm/s elemental carbon

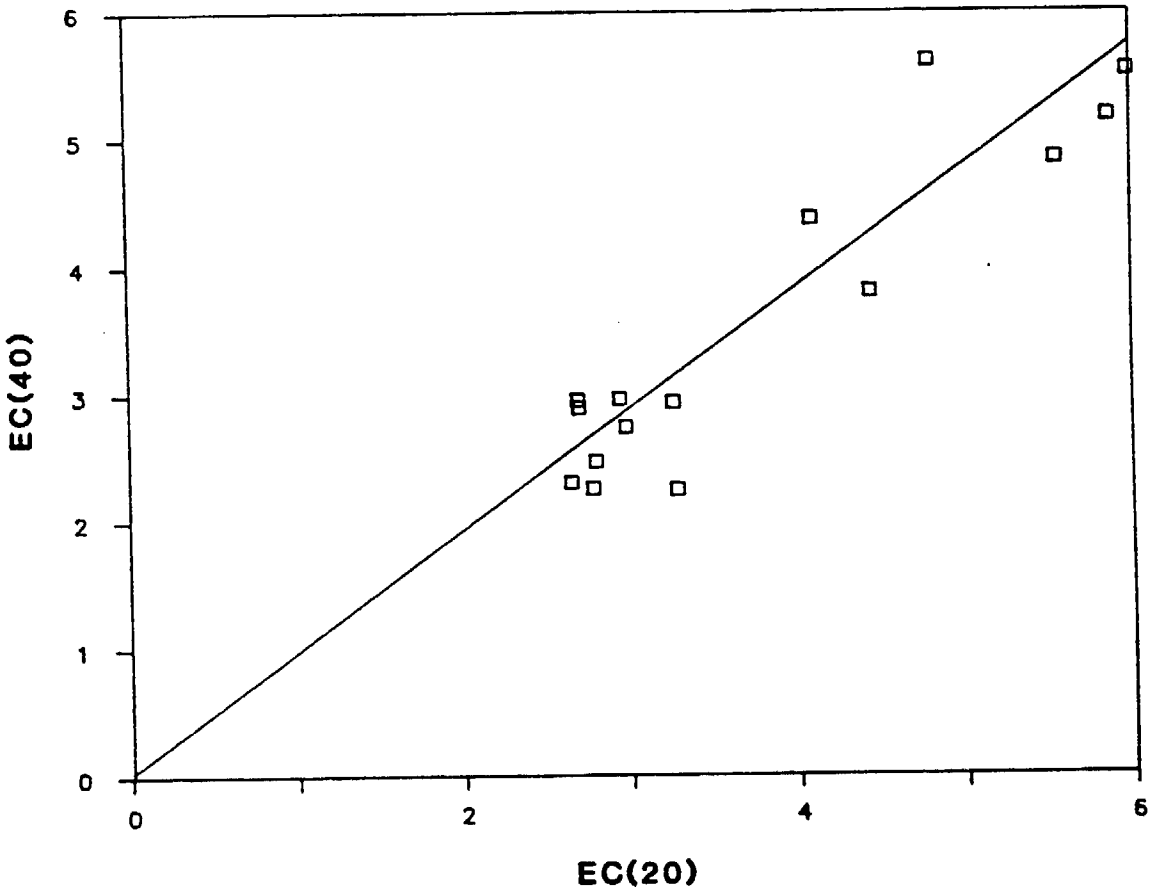

Figure 24. Comparison of elemental carbon concentrations ($\mu gC/m^3$) for quartz fiber front filters at face velocities of 20 and 40 cm/s. The solid line is the linear least squares fit of Table 5.

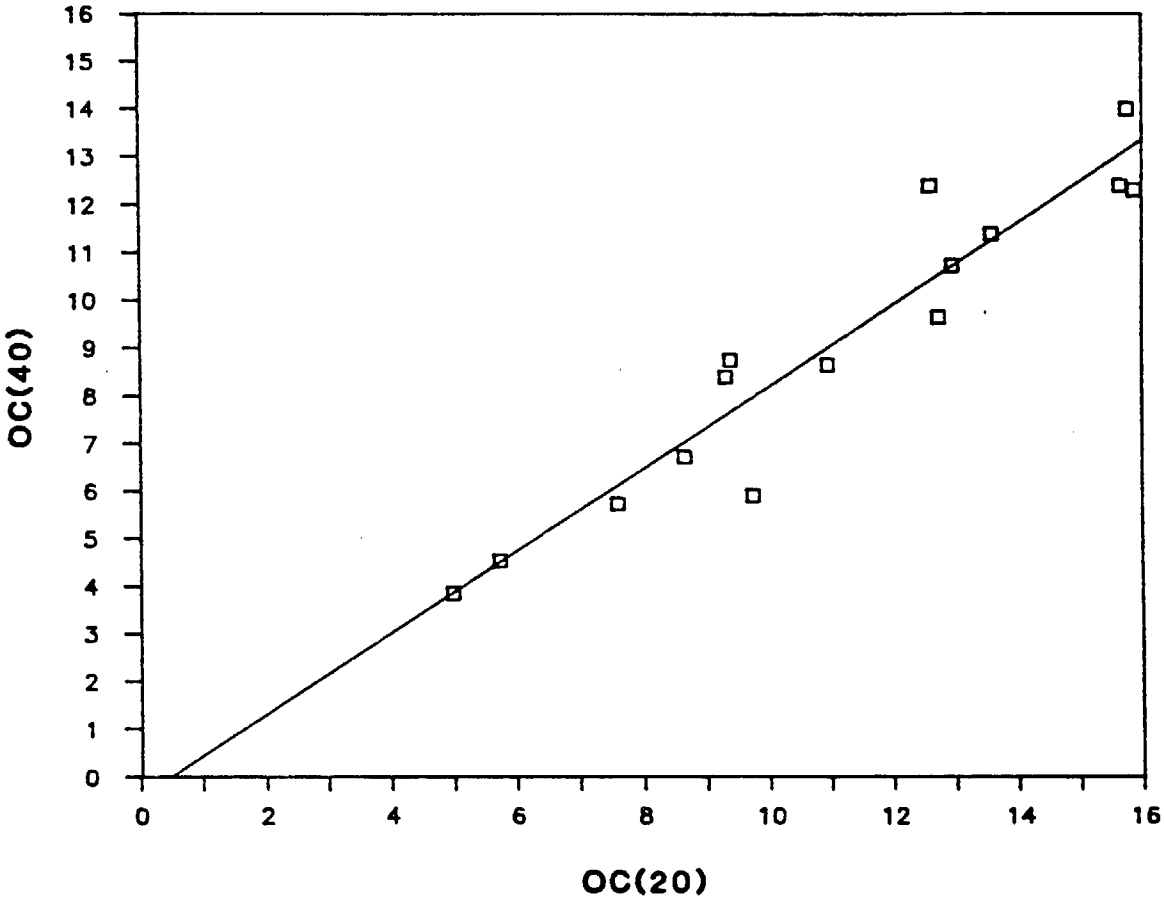

Figure 25. Comparison of organic carbon concentrations ($\mu gC/m^3$) for quartz fiber front filters at face velocities of 20 and 40 cm/s. The solid line is the linear least squares fit of Table 5.

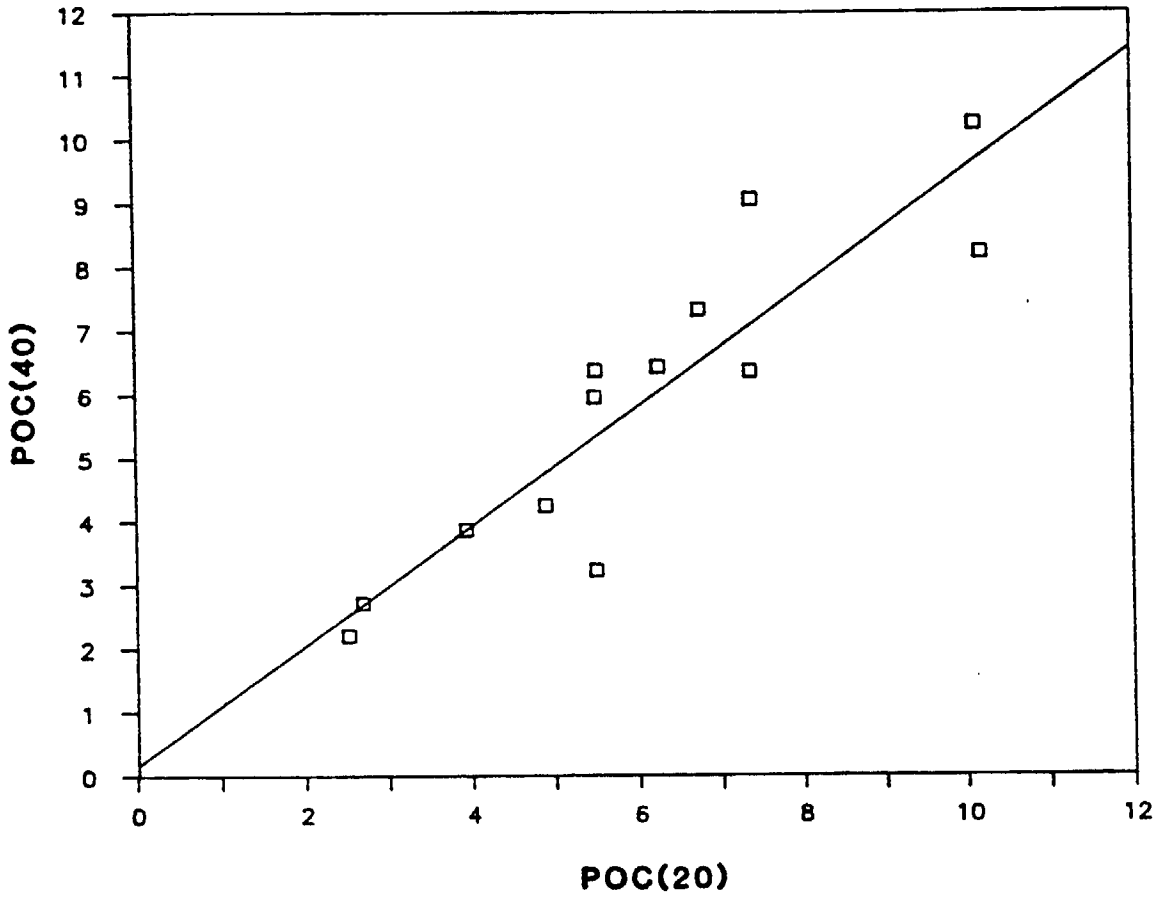

Figure 26. Comparison of "artifact corrected," particulate organic carbon concentrations (POC) ($\mu gC/m^3$) at face velocities of 20 and 40 cm/s. Correction for vapor adsorption is accomplished by subtracting the quartz fiber backup filter behind the Teflon filter from the quartz fiber front filter. The solid line is the linear least squares fit of Table 5.

concentrations at the 95% confidence level. The 20 cm/s face velocity OC values are higher than the 40 cm/s values not only at the 95 but also at the 99% confidence level as demonstrated by a single sided t-test. Linear regression results are listed in Table 5. When the measured concentrations of organic carbon on the TQ backup filters are subtracted from the corresponding apparent OC concentrations on the QQ front filters, the face velocity dependence is virtually eliminated. A two-sided t-test shows no significant difference between 20 and 40 cm/s "corrected" OC values at 95% confidence levels. These results suggest that adsorption of organic vapors is the dominant artifact in the sampling of organic aerosol.

A comparison with McDow's (1986) Portland experiments is shown in Table 6. Carbon loadings in the two experiments are comparable. The ratio of 20 to 40 cm/s uncorrected organic carbon concentrations is larger for the Glendora samples than for the Portland samples. For an average organic aerosol loading of 6 μgC/m3 at a face velocity of 40 cm/s about 30% of the organic material deposited on the filter was attributed to vapor adsorption in the Glendora experiment. This compares with 10 to 15% at the same face velocity for an average organic aerosol loading of 7 $\mu gC/m^3$ in Portland. As in the CSMCS experiments, the face velocity dependence in the Portland experiments was greatly reduced by backup filter subtraction. These results suggest that adsorbed vapor played a more significant role in the sampling of organic carbon in the conditions present during the CSMCS in Glendora, California, than in typical Portland conditions.

Taken as a whole, these ambient South Coast Air Basin results are consistent with those obtained in Portland by McDow (1986) and suggest that adsorption of organic vapors is the dominant artifact in the sampling of organic aerosol.

Table 5. REGRESSION RESULTS FOR COMPARISON OF FACE VELOCITY SAMPLER FRONT FILTERS.

Uncertainties are 95% confidence intervals. The number of samples comprising the regression is indicated by n, R^2 is the percentage of the variance explained by the regression and the ratio expressed is the ratio of mean 20 cm/s to mean 40 cm/s concentrations. A one sided t-test shows that 20 cm/s uncorrected OC concentrations are significantly larger than 40 cm/s uncorrected OC concentrations with 95% confidence ($t = 7.1$). Elemental carbon and vapor corrected organic carbon are not significantly different ($t_{EC} = 1.9$; $t_{POC} = 0.6$).

(40 cm/s) = a + b (20 cm/s)

	a	b	RATIO (20)/(40)	R^2	n
EC	0.04 ± 0.9	0.93 ± 0.2	1.07	85%	15
UNCORRECTED OC	-0.4 ± 2	0.86 ± 0.2	1.22	91%	15
CORRECTED OC	0.2 ± 2	0.94 ± 0.3	1.03	81%	13

Table 6. COMPARISON OF THE FACE VELOCITY DEPENDENCE OF CARBON LOADING FOR PORTLAND AND CSMCS GLENDORA, CALIFORNIA, EXPERIMENTS.

Ratios are of the mean 20 cm/s face velocity concentration to the mean 40 cm/s face velocity concentration. POC corresponds to particulate organic carbon which refers to the vapor-corrected concentrations. Carbon loadings in the two experiments are similar. The numbers in parenthesis for Portland are ratios of 15 cm/s face velocity concentrations to 40 cm/s concentrations.

	RATIOS OF THE MEANS	
	PORTLAND	GLENDORA (CSMCS)
EC(20)/EC(40)	0.95 (0.91)	1.07
OC(20)/OC(40)	1.09 (1.14)	1.22
POC(20)/POC(40)	(0.99)	1.03

CHAPTER 6: DILUTION SAMPLER STUDY

The two-port assembly was used as described in Chapter 4 through period "56", which ended at 2000 hr PDT 8/15/86. A third port was then added enabling the sampler to also be used to investigate the vapor artifact in an experiment of Susanne Hering's design. All ports operated at 25 l/min and large particles were removed with a 2.5 μm cut-point impactor. One port contained a TQ filter combination, and two held QQ filter combinations. In one of the two QQ ports a fraction of the input air was stripped of aerosol by drawing it through a Teflon pre-filter with a bellows pump and re-injecting it into the sample stream; these samples are designated DQQ. The experiment was designed to determine the relative importance of adsorption and volatilization artifacts in the sampling of organic aerosol. Three ports sampled with different combinations of three unknowns: adsorbed organic vapor, volatilized organic material, and organic aerosol. Thus the relative artifact contributions are solutions of the sampling matrix.

The fraction of the input air which was stripped of aerosol ($1-\beta$) is given in Table 7. The dilution experiment data are given with the two-port data in Appendix B. Elemental carbon concentrations again provide a good quality assurance check because they are not subject to sampling artifacts. When the DQQ (front filter) elemental carbon values were compared with the QQ (front filter) EC values multiplied by the fraction of unstripped air (β) entering the DQQ port (DQQ vs βQQ) good agreement was found except for Runs 66, 67, 106, and 107 (Day 6, 8/16/86 and Day 10, 8/20/86). This could have resulted from some of the dilution air escaping out the sampler inlet. Although it is possible to estimate the fraction of particle-stripped air which escaped, this was not done, and the questionable runs were excluded from the analysis.

Several scenarios for data interpretation were considered. First, if no adsorption occurred, TQ and QQ backup filters would not contain any organic carbon. This is clearly not the case. If all adsorbed organic carbon on the backup filters originated from particulate material which was collected on the front filter and subsequently volatilized and adsorbed on the backup filter, then TQ and QQ backup concentrations would

Table 7. PERCENTAGE OF INPUT AIR STRIPPED OF AEROSOL

RUN	%
57	19.3
66	19.0
67	19.7
76	20.4
77	19.6
86	39.2
87	47.4
96	48.7
97	71.2
106	72.9
107	18.7

be identical. This is also not the case. When it was assumed that volatilization is proportional to particle loading and all volatilized material from the front filter is adsorbed on the backup filter the following equations resulted:

$$QQF = P + A - V$$

$$DQQF = \beta P + A - \beta V + C$$

$$TQB = A + V$$

where P represents particulate organic carbon; A, adsorption; V, volatilization; β, the fraction of unstripped ambient air, and C the amount of organic contamination originating in the dilution system. Finally, if volatilization is the result of a pressure drop across the filter, volatilization would occur because of a drop in the concentrations of organics near the filter surface, and the rate of volatilization should be constant, other factors being equal. The following equations describe this scenario:

$$QQF = P + A - V$$

$$DQQF = \beta P + A - V + C$$

$$TQB = A + V$$

A contamination term is included in the above models because GC/MS results from DQQ backup filters showed strong phthalate peaks which were undoubtedly associated with contamination. The source of the contamination is not known but is most likely the bellows pump or some other component of the dilution system. The degree of contamination on the DQQ front filter can be estimated by comparing DQQ and QQ backup filters. These filters are exposed to the same concentration of organic vapor assuming that (1) redistribution between vapor and particulate phases between the dilution sampler inlet and the front filter is small; and (2) volatilization of particulate material from the front filter is small. The difference in DQQ and QQ backup filter organic carbon loadings was 1.5 $\mu gC/cm^2$ on average. Because the first quartz fiber filter in a QQ or DQQ pair depletes the air of adsorbable vapor, this difference is a lower limit. An upper limit can be obtained by multiplying this estimate by the ratio TQB/QQB. This yields an average upper limit contamination estimate of 2.0 $\mu gC/cm^2$ or 15% on the DQQ front filter.

Table 8 describes the average adsorbed organic vapor, volatilized organic material and particulate organic material from solutions of the sampling matrix. Solutions are given for cases where volatilization was assumed to be proportional to particle loading and where a constant rate of volatilization was assumed, using use both upper and lower limit contamination estimates. Adsorbed vapor comprised about 4 to 6 $\mu gC/cm^2$ of the material on the filter and particulate organic carbon accounted for about 10 to 14 $\mu gC/cm^2$ on average. In contrast, none of the volatilization estimates are significantly different from zero (as determined by a two-sided paired t-test with 95% confidence intervals).

Contamination in the dilution port has shed some uncertainty in the results of this experiment and prompted the development of a similar experiment for the Southern California Air Quality Study in 1987. However, the results are conclusive enough to verify the importance of vapor adsorption artifacts as the dominant artifacts in the sampling of organic aerosols on quartz fiber filters.

Table 8. RELATIVE ARTIFACT CONTRIBUTIONS DETERMINED FROM DILUTION EXPERIMENT

Values describe average adsorbed organic vapor (A), volatilized organic material (V) and particulate organic material (P) from solutions of the sampling matrix. Solutions are given for cases where volatilization was assumed to be proportional to particle loading and where a constant rate of volatilization was assumed. Results using upper and lower limit contamination estimates are given. The number of samples is 7. Values are filter loadings in $\mu gC/cm^2$.

VOLATILIZATION ASSUMPTION	CONTAMINATION ESTIMATE LOWER LIMIT	UPPER LIMIT
PROPORTIONAL TO LOADING	A = 6.2 V = -1.3 P = 9.9	A = 5.7 V = -0.8 P = 10.9
CONSTANT RATE	A = 4.8 V = 0.1 P = 12.7	A = 4.3 V = 0.6 P = 13.7

CHAPTER 7: GC/MS STUDY OF ORGANIC COMPOUNDS ON AEROSOL AND BACKUP FILTERS

The quartz fiber filters from the two-port sampler were also analyzed for specific organic compounds using thermal desorption/gas chromatography/mass spectroscopy (TD/GC/MS). This technique is an adaptation of a method (adsorption/thermal desorption) developed by Pankow and collaborators (Pankow and Isabelle, 1982) at OGC for organic analysis of rain samples. Samples are thermally desorbed onto a 25 m long, 0.32 mm diameter fused silica capillary column with a 0.25μm film thickness (Chrompack CP-SIL 8 CB) mounted in an HP 5790 gas chromatograph. The gas chromatograph is interfaced to a Finnigan 4000 mass spectrometer/data system as described by Pankow and Isabelle (1984).

In the analysis procedure, a 1 - 1.5 cm^2 section of the filter sample was placed in the desorption apparatus and an internal standard was injected onto the filter. The desorber was purged with He at a rate of 5 ml/min for 5 min to remove solvent from the internal standard and ambient O_2 from the system. Filters were desorbed at 250 C for 20 min at a pressure of 30 psi, and target compounds were trapped at the head of the column by maintaining an oven temperature of -80 C. When desorption was complete, the GC oven was heated from -10 C to 320 C at a rate of 10 C/min. Mass spectra were obtained by scanning from 50 - 450 amu at 0.5 s/scan with an electron energy of 70 eV and the electron multiplier at 1300 V.

A calibration curve for each of the 119 target compounds was obtained by analyzing standards containing each compound in concentrations of 5, 20 and 50 ng/μl. These data were used to determine compound retention times and response factors. All three levels of standards were analyzed daily as a quality assurance measure. Positive identification was assigned only when the GC relative retention times and mass spectra matched that of the standards.

The filter samples were doped with internal standards to evaluate losses in thermal desorption, determine relative retention times, and facilitate quantitative analysis. The use of internal standards was

particularly important because build-up of polar compounds at the head of the column would degrade the peak shape, requiring that the column be shortened by 0.5 m every 5 or 6 runs to avoid co-elution of normally separated compounds. The internal standards consisted of deuterated compounds from three major classes: alkanes (eicosane, D_{42}); acids and alcohols (decanoic acid, D_{19} and hexadecanoic acid, D_{31}); and polycyclic aromatic hydrocarbons (PAH's) and remaining compounds (naphthalene, D_8; acenaphthylene, D_{10}; fluorene, D_{10}; benzophenone, D_{10}; phenanthrene, D_{10}; fluoranthene, D_{10}; chrysene, D_{12}; and perylene, D_{12}).

Average concentrations for the front (QQF) and backup (QQB) filters of the QQ combination and for the backup filter (TQB) of the TQ combination are presented in Appendix E. Because of time constraints only a limited amount of exploratory data analysis was performed on the GC/MS data set.

Large concentrations of carboxylic acids were found on both front and backup filters and were present mostly as hexadecanoic, octadecanoic, and tetradecanoic acid. The lower vapor pressure acids (dodecanoic - octadecanoic) showed a substantial difference between day and night concentrations with elevated concentrations occurring during the day on both front and backup filters. This is consistent with the suggested photochemical origin of these compounds. One compound, hexadecanoic acid, was examined in more detail. A single-sided paired t-test comparing hexadecanoic acid concentrations found on QQ front and TQ backup filters indicated that QQ front filter concentrations were significantly larger with 95% confidence. The ratio of the means is about 1.6 indicating that hexadecanoic acid is present in significant quantities in particulate form. This suggests at least some secondary organic aerosol formation during the CSMCS. Due to a large variation in the means, TQB and QQB results are not significantly different but the ratio of their means is 2.7. Thus no decisive conclusions can be made regarding adsorption of hexadecanoic acid on quartz filters.

PAH's were found almost entirely on the front filter, with a ratio of mean QQF to mean QQB of 12.1. A comparison of QQ front and backup filter averages with TQ backup filter averages for the three major compound classes of interest is given in Table 9. Ratios listed in Table

Table 9. COMPARISON OF QQ FRONT AND BACKUP FILTERS WITH TQ BACKUPS FOR THE MAJOR COMPOUND CLASSES.

Values are in ng/m^3. Periods for which there were no TQB results are excluded from the analysis.

	QQF	QQB	TQB	QQF/TQB	TQB/QQB
CARBOXYLIC ACIDS	163	43	75	2.2	1.8
PAH's AND ALKYL PAH's	6.7	0.6	1.8	3.6	3.1
ALKANES	58	11	13	4.4	1.1

9 are from QQF, QQB and TQB averages which exclude sample periods where TQ backups were missing. Theory predicts that vapor/particle partitioning is a function of vapor pressure (Junge, 1977). Quartz fiber filters absorb only a portion of the material present in the vapor phase. The mean concentration of PAH's on the TQ backups was substantially higher than the mean concentration on the QQ backups, suggesting that vapor phase PAH's adsorb readily on quartz fiber filters. However, the large QQF/QQB ratio and QQF/TQB ratio indicates that most of the material on the filter is in particulate form. The PAH's included as target compounds span a wide range of vapor pressures (Ligocki, 1986).

The dominant alkanes identified were tetracosane through nonacosane (C_{24} - C_{29}). As was the case for the PAH's, the QQ front filter alkane concentrations are much higher than the TQ backup filter concentrations, indicating that a substantial fraction of the material on the filter is in particulate form. However, little difference is seen between TQ and QQ backup filter concentrations indicating that the capacity for adsorption on quartz fiber filters is minimal. One compound, tetracosane, was examined in more detail. Results of paired t-tests comparing QQF and TQB concentrations and comparing TQB and QQB concentrations agreed with the general conclusions above (QQF > TQB with 95% confidence but TQB and QQB are not significantly different). For tetracosane, QQF/TQB and TQB/QQB ratios are 4.1 and 1.1 respectively. In Table 10 QQ front (QQF)and TQ backup (TQB) filter results are averaged over all sampling periods for each alkane identified and the QQF/TQB ratio is presented. Concentrations of pentadecane through heneicosane (C_{15} - C_{21}) are often below detection limits based on analysis of filter blanks. The QQF/TQB ratio increased as a function of carbon number for docosane through heptacosane (C_{22} - C_{27}) indicating an increasing particulate phase with decreasing vapor pressure. However, the ratio declines between C_{27} and C_{29}. A desorption temperature of 250 C might be insufficient to efficiently remove these higher molecular weight compounds from the filter. Tricosane through nonacosane exhibited a diurnal variation on the QQ front filter with higher concentrations occurring at night. The reason for this is not well understood.

Table 10. AVERAGES FOR ALKANES: QQF, TQB, AND QQF/TQB (ng/m^3)

Carbon No.	Compound	QQF	TQB	QQF/TQB
C15	pentadecane	0.238	0.176	1.35
C16	hexadecane	0.75	0.74	1.01
C17	heptadecane	0.015	0.25	0.06
C18	octadecane	0.427	1.11	0.38
C19	nonadecane	1.156	1.283	0.90
C20	eicosane	0.45	0.883	0.52
C21	heneicosane	0.917	1.194	0.77
C22	docosane	2.253	1.844	1.22
C23	tricosane	5.501	1.502	3.66
C24	tetracosane	10.131	2.495	4.06
C25	pentacosane	10.984	1.761	6.24
C26	hexacosane	7.703	0.655	11.76
C27	heptacosane	6.736	0.535	12.59
C28	octacosane	8.791	0.792	11.10
C29	nonacosane	8.433	1.172	7.20

A great deal of information can be derived from this expansive collection of data. This data set could contain valuable insights into sampling artifact and aerosol formation questions, and therefore an investigative analysis will continue.

CHAPTER 8: OTHER EXPERIMENTAL RESULTS

Adsorbed vapor: saturation

A laboratory experiment was conducted in which a relatively constant concentration of organic vapor in air with a low aerosol content was sampled by the in situ carbon analyzer with varying collection times. Air from a pure air generator (AADCO 737) flowed into a sampling chamber at a flow rate of 22 l/min where it was sampled by aerosol and vapor side sampling inlets of the in situ carbon analyzer. On the vapor side a Teflon pre-filter removes all particles so that only adsorbed vapor is collected on the quartz fiber sampling filter whereas on the aerosol side, both aerosol and adsorbed vapor is collected on the quartz fiber sampling filter. Aerosol concentrations are determined by subtracting the vapor side result from the aerosol side result. The "clean air" generator provided a only a moderately constant source with aerosol concentrations which varied from 4.5 to 8.5 $\mu gC/m^3$. Despite the variation, the results clearly indicate a trend towards saturation of vapor adsorption sites as collection time increases.

The results of the 8 run experiment are presented as mass loading vs collection time in Figure 27 with an expanded view of vapor loadings in Figure 28. The excellent correlation between aerosol loading and collection time (R^2 = 98.9%), expressed by the linear regression results in Table 11, demonstrates that source variability did not influence the results. Aerosol collection doubles with doubling of collection time while the marginal increase in vapor loading diminishes with increased sampling duration. Increases in vapor loading become insignificant for collection times longer than 200 minutes and the loadings approach a steady state of about 4 μgC on the 1.5 cm diameter double filter. This result suggests that longer sampling durations will reduce the percentage of collected organic material which is adsorbed vapor and that with long enough collection time vapor adsorption will approach filter site saturation.

Saturation phenomena were not observed in the CSMCS data. The mass of adsorbed vapor per cm^2 of filter is plotted as a function of particulate organic carbon loading ($\mu gC/cm^2$) for the two-port, in situ

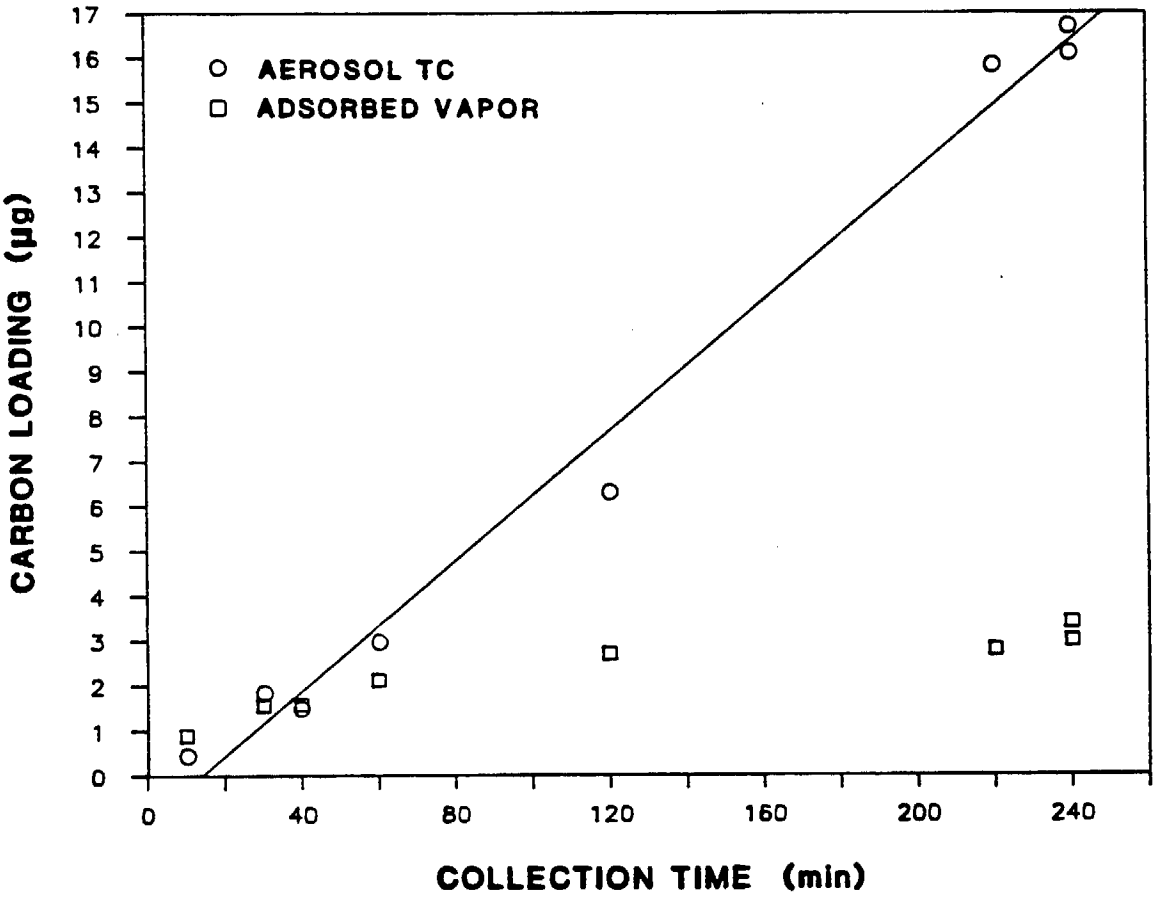

Figure 27. Aerosol total carbon and adsorbed vapor loadings (µg) as a function of collection time (min) in laboratory vapor saturation experiment. The filter area is 1.77 cm^2. The solid line is the linear least squares fit for aerosol total carbon of Table 11.

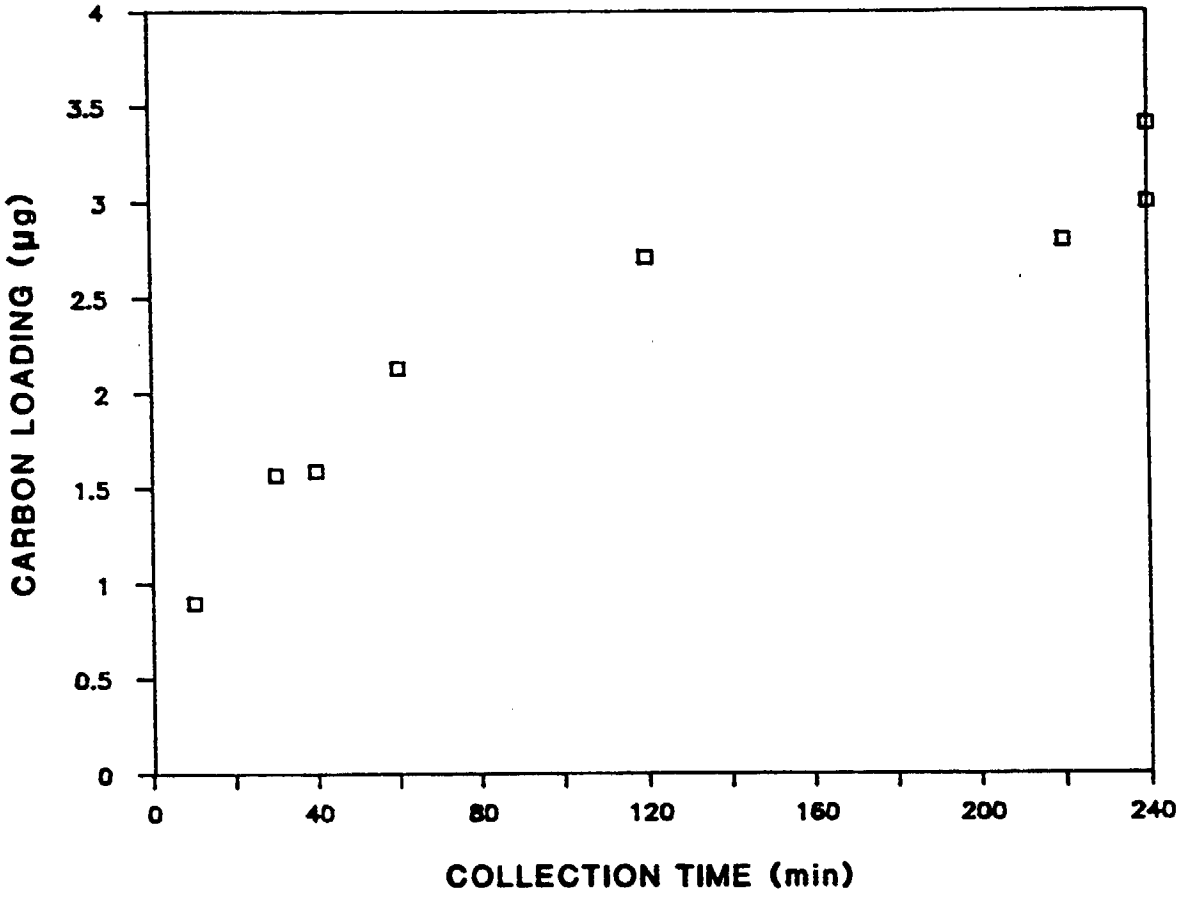

Figure 28. Expanded view of adsorbed vapor loading (µg) as a function of collection time (min) in laboratory vapor saturation experiment. The filter area is 1.77 cm^2.

Table 11. REGRESSION RESULTS FOR THE LABORATORY VAPOR ARTIFACT EXPERIMENT: AEROSOL LOADING (μg) AS A FUNCTION OF COLLECTION TIME (min).

Uncertainties are 95% confidence intervals. The number of samples comprising the regression is indicated by n, and R^2 is the percentage of the variance explained by the regression.

(AEROSOL TC) = a + b (COLLECTION TIME)

	a	b	R^2	n
LINEAR REGRESSION	-1.0 ± 1.2	0.07 ± 0.008	99%	8

and face velocity samples in Figures 29-32. Regressions are presented in Table 12. Since vapor adsorption is face velocity dependent, results are presented by sampler. The dependence on loading demonstrates that the filters are not saturated with adsorbed vapor.

Quality Control: Consistency Between Samplers

Consistency within individual sampling systems was considered within the context of the chapters devoted to those systems. A comparison of *in situ* aerosol data and two-port sampler data was presented in Chapter 4. The face velocity sampler operated with a particle cut point of 1.0 μm instead of the 2.5 μm cut point used in the other samplers and so aerosol carbon values could not be compared. However, 40 cm/s TQ and QQ backup concentrations from the face velocity sampler can be compared with two-port backups since the two-port sampler operated at a face velocity of 43 cm/s. The comparison is shown in Figures 33 and 34 with regression results in Table 13. A two sided paired t-test shows no significant difference between samplers for either TQ or QQ backups at the 95% confidence level. However, the agreement is better for TQ backups than QQ backups as is the least squares fit (R^2 = 90.8% for TQ and R^2 = 79.9% for QQ). The good agreement between backup filter results not only serves as a quality control check between samplers, but it also validates the use of 40 cm/s face velocity sampler TQ backup carbon concentrations to correct for vapor adsorption in two-port samples when the corresponding two-port TQ backups are not available.

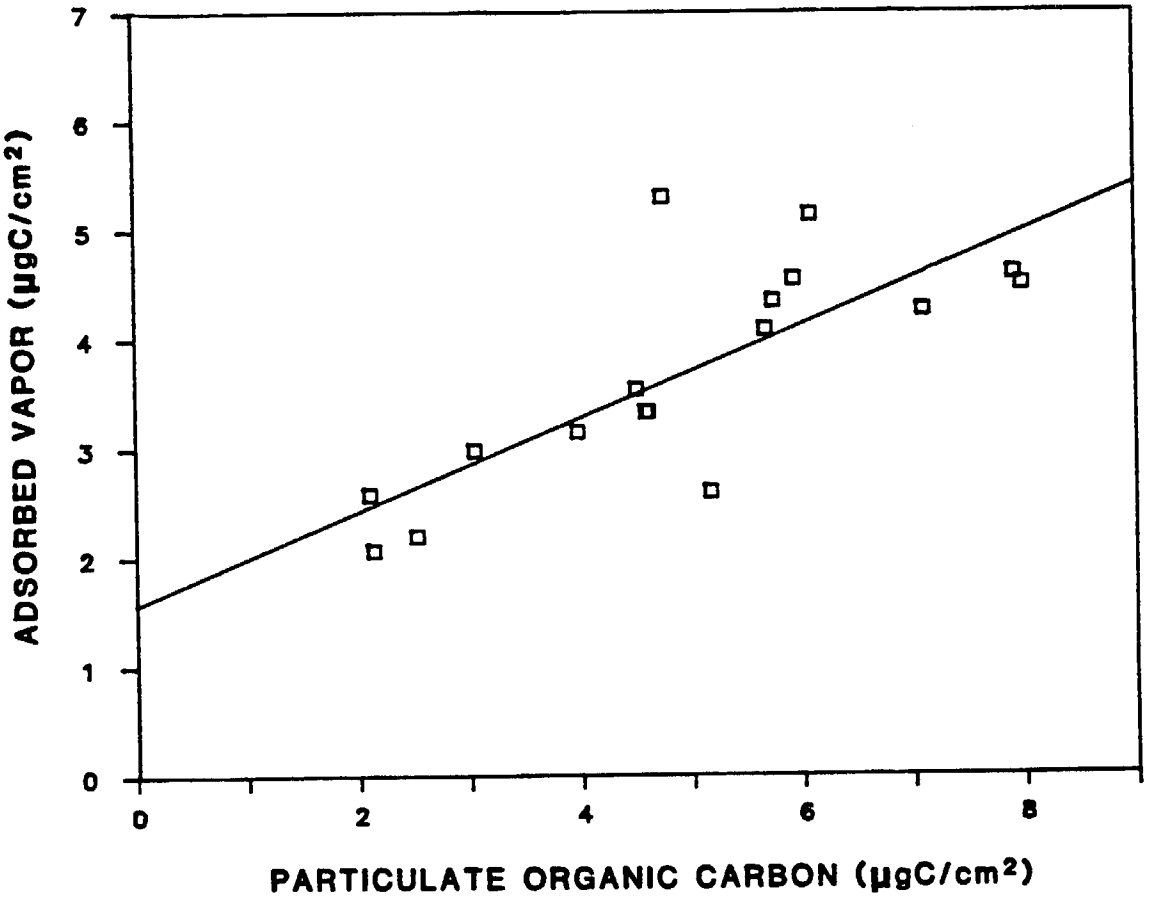

Figure 29. Adsorbed vapor as a function of particulate organic carbon loading ($\mu g/cm^2$) for 20 cm/s CSMCS face velocity samples. The solid line is the linear least squares fit of Table 12.

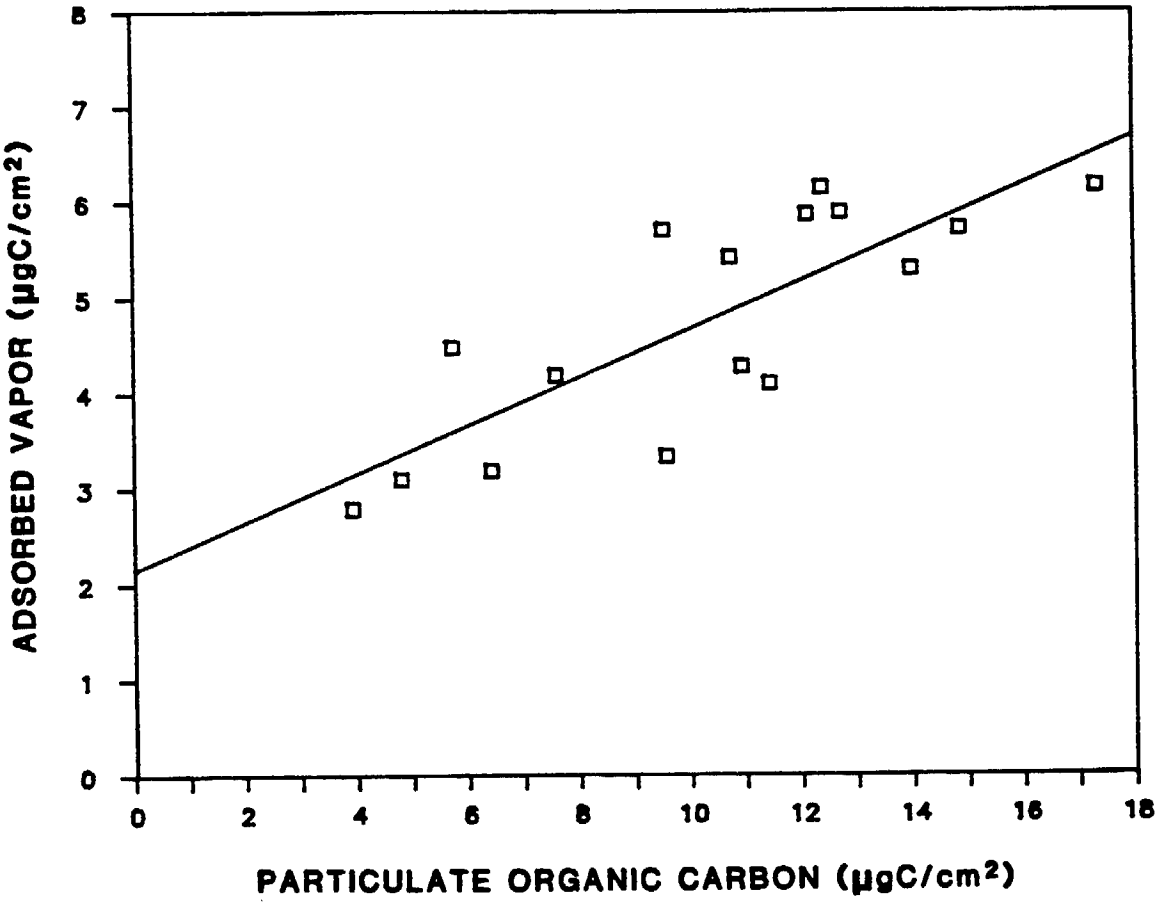

Figure 30. Adsorbed vapor as a function of particulate organic carbon loading ($\mu g/cm^2$) for 40 cm/s CSMCS face velocity samples. The solid line is the linear least squares fit of Table 12.

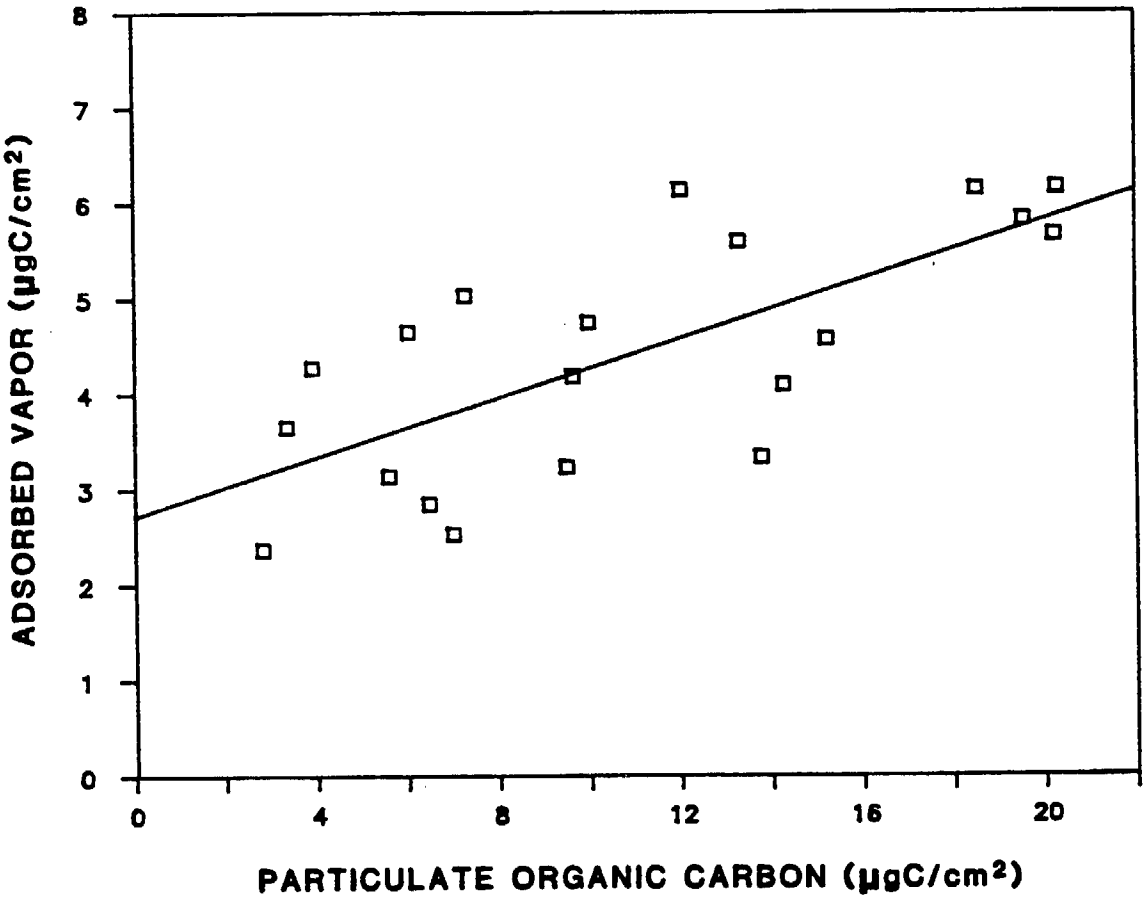

Figure 31. Adsorbed vapor as a function of particulate organic carbon loading (µg/cm^2) for CSMCS two-port samples. The solid line is the linear least squares fit of Table 12.

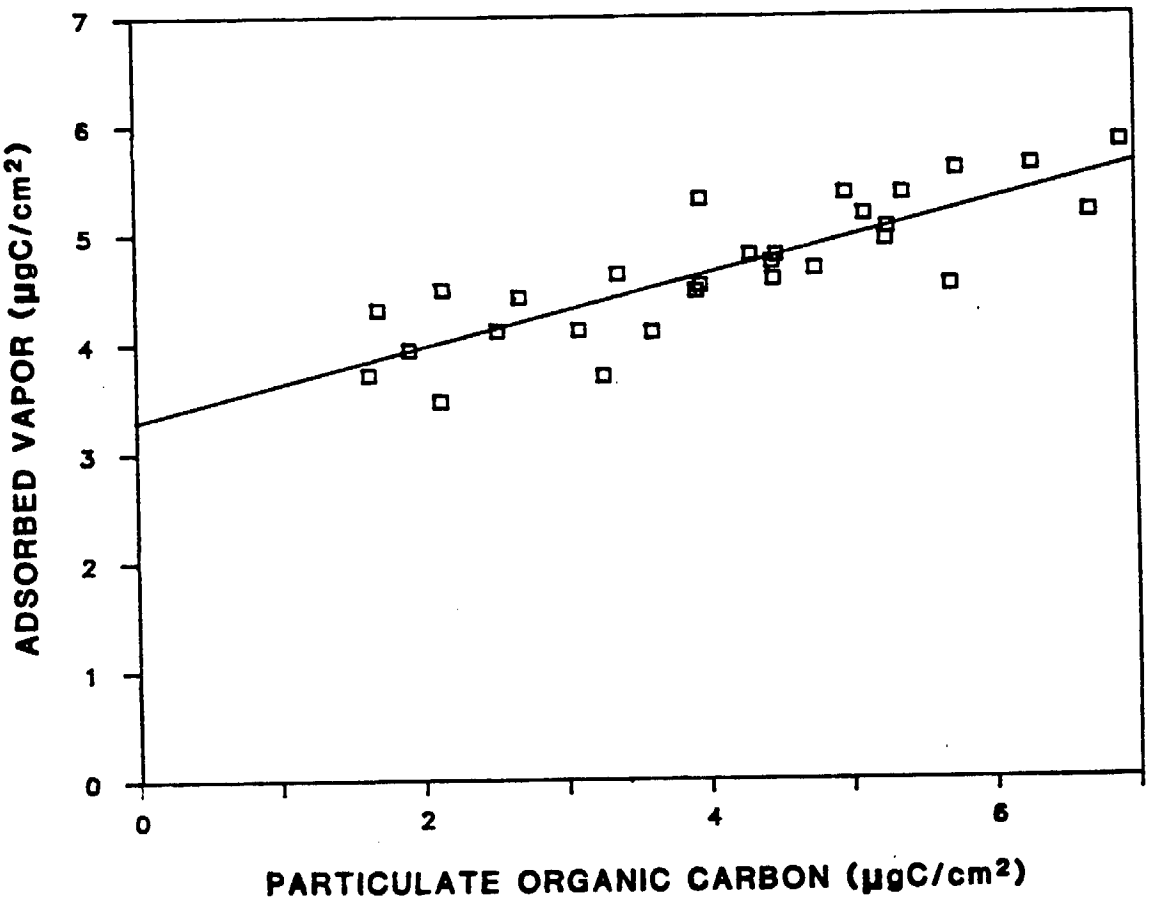

Figure 32. Adsorbed vapor as a function of particulate organic carbon loading ($\mu g/cm^2$) for CSMCS in situ carbon analyzer samples. The solid line is the linear least squares fit of Table 12.

Table 12. REGRESSION RESULTS FOR COMPARISON OF ADSORBED VAPOR AND PARTICULATE ORGANIC CARBON LOADINGS ($\mu gC/cm^2$).

Uncertainties are 95% confidence intervals. The number of samples comprising the regression is indicated by n, and R^2 is the percentage of the variance explained by the regression.

(ADSORBED VAPOR) = a + b (PARTICULATE OC)

	a	b	R^2	n
FACE VELOCITY SAMPLER 20 cm/s	1.6 ± 1.0	0.43 ± 0.2	60%	17
IN SITU SAMPLER	3.3 ± 0.4	0.34 ± 0.09	69%	29
FACE VELOCITY SAMPLER 40 cm/s	2.2 ± 1.2	0.25 ± 0.1	64%	16
TWO-PORT SAMPLER	2.7 ± 0.9	0.16 ± 0.08	51%	20

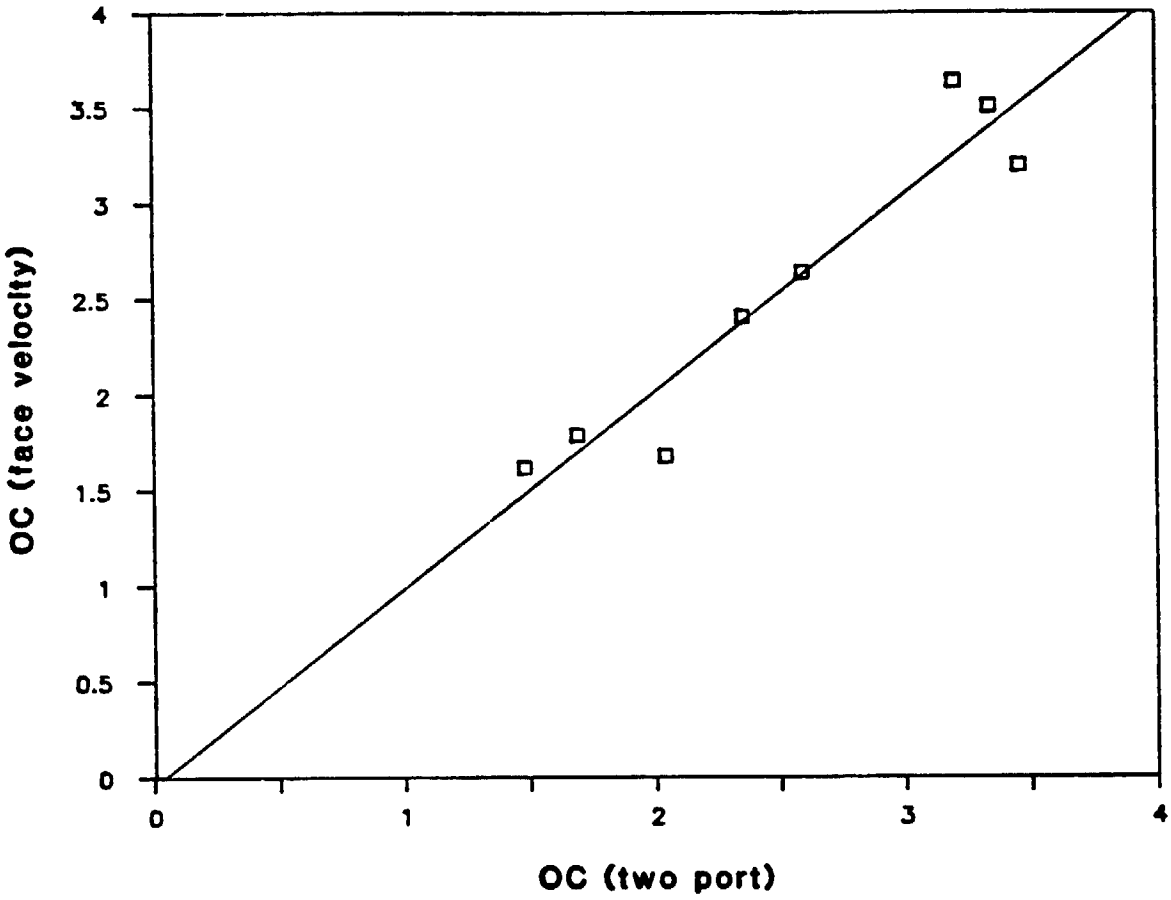

Figure 33. Comparison of quartz fiber backup filters behind Teflon front filters for two-port (43 cm/s) and 40 cm/s face velocity samples. The solid line is the linear least squares fit of Table 13.

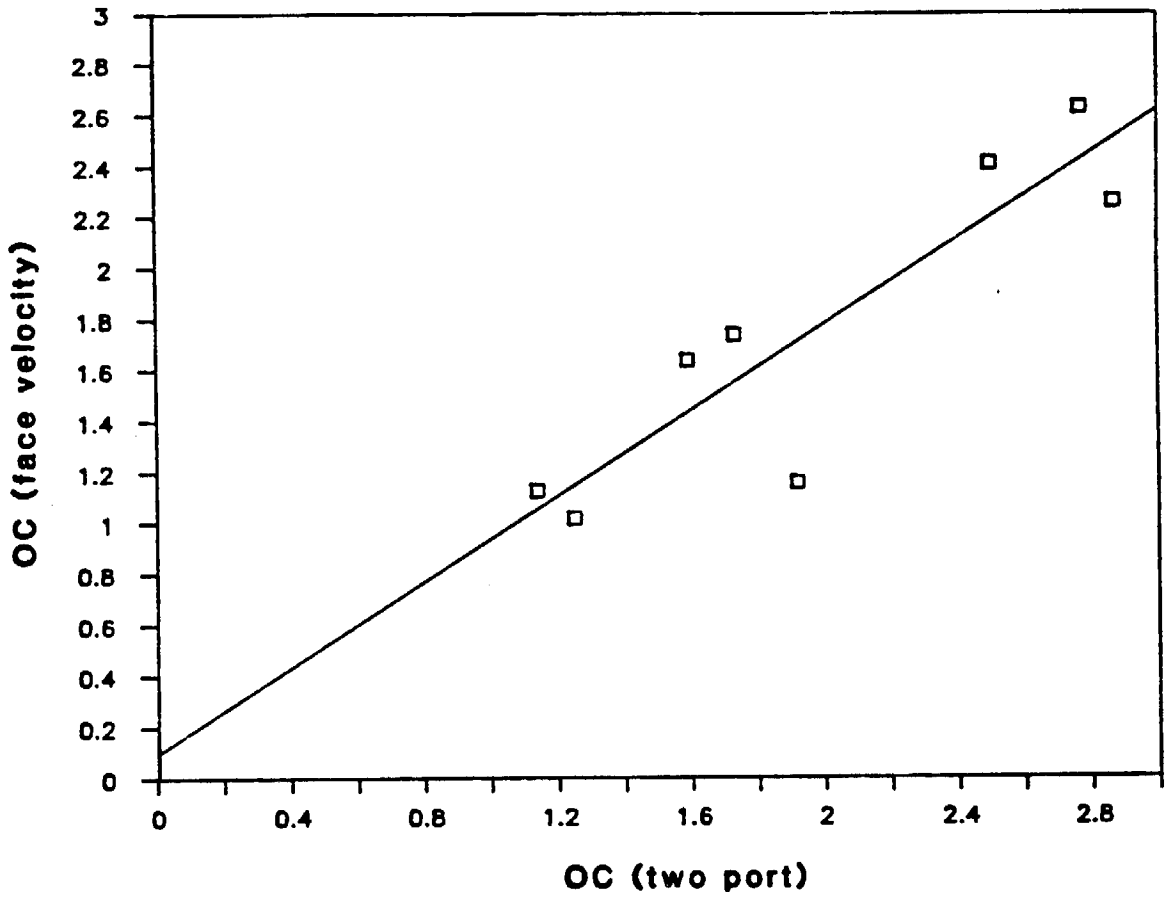

Figure 34. Comparison of quartz fiber backup filters behind quartz fiber front filters for two-port (43 cm/s) and 40 cm/s face velocity samples. The solid line is the linear least squares fit of Table 13.

Table 13. REGRESSION RESULTS FOR COMPARISON OF TWO-PORT (43 cm/s) AND FACE VELOCITY SAMPLER (40 cm/s) BACKUP FILTERS.

Uncertainties are 95% confidence intervals. The number of samples comprising the regression is indicated by n, and R^2 is the percentage of the variance explained by the regression.

(FACE VELOCITY) = a + b (TWO-PORT)

	a	b	R^2	n
TQ BACKUP - TC	-0.04 ± 0.9	1.0 ± 0.3	91%	8
QQ BACKUP - TC	0.10 ± 0.9	0.8 ± 0.4	80%	8

REFERENCES

Appel, B. R., Hoffer, E. M., Kothny, E. L., Wall, S. M., Haik, M.,and Knights, R. L. (1979). Environ. Sci. Technol. 13:98-104.

Cadle, S. H., Groblicki, P. J., and Mulawa, P. A. (1983). Atmos. Environ. 17:593-600.

Cheng, Y. S., and Yeh, H. C. (1979). Environ. Sci. Technol. 13:1392-1396.

Countess, R. J. (1988). submitted to Aerosol Sci. Technol.

Esman, N. A., Ziegler, P., and Whitfield, R. (1978). J. Aerosol Sci. 9:547-556.

Gray, H. A., Cass, G. R., Huntzicker, J. J., Heyerdahl, E. K., and Rau, J. A. (1984). Sci. Total Environ. 36:17-25.

Gundel, L. A., Dod, R. L., Rosen, H., and Novakov, T. (1984). Sci. Total Environ. 36:197-202.

Heisler, S. L., and Friedlander, S. K. (1977). Atmos. Environ. 11:157-168.

Hidy, G. M., Appel, B. R., Charlson, R. J., Clark, W., E., Friedlander, S. K., Hutchinson, D. H., Smith, T. B., Suder, J., Wesolowski, J. J., and Whitby, K. T. (1975). J. Air Poll. Control Assoc. 25:1106-1114.

Hogan, A., Ahmed, N., Black, J., and Barnard, S. (1985). J. Aerosol Sci. 16:391-397.

Huntzicker, J. J., Johnson, R. L., Shah, J. J., and Cary, R. A. (1982). In Particulate Carbon: Atmospheric Life Cycle (G. T. Wolff and R. L. Klimisch, eds.). Plenum, New York, pp. 79-88.

Johnson, R. L., Shah, J. J., Cary, R. A., and Huntzicker, J. J. (1981). In ACS Symposium Series No. 167: Atmospheric Aerosol: Source/Air Quality Relationships, (E. S. Macias and P. K. Hopke, eds.), American Chemical Society, Washington, D.C., pp. 223-233.

Junge, C. E. (1977). In Fate of Pollutants in the Air and Water Environments, (I. H. Suffet, ed.), John Wiley & Sons, New York, pp. 7-25.

Ligocki, M. P. (1986). The Scavenging of Atmospheric Trace Organic Compounds by Rain. Ph.D. Thesis, Oregon Graduate Center, Beaverton, Oregon, 97006.

Marple, V. A., and Liu, B. Y. H. (1974). Environ. Sci. Technol. 8:648-654.

Marple, V. A., and Liu, B. Y. H. (1975). J. Colloid Interface Sci. 53:31-34.

McDow, S. R. (1986). The Effect of Sampling Procedures on Organic Aerosol Measurement. Ph.D. Thesis, Oregon Graduate Center, Beaverton, OR 97006.

McMurry, P. H., and Grosjean, D. (1985). Atmos. Environ. 19:1445-1451.

Pankow, J. F., and Isabelle, L. M. (1982). J. Chromatog. 237: 25-39.

Pankow, J. F., and Isabelle, L. M. (1984). Anal. Chem. 56: 2997-2999.

Shah, J. J., Johnson, R. L., Heyerdahl, E. K., and Huntzicker, J. J. (1986). J. Air Pollution Control Assoc. 36:254-257.

Schwartz, G. P., Daisey, J. M., Lioy, P. J. (1981). Am. Ind. Hyg. Assoc. J. 42:258-263.

Turpin, B. J., Cary, R. A., and Huntzicker, J. J., An In Situ Analyzer for Organic and Elemental Carbon. Submitted to Aerosol Science and Technology, January 1988.

GLOSSARY OF SYMBOLS

b	Extinction coefficient ($cm^2/\mu g$)
n	Number of samples comprising regression
u	Fluid velocity through the jet (cm/s)
v	Kinematic viscosity of the fluid (cm^2/s)
w	Jet diameter
A	Adsorption
C	Concentration ($\mu gC/cm^2$)
I	Intensity of transmitted light for the sample
I_0	Intensity of transmitted light for the blank
P_2	Particulate organic carbon
R^2	Percentage of variance explained by the regression
V	Volatilization
$(1-\beta)$	Fraction of ambient air stripped of particles
σ	Standard deviation

GLOSSARY OF ABBREVIATIONS

i.d.	Inner diameter
pphm	Parts per hundred million
ABS	Optical absorbance
ARB	Air Resources Board
BV	Ball valve
CSMCS	Carbonaceous Species Methods Comparison Study
DQQ	Quartz fiber front filter followed by a quartz fiber backup filter in the "dilution" port
DQQB	Backup filter of a quartz-quartz filter combination in the "dilution" port
DQQF	Front filter of a quartz-quartz filter combination in the "dilution" port
EC	Elemental carbon
EC(20)	Elemental carbon loading for 20 cm/s face velocity sample
EC(40)	Elemental carbon loading for 40 cm/s face velocity sample
EMSI	Environmental Monitoring and Services, Inc.
FID	Flame ionization detector
GC/MS	Gas chromatography/mass spectrometry
OC	Organic carbon
OC(20)	Organic carbon loading for 20 cm/s face velocity sample
OC(40)	Organic carbon loading for 40 cm/s face velocity sample
OGC	Oregon Graduate Center
PAH's	Polycyclic aromatic hydrocarbons
PDT	Pacific daylight time
POC	Particulate organic carbon
POC(20)	Particulate organic carbon loading for 20 cm/s face velocity sample
POC(40)	Particulate organic carbon loading for 40 cm/s face velocity sample
QQ	Quartz fiber front filter followed by a quartz fiber backup filter
QQB	Backup filter of a quartz-quartz filter combination

GLOSSARY OF ABBREVIATIONS (cont.)

QQB(20)	QQ backup collected at a face velocity of 20 cm/s
QQB(40)	QQ backup collected at a face velocity of 40 cm/s
QQF	Front filter of a quartz-quartz filter combination
QTQ	Teflon filter inserted between two quartz fiber filters
SCAQS	Southern California Air Quality Study
SV	Solenoid valve
TC	Total carbon
TOC	Total organic carbon (particulate & adsorbed vapor)
TQ	Teflon front filter followed by quartz fiber backup filter
TQB	Backup filter of a Teflon-quartz filter combination
TQB(20)	TQ backup collected at a face velocity of 20 cm/s
TQB(40)	TQ backup collected at a face velocity of 40 cm/s
TQB(80)	TQ backup collected at a face velocity of 80 cm/s
TQQ	Teflon filter followed by two quartz fiber filters
μgC	μg of carbon

APPENDIX A: ROUND ROBIN SAMPLES

Table A.1. FILTER SAMPLES

SAMPLE I.D.	TOTAL CARBON LOADING $\mu gC/cm^2$	TOTAL CARBON ERROR $\mu gC/cm^2$	ORGANIC CARBON LOADING $\mu gC/cm^2$	ORGANIC CARBON ERROR $\mu gC/cm^2$	ELEMENTAL CARBON LOADING $\mu gC/cm^2$	ELEMENTAL CARBON ERROR $\mu gC/cm^2$
Y01-20	41.2	2.9	30.7	2.6	10.4	0.7
Y02-11	27.3	1.9	20.0	1.7	7.3	0.5
Y03-07	26.6	1.9	21.3	1.8	5.3	0.4
Y04-20	32.4	2.3	25.1	2.1	7.4	0.5
Y05-18	27.7	1.9	20.7	1.7	7.0	0.5
Y06-18	35.4	2.5	27.1	2.3	8.3	0.6
Y07-06	35.7	2.5	9.0	0.8	26.7	1.8
Y08-26	29.7	2.1	21.9	1.8	7.8	0.5
Y09-03	3.4	0.2	3.4	0.3	.0	0.1
Y10-07	36.7	2.6	25.9	2.2	10.8	0.7
Y11-06	123.3	8.6	41.2	18.8	82.1	19.3
Y12-06	18.4	1.3	6.3	0.5	12.1	0.8
Y13-06	101.8	7.1	75.2	6.3	26.6	1.8
Y14-28	31.2	2.2	23.9	2.0	7.3	0.5
Y15-06	397.3	27.8	302.6	25.4	94.7	6.5
Y16-30	41.8	2.9	30.7	2.6	11.1	0.8
Y17-07	38.4	2.7	29.3	2.5	9.0	0.6
Y18-08	71.7	5.0	48.9	4.1	22.8	1.6
Y19-06	10.1	0.7	10.1	0.9	.0	0.1
Y20-29	37.3	2.6	28.2	2.4	9.1	0.6

Table A.2. SOLID SAMPLES

SAMPLE I.D.	TOTAL CARBON $\mu gC/\mu g$ SAMPLE LOADING	TOTAL CARBON $\mu gC/\mu g$ SAMPLE ERROR	ORGANIC CARBON $\mu gC/\mu g$ SAMPLE LOADING	ORGANIC CARBON $\mu gC/\mu g$ SAMPLE ERROR	ELEMENTAL CARBON $\mu gC/\mu g$ SAMPLE LOADING	ELEMENTAL CARBON $\mu gC/\mu g$ SAMPLE ERROR
Y21	0.20		0.15		0.056	
Y22	0.049		0.049		0.00	
Y23	0.11		0.086		0.021	

APPENDIX B: TWO-PORT SAMPLER DATA

Table B.1. PARTICULATE CARBON CONCENTRATIONS

SAMPLING PERIOD	START TIME PDT	STOP TIME PDT	PARTICULATE TOTAL CARBON $\mu gC/m^3$	error	PARTICULATE ORGANIC CARBON $\mu gC/m^3$	error	PARTICULATE ELEMENTAL CARBON $\mu gC/m^3$	error
21	08:00	12:00	18.2	1.3	10.3	1.0	8.0	0.6
22	12:00	16:00	17.1	1.3	11.8	1.0	5.3	0.4
23	16:00	20:00	10.0	0.9	6.5	0.8	3.5	0.3
24	20:00	24:00	9.1	0.7	5.2	0.5	3.9	0.3
25	24:00	08:00	9.0	0.5	4.4	0.3	4.6	0.3
31	08:00	12:00	15.2	1.2	8.1	0.9	7.1	0.5
32	12:00	16:00					4.6	0.3
33	16:00	20:00					4.7	0.4
37	20:00	08:00	8.9	0.5	5.2	0.3	3.7	0.3
46*	08:00	20:00	17.8	1.0	12.3	0.7	5.4	0.4
47	20:00	08:00	6.7	0.4	3.5	0.3	3.2	0.2
56	08:00	20:00	16.8	0.9	11.7	0.7	5.1	0.4
57	20:00	08:00	7.0	0.4	3.9	0.3	3.2	0.2
66*	08:00	20:00	14.7	0.9	11.5	0.8	3.2	0.2
67*	20:00	08:00	9.7	0.6	7.1	0.4	2.6	0.2
76*	08:00	20:00	15.2	0.9	12.0	0.7	3.3	0.2
77*	20:00	08:00	7.9	0.5	5.2	0.4	2.7	0.2
86	08:00	20:00	11.6	0.7	6.7	0.5	4.9	0.4
87	20:00	08:00	8.2	0.5	5.4	0.4	2.8	0.2
96*	08:00	20:00	11.3	0.7	7.4	0.5	3.9	0.3
97	20:00	08:00	11.4	0.7	7.9	0.5	3.5	0.3
106	08:00	20:00	17.1	1.0	11.3	0.7	5.8	0.4
107*	20:00	08:00	12.4	0.7	7.8	0.4	4.6	0.3

* The tag indicates runs in which the two-port TQ backup is missing and vapor correction was accomplished by subtracting the 40 cm/s TQ backup from the face velocity sampler instead. A consistency check comparing the backups from the two-port sampler (43 cm/s) with those from the 40 cm/s port of the face velocity sampler proved favorable (see chapter 8).

Table B.2. MEASURED TWO-PORT QQ FRONT FILTER CONCENTRATIONS

SAMPLING PERIOD	START TIME PDT	STOP TIME PDT	MEASURED					
			TOTAL CARBON $\mu gC/m^3$	error	ORGANIC CARBON $\mu gC/m^3$	error	ELEMENTAL CARBON $\mu gC/m^3$	error
21	08:00	12:00	25.9	1.2	17.9	0.8	8.0	0.6
22	12:00	16:00	25.0	1.2	19.7	0.8	5.3	0.4
23	16:00	20:00	16.8	0.8	13.2	0.6	3.5	0.3
24	20:00	24:00	13.0	0.6	9.1	0.4	3.9	0.3
25	24:00	08:00	11.3	0.5	6.7	0.3	4.6	0.3
31	08:00	12:00	23.6	1.1	16.5	0.7	7.1	0.5
32	12:00	16:00	21.0	1.0	16.5	0.7	4.6	0.3
33	16:00	20:00	19.7	0.9	15.0	0.6	4.7	0.4
37	20:00	08:00	10.6	0.5	6.9	0.3	3.7	0.3
46*	08:00	20:00	21.4	1.0	15.9	0.7	5.4	0.4
47	20:00	08:00	8.2	0.4	5.0	0.2	3.2	0.2
56	08:00	20:00	20.0	0.9	14.9	0.6	5.1	0.4
57	20:00	08:00	9.1	0.4	5.9	0.3	3.2	0.2
66*	08:00	20:00	18.8	0.9	15.6	0.7	3.2	0.2
67*	20:00	08:00	12.0	0.6	9.4	0.4	2.6	0.2
76*	08:00	20:00	18.9	0.9	15.7	0.7	3.3	0.2
77*	20:00	08:00	10.3	0.5	7.6	0.3	2.7	0.2
86	08:00	20:00	15.1	0.7	10.1	0.4	4.9	0.4
87	20:00	08:00	10.8	0.5	8.0	0.3	2.8	0.2
96*	08:00	20:00	14.7	0.7	10.8	0.5	3.9	0.3
97	20:00	08:00	13.8	0.6	10.2	0.4	3.5	0.3
106	08:00	20:00	20.5	0.9	14.7	0.6	5.8	0.4
107*	20:00	08:00	14.7	0.7	10.1	0.4	4.6	0.3

Table B.3. MEASURED TWO-PORT QQ BACKUP FILTER CONCENTRATIONS

SAMPLING PERIOD	START TIME PDT	STOP TIME PDT	TOTAL CARBON $\mu gC/m^3$	error
21	08:00	12:00	5.1	0.3
22	12:00	16:00	4.8	0.3
23	16:00	20:00	3.5	0.2
24	20:00	24:00	1.8	0.1
25	24:00	08:00	1.4	0.1
31	08:00	12:00	6.3	0.4
32	12:00	16:00	5.1	0.3
33	16:00	20:00	4.1	0.3
37	20:00	08:00	1.9	0.1
46	08:00	20:00	2.8	0.2
47	20:00	08:00	1.3	0.1
56	08:00	20:00	2.5	0.2
57	20:00	08:00	1.1	0.1
66	08:00	20:00	2.7	0.2
67	20:00	08:00	1.5	0.1
76	08:00	20:00	3.0	0.2
77	20:00	08:00	1.5	0.1
86	08:00	20:00	2.9	0.2
87	20:00	08:00	1.7	0.1
96	08:00	20:00	2.7	0.2
97	20:00	08:00	1.6	0.1
106	08:00	20:00	2.8	0.2
107	20:00	08:00	1.6	0.1

Table B.4. MEASURED TWO-PORT TQ BACKUP FILTER CONCENTRATIONS

SAMPLING PERIOD	START TIME PDT	STOP TIME PDT	TOTAL CARBON $\mu gC/m^3$	error
21	08:00	12:00	7.6	0.5
22	12:00	16:00	7.9	0.5
23	16:00	20:00	6.8	0.5
24	20:00	24:00	3.9	0.3
25	24:00	08:00	2.3	0.2
31	08:00	12:00	8.4	0.6
32	12:00	16:00		
33	16:00	20:00		
37	20:00	08:00	1.7	0.1
46	08:00	20:00		
47	20:00	08:00	1.5	0.1
56	08:00	20:00	3.2	0.2
57	20:00	08:00	2.0	0.1
66	08:00	20:00		
67	20:00	08:00		
76	08:00	20:00		
77	20:00	08:00		
86	08:00	20:00	3.5	0.2
87	20:00	08:00	2.6	0.2
96	08:00	20:00		
97	20:00	08:00	2.3	0.2
106	08:00	20:00	3.3	0.2
107	20:00	08:00		

Table B.5. MEASURED DILUTION PORT (DQQ) FRONT FILTER CONCENTRATIONS

SAMPLING PERIOD	START TIME PDT	STOP TIME PDT	MEASURED TOTAL CARBON $\mu gC/m^3$	error	ORGANIC CARBON $\mu gC/m^3$	error	ELEMENTAL CARBON $\mu gC/m^3$	error
57	20:00	08:00	8.0	0.4	5.5	0.2	2.6	0.2
66	08:00	20:00	17.5	0.8	14.3	0.6	3.1	0.2
67	20:00	08:00	10.5	0.5	8.2	0.4	2.3	0.2
76	08:00	20:00	16.1	0.7	13.3	0.6	2.7	0.2
77	20:00	08:00	8.2	0.4	6.0	0.3	2.2	0.2
86	08:00	20:00	11.4	0.5	8.4	0.4	3.0	0.2
87	20:00	08:00	7.3	0.3	5.8	0.3	1.5	0.1
96	08:00	20:00	11.6	0.5	9.2	0.4	2.4	0.2
97	20:00	08:00	6.7	0.3	5.5	0.2	1.2	0.1
106	08:00	20:00	12.2	0.6	9.9	0.4	2.2	0.2
107	20:00	08:00	12.4	0.6	9.1	0.4	3.3	0.2

TABLE B.6. MEASURED DILUTION PORT (DQQ) BACKUP FILTER CONCENTRATIONS

SAMPLING PERIOD	START TIME PDT	STOP TIME PDT	TOTAL CARBON $\mu gC/m^3$	error
57	20:00	08:00	2.0	0.1
66	08:00	20:00	3.7	0.2
67	20:00	08:00	2.2	0.1
76	08:00	20:00	3.5	0.2
77	20:00	08:00	1.9	0.1
86	08:00	20:00	3.9	0.3
87	20:00	08:00	2.5	0.2
96	08:00	20:00	3.8	0.3
97	20:00	08:00	2.6	0.2
106	08:00	20:00	3.9	0.3
107	20:00	08:00	2.2	0.1

APPENDIX C: IN SITU CARBON ANALYZER DATA

Table C.1. PARTICULATE CARBON VALUES AVERAGED OVER SAMPLING PERIODS

SAMPLING PERIOD	START TIME PDT	STOP TIME PDT	PARTICULATE TOTAL CARBON $\mu gC/m^3$	error	PARTICULATE ORGANIC CARBON $\mu gC/m^3$	error	PARTICULATE ELEMENTAL CARBON $\mu gC/m^3$	error
21	08:00	12:00						
22	12:00	16:00						
23	16:00	20:00	10.5	0.6				
24	20:00	00:00						
25	00:00	08:00	8.4	0.3				
31	08:00	12:00						
32	12:00	16:00						
33	16:00	20:00	17.0	0.6				
34	20:00	00:00	10.7	0.4				
35	00:00	08:00	10.3	0.4				
41	08:00	12:00	17.5	0.6				
42	12:00	16:00	17.8	0.6				
43	16:00	20:00	22.2	0.8				
44	20:00	00:00						
45	00:00	08:00	7.1	0.2				
51	08:00	12:00	16.0	0.5				
52	12:00	16:00	24.6	0.8				
53	16:00	20:00						
54	20:00	00:00	9.5	0.4				
55	00:00	08:00	9.8	0.4				
61	08:00	12:00						
62	12:00	16:00						
63	16:00	20:00	14.9	0.7				
64	20:00	00:00	8.4	0.5				
65	00:00	08:00	10.1	0.5				
71	08:00	12:00	15.7	0.6				
72	12:00	16:00	16.9	0.7				
73	16:00	20:00	12.3	0.6				
74	20:00	00:00	7.3	0.3				
75	00:00	08:00	8.5	0.4				
81	08:00	12:00	16.9	0.7	10.6	2.2	6.3	0.6
82	12:00	16:00	15.6	0.7	11.7	2.4	3.9	0.4
83	16:00	20:00						
84	20:00	00:00						
85	00:00	08:00	7.6	0.4	5.4	1.4	2.3	0.2
91	08:00	12:00	15.1	0.7	11.1	2.3	4.0	0.4
92	12:00	16:00	16.8	0.7	12.8	2.6	4.0	0.4
93	16:00	20:00	6.7	0.5	4.4	1.5	2.3	0.2
94	20:00	00:00	8.0	0.4	5.2	1.2	2.8	0.3
95	00:00	08:00	10.7	0.5	7.6	1.6	3.0	0.3
101	08:00	12:00	23.7	0.9	15.1	3.1	8.6	0.9
102	12:00	16:00	21.2	0.9	17.2	3.3	4.1	0.4
103	16:00	20:00	10.6	0.6	7.6	2.1	3.0	0.3
104	20:00	00:00	10.9	0.4	8.0	1.6	2.8	0.3
105	00:00	08:00	13.3	0.5	9.3	1.8	4.0	0.4

Table C.2a. MEASURED CARBON VALUES AVERAGED OVER SAMPLING PERIODS.
Organic and Elemental Carbon

SAMPLING PERIOD	START TIME PDT	STOP TIME PDT	MEASURED VALUES ORGANIC CARBON $\mu gC/m^3$	error	ELEMENTAL CARBON $\mu gC/m^3$	error
81	08:00	12:00	21.7	2.2	6.3	0.6
82	12:00	16:00	23.9	2.4	3.9	0.4
83	16:00	20:00				
84	20:00	00:00				
85	00:00	08:00	13.6	1.4	2.3	0.2
91	08:00	12:00	23.3	2.3	4.0	0.4
92	12:00	16:00	26.2	2.6	4.0	0.4
93	16:00	20:00	15.1	1.5	2.3	0.2
94	20:00	00:00	12.2	1.2	2.8	0.3
95	00:00	08:00	15.9	1.6	3.0	0.3
101	08:00	12:00	30.4	3.0	8.6	0.9
102	12:00	16:00	33.2	3.3	4.1	0.4
103	16:00	20:00	21.3	2.1	3.0	0.3
104	20:00	00:00	15.8	1.6	2.8	0.3
105	00:00	08:00	17.5	1.7	4.0	0.4

Table C.2b. MEASURED CARBON VALUES AVERAGED OVER SAMPLING PERIODS.
Total and Vapor Carbon

SAMPLING PERIOD	START TIME PDT	STOP TIME PDT	MEASURED VALUES — TOTAL CARBON $\mu gC/m^3$	error	VAPOR CARBON $\mu gC/m^3$	error
21	08:00	12:00				
22	12:00	16:00				
23	16:00	20:00	22.7	0.5	12.2	0.3
24	20:00	00:00				
25	00:00	08:00	13.0	0.3	4.6	0.1
31	08:00	12:00				
32	12:00	16:00				
33	16:00	20:00	26.8	0.6	9.8	0.2
34	20:00	00:00	18.5	0.4	7.8	0.2
35	00:00	08:00	17.6	0.4	7.2	0.2
41	08:00	12:00	27.1	0.6	9.6	0.2
42	12:00	16:00	27.4	0.6	9.7	0.2
43	16:00	20:00	33.6	0.7	11.4	0.3
44	20:00	00:00				
45	00:00	08:00	9.7	0.2	2.6	0.1
51	08:00	12:00	22.7	0.5	6.7	0.1
52	12:00	16:00	33.3	0.7	8.7	0.2
53	16:00	20:00				
54	20:00	00:00	15.5	0.3	6.0	0.1
55	00:00	08:00	15.1	0.3	5.2	0.1
61	08:00	12:00				
62	12:00	16:00				
63	16:00	20:00	28.5	0.6	13.6	0.3
64	20:00	00:00	19.0	0.4	10.6	0.2
65	00:00	08:00	18.7	0.4	8.6	0.2
71	08:00	12:00	27.1	0.6	11.4	0.3
72	12:00	16:00	30.0	0.7	13.1	0.3
73	16:00	20:00	25.0	0.6	12.7	0.3
74	20:00	00:00	13.7	0.3	6.4	0.1
75	00:00	08:00	14.7	0.3	6.3	0.1
81	08:00	12:00	28.0	0.6	11.2	0.2
82	12:00	16:00	27.8	0.6	12.2	0.3
83	16:00	20:00				
84	20:00	00:00				
85	00:00	08:00	15.8	0.3	8.2	0.2
91	08:00	12:00	27.3	0.6	12.3	0.3
92	12:00	16:00	30.2	0.7	13.5	0.3
93	16:00	20:00	17.5	0.4	10.8	0.2
94	20:00	00:00	15.1	0.3	7.1	0.2
95	00:00	08:00	18.9	0.4	8.2	0.2
101	08:00	12:00	39.1	0.9	15.4	0.3
102	12:00	16:00	37.2	0.8	16.0	0.4
103	16:00	20:00	24.2	0.5	13.6	0.3
104	20:00	00:00	18.6	0.4	7.8	0.2
105	00:00	08:00	21.5	0.5	8.1	0.2

Table C.3. PARTICULATE CARBON VALUES FOR INDIVIDUAL RUNS

DATE	START TIME PDT	STOP TIME PDT	PARTICULATE TOTAL CARBON $\mu gC/m^3$	error	ORGANIC CARBON $\mu gC/m^3$	error	ELEMENTAL CARBON $\mu gC/m^3$	error
08/12	16:28	17:24	10.7	0.7				
08/12	18:08	19:28	10.3	0.5				
08/12	23.58	01:18	9.4	0.4				
08/13	01:57	07:57	8.2	0.3				
08/13	13:26	15:21	20.1	0.7				
08/13	16:18	18:38	19.0	0.7				
08/13	19:17	21:37	10.4	0.4				
08/13	22:16	00:36	11.0	0.4				
08/14	01:15	03:35	9.4	0.4				
08/14	04:14	06:34	9.2	0.4				
08/14	07:13	09:33	15.8	0.6				
08/14	10:19	12:39	19.0	0.7				
08/14	13:18	15:38	17.4	0.6				
08/14	16:17	18:37	22.4	0.7				
08/14	19:18	19:41	20.6	1.0				
08/14	22:59	07:19	7.1	0.2				
08/15	08:05	10:25	13.9	0.5				
08/15	11:04	13:24	21.3	0.7				
08/15	14:04	16:23	27.0	0.8				
08/15	20:33	22:53	9.4	0.4				
08/15	23:32	01:52	9.7	0.4				
08/16	02:31	04:51	9.4	0.3				
08/16	05:30	07:50	10.4	0.4				
08/16	16:54	17:54	17.6	0.8				
08/16	18:33	19:33	12.2	0.6				
08/16	20:12	21:12	8.7	0.5				
08/16	21:59	23:19	8.2	0.5				
08/16	23:58	01:18	7.0	0.4				
08/17	01:57	03:17	10.4	0.5				
08/17	03:56	05:16	12.3	0.5				
08/17	05:55	07:15	10.3	0.4				
08/17	07:54	09:14	12.9	0.5				
08/17	09:53	11:13	17.9	0.7				
08/17	11:52	13:12	18.8	0.8				
08/17	13:51	15:11	15.4	0.7				
08/17	15:50	17:10	15.5	0.7				
08/17	17:49	19:09	9.5	0.5				
08/17	20:45	23:05	7.2	0.3				
08/17	23:44	02:04	7.7	0.4				
08/18	02:43	05:03	7.7	0.3				
08/18	05:42	08:02	10.0	0.4				
08/18	08:44	10:04	14.0	0.6	8.6	1.9	5.4	0.5
08/18	10:43	12:03	19.7	0.8	12.5	2.5	7.2	0.7
08/18	12:42	14:02	13.0	0.6	9.5	2.1	3.5	0.3
08/18	14:41	16:01	18.2	0.8	13.9	2.7	4.3	0.4
08/18	21:49	23:44	8.3	0.4	5.7	1.3	2.6	0.3

Table C.3. PARTICULATE CARBON VALUES FOR INDIVIDUAL RUNS (cont.)

DATE	START TIME PDT	STOP TIME PDT	PARTICULATE TOTAL CARBON $\mu gC/m^3$	error	PARTICULATE ORGANIC CARBON $\mu gC/m^3$	error	PARTICULATE ELEMENTAL CARBON $\mu gC/m^3$	error
08/18	00:23	02:18	5.8	0.4	3.9	1.2	1.9	0.2
08/19	02:57	04:52	6.4	0.4	4.9	1.3	1.5	0.1
08/19	05:31	07:26	10.6	0.5	7.2	1.6	3.5	0.3
08/19	08:08	09:28	14.6	0.6	10.4	2.3	4.2	0.4
08/19	10:07	11:27	15.5	0.7	11.8	2.4	3.8	0.4
08/19	12:06	13:26	15.1	0.7	11.3	2.4	3.8	0.4
08/19	14:05	15:25	18.5	0.8	14.2	2.9	4.3	0.4
08/19	16:04	17:24	6.7	0.5	4.5	1.6	2.2	0.2
08/19	18:03	19:23	6.7	0.4	4.3	1.4	2.4	0.2
08/19	20:51	23:11	8.0	0.4	5.1	1.2	2.9	0.3
08/19	23:50	02:10	8.3	0.4	6.0	1.4	2.3	0.2
08/20	02:49	05:09	9.6	0.4	7.5	1.6	2.1	0.2
08/20	05:48	08:08	14.1	0.5	9.5	1.8	4.7	0.5
08/20	08:51	10:11	26.0	1.0	15.1	3.0	10.9	1.1
08/20	10:53	11:53	21.9	0.9	15.8	3.3	6.1	0.6
08/20	12:32	13:32	25.5	1.0	20.0	3.6	5.4	0.5
08/20	14:11	15:11	18.6	0.8	15.7	3.2	2.9	0.3
08/20	15:50	16:50	11.8	0.7	8.9	2.4	2.9	0.3
08/20	17:29	18:29	9.3	0.6	6.7	2.1	2.6	0.3
08/20	19:08	20:08	11.0	0.6	7.5	2.0	3.5	0.3
08/20	20:50	23:10	10.7	0.4	7.9	1.6	2.8	0.3
08/20	23:49	02:09	13.1	0.5	10.1	1.8	3.1	0.3
08/21	02:48	05:08	11.1	0.4	7.7	1.6	3.4	0.3
08/21	05:47	08:07	15.9	0.6	10.4	1.9	5.5	0.6

Table C.4a. MEASURED CARBON VALUES FOR INDIVIDUAL RUNS. Organic and Elemental Carbon

DATE	START TIME PDT	STOP TIME PDT	MEASURED VALUES — ORGANIC CARBON $\mu gC/m^3$	error	ELEMENTAL CARBON $\mu gC/m^3$	error
08/18	08:44	10:04	18.4	1.8	5.4	0.5
08/18	10:43	12:03	25.0	2.5	7.2	0.7
08/18	12:42	14:02	20.5	2.1	3.5	0.3
08/18	14:41	16:01	27.3	2.7	4.3	0.4
08/18	21:49	23:44	13.3	1.3	2.6	0.3
08/18	00:23	02:18	12.2	1.2	1.9	0.2
08/19	02:57	04:52	13.0	1.3	1.5	0.1
08/19	05:31	07:26	15.4	1.5	3.5	0.3
08/19	08:08	09:28	22.4	2.2	4.2	0.4
08/19	10:07	11:27	24.3	2.4	3.8	0.4
08/19	12:06	13:26	24.0	2.4	3.8	0.4
08/19	14:05	15:25	28.4	2.8	4.3	0.4
08/19	16:04	17:24	16.0	1.6	2.2	0.2
08/19	18:03	19:23	14.3	1.4	2.4	0.2
08/19	20:51	23:11	12.1	1.2	2.9	0.3
08/19	23:50	02:10	14.1	1.4	2.3	0.2
08/20	02:49	05:09	15.6	1.6	2.1	0.2
08/20	05:48	08:08	18.0	1.8	4.7	0.5
08/20	08:51	10:11	29.9	3.0	10.9	1.1
08/20	10:53	11:53	32.8	3.3	6.1	0.6
08/20	12:32	13:32	36.0	3.6	5.4	0.5
08/20	14:11	15:11	31.9	3.2	2.9	0.3
08/20	15:50	16:50	23.6	2.4	2.9	0.3
08/20	17:29	18:29	20.7	2.1	2.6	0.3
08/20	19:08	20:08	19.7	2.0	3.5	0.3
08/20	20:50	23:10	15.4	1.5	2.8	0.3
08/20	23:49	02:09	17.9	1.8	3.1	0.3
08/21	02:48	05:08	15.5	1.5	3.4	0.3
08/21	05:47	08:07	19.2	1.9	5.5	0.6

Table C.4b. MEASURED CARBON VALUES FOR INDIVIDUAL RUNS. Total and Vapor Carbon

DATE	START TIME PDT	STOP TIME PDT	MEASURED VALUES — TOTAL CARBON $\mu gC/m^3$	error	VAPOR CARBON $\mu gC/m^3$	error
08/12	16:28	17:24	27.4	0.6	16.7	0.4
08/12	18:08	19:28	19.4	0.4	9.1	0.2
08/12	23:58	01:18	17.5	0.4	8.1	0.2
08/13	01:57	07:57	12.0	0.3	3.8	0.1
08/13	13:26	15:21	29.8	0.7	9.7	0.2
08/13	16:18	18:38	29.3	0.6	10.3	0.2
08/13	19:17	21:37	18.5	0.4	8.1	0.2
08/13	22:16	00:36	18.5	0.4	7.5	0.2
08/14	01:15	03:35	16.3	0.4	6.9	0.2
08/14	04:14	06:34	16.2	0.4	7.0	0.2
08/14	07:13	09:33	24.6	0.5	8.8	0.2
08/14	10:19	12:39	29.4	0.6	10.4	0.2
08/14	13:18	15:38	26.9	0.6	9.5	0.2
08/14	16:17	18:37	32.4	0.7	10.0	0.2
08/14	19:18	19:41	40.8	0.9	20.2	0.4
08/14	22:59	07:19	9.7	0.2	2.6	0.1
08/15	08:05	10:25	20.2	0.4	6.3	0.1
08/15	11:04	13:24	29.1	0.6	7.8	0.2
08/15	14:04	16:23	36.4	0.8	9.4	0.2
08/15	20:33	22:53	15.5	0.3	6.1	0.1
08/15	23:32	01:52	15.2	0.3	5.5	0.1
08/16	02:31	04:51	14.4	0.3	5.0	0.1
08/16	05:30	07:50	15.6	0.3	5.2	0.1
08/16	16:54	17:54	32.6	0.7	15.0	0.3
08/16	18:33	19:33	24.3	0.5	12.1	0.3
08/16	20:12	21:12	20.3	0.4	11.6	0.3
08/16	21:59	23:19	18.0	0.4	9.8	0.2
08/16	23:58	01:18	15.5	0.3	8.5	0.2
08/17	01:57	03:17	19.5	0.4	9.1	0.2
08/17	03:56	05:16	21.3	0.5	9.0	0.2
08/17	05:55	07:15	18.2	0.4	7.9	0.2
08/17	07:54	09:14	22.5	0.5	9.6	0.2
08/17	09:53	11:13	30.8	0.7	12.9	0.3
08/17	11:52	13:12	32.3	0.7	13.5	0.3
08/17	13:51	15:11	28.1	0.6	12.7	0.3
08/17	15:50	17:10	28.9	0.6	13.4	0.3
08/17	17:49	19:09	21.6	0.5	12.1	0.3
08/17	20:45	23:05	13.6	0.3	6.4	0.1
08/17	23:44	02:04	14.5	0.3	6.8	0.1
08/18	02:43	05:03	14.1	0.3	6.4	0.1
08/18	05:42	08:02	15.6	0.3	5.6	0.1
08/18	08:44	10:04	23.8	0.5	9.8	0.2
08/18	10:43	12:03	32.2	0.7	12.5	0.3
08/18	12:42	14:02	24.0	0.5	11.0	0.2
08/18	14:41	16:01	31.6	0.7	13.4	0.3

Table C.4b. MEASURED CARBON VALUES FOR INDIVIDUAL RUNS. Total and Vapor Carbon (cont.)

DATE	START TIME PDT	STOP TIME PDT	MEASURED VALUES — TOTAL CARBON $\mu gC/m^3$	error	VAPOR CARBON $\mu gC/m^3$	error
08/18	21:49	23:44	15.9	0.3	7.6	0.2
08/18	00:23	02:18	14.1	0.3	8.3	0.2
08/19	02:57	04:52	14.5	0.3	8.1	0.2
08/19	05:31	07:26	18.8	0.4	8.2	0.2
08/19	08:08	09:28	26.6	0.6	12.0	0.3
08/19	10:07	11:27	28.0	0.6	12.5	0.3
08/19	12:06	13:26	27.8	0.6	12.7	0.3
08/19	14:05	15:25	32.7	0.7	14.2	0.3
08/19	16:04	17:24	18.2	0.4	11.5	0.3
08/19	18:03	19:23	16.7	0.4	10.0	0.2
08/19	20:51	23:11	15.0	0.3	7.0	0.2
08/19	23:50	02:10	16.4	0.4	8.1	0.2
08/20	02:49	05:09	17.7	0.4	8.1	0.2
08/20	05:48	08:08	22.6	0.5	8.5	0.2
08/20	08:51	10:11	40.8	0.9	14.8	0.3
08/20	10:53	11:53	38.9	0.9	17.0	0.4
08/20	12:32	13:32	41.5	0.9	16.0	0.4
08/20	14:11	15:11	34.8	0.8	16.2	0.4
08/20	15:50	16:50	26.5	0.6	14.7	0.3
08/20	17:29	18:29	23.3	0.5	14.0	0.3
08/20	19:08	20:08	23.2	0.5	12.2	0.3
08/20	20:50	23:10	18.2	0.4	7.5	0.2
08/20	23:49	02:09	20.9	0.5	7.8	0.2
08/21	02:48	05:08	18.9	0.4	7.8	0.2
08/21	05:47	08:07	24.7	0.5	8.8	0.2

APPENDIX D: FACE VELOCITY SAMPLER DATA

Table D.1. PARTICULATE CARBON VALUES ESTIMATED FROM 20 cm/s FACE VELOCITY PORT

SAMPLING PERIOD	START TIME PDT	STOP TIME PDT	PARTICULATE ORGANIC CARBON $\mu gC/m^3$	error	PARTICULATE ELEMENTAL CARBON $\mu gC/m^3$	error	PARTICULATE TOTAL CARBON $\mu gC/m^3$	error
26	08:00	20:00	6.7	0.7	4.8	0.4	11.5	0.9
27	20:00	08:00	3.9	0.4	2.9	0.2	6.9	0.5
36	08:00	20:00	7.4	0.6	6.0	0.4	13.4	0.9
37	20:00	08:00	2.7	0.3	2.7	0.2	5.4	0.4
46	08:00	20:00	7.7	0.7	5.6	0.4	13.3	1.0
47	20:00	08:00	2.5	0.3	2.8	0.2	5.3	0.4
56	08:00	20:00						
57	20:00	08:00	3.3	0.3	3.1	0.2	6.4	0.5
66	08:00	20:00	10.2	0.8	3.3	0.2	13.5	1.0
67	20:00	08:00	7.4	0.5	2.7	0.2	10.0	0.7
76	08:00	20:00	10.1	0.8	3.3	0.2	13.4	1.0
77	20:00	08:00	4.9	0.4	3.0	0.2	7.9	0.6
86	08:00	20:00	6.3	0.7	4.1	0.3	10.4	0.9
87	20:00	08:00	5.5	0.5	2.8	0.2	8.3	0.6
96	08:00	20:00	7.5	0.7	3.9	0.3	11.4	0.9
97	20:00	08:00	5.5	0.5	2.7	0.2	8.2	0.6
106	08:00	20:00						
107	20:00	08:00	5.5	0.5	4.4	0.3	9.9	0.7

Table D.2. PARTICULATE CARBON VALUES ESTIMATED FROM 40 cm/s FACE VELOCITY PORT

SAMPLING PERIOD	START TIME PDT	STOP TIME PDT	PARTICULATE ORGANIC CARBON $\mu gC/m^3$	error	PARTICULATE ELEMENTAL CARBON $\mu gC/m^3$	error	PARTICULATE TOTAL CARBON $\mu gC/m^3$	error
26	08:00	20:00	7.3	0.6	5.6	0.4	12.9	0.9
27	20:00	08:00	3.9	0.3	3.0	0.2	6.8	0.5
36	08:00	20:00	9.1	0.6	5.5	0.4	14.6	0.9
37	20:00	08:00	2.7	0.3	3.0	0.2	5.7	0.4
46	08:00	20:00						
47	20:00	08:00	2.2	0.2	2.5	0.2	4.7	0.3
56	08:00	20:00	6.0	0.5	3.7	0.3	9.7	0.7
57	20:00	08:00						
66	08:00	20:00	8.2	0.7	2.3	0.2	10.5	0.8
67	20:00	08:00	6.4	0.4	2.3	0.2	8.7	0.6
76	08:00	20:00	10.2	0.7	2.9	0.2	13.2	0.9
77	20:00	08:00	4.2	0.4	2.7	0.2	7.0	0.5
86	08:00	20:00	6.4	0.6	4.4	0.3	10.8	0.8
87	20:00	08:00	3.2	0.4	2.3	0.2	5.5	0.5
96	08:00	20:00						
97	20:00	08:00	6.0	0.4	2.9	0.2	8.8	0.6
106	08:00	20:00	8.9	0.5	5.2	0.4	14.0	0.8
107	20:00	08:00	6.4	0.5	3.8	0.3	10.2	0.6

Table D.3. MEASURED CONCENTRATIONS FROM 20 cm/s FACE VELOCITY QQ FRONT FILTERS

SAMPLING PERIOD	START TIME PDT	STOP TIME PDT	MEASURED CONCENTRATIONS — ORGANIC CARBON $\mu gC/m^3$	error	ELEMENTAL CARBON $\mu gC/m^3$	error	TOTAL CARBON $\mu gC/m^3$	error
26	08:00	20:00	12.9	0.6	4.8	0.4	17.7	0.8
27	20:00	08:00	7.6	0.3	2.9	0.2	10.5	0.5
36	08:00	20:00	12.6	0.5	6.0	0.4	18.6	0.9
37	20:00	08:00	5.7	0.2	2.7	0.2	8.4	0.4
46	08:00	20:00	13.6	0.6	5.6	0.4	19.1	0.9
47	20:00	08:00	5.0	0.2	2.8	0.2	7.8	0.4
56	08:00	20:00						
57	20:00	08:00	6.0	0.3	3.1	0.2	9.2	0.4
66	08:00	20:00	15.9	0.7	3.3	0.2	19.2	0.9
67	20:00	08:00	10.9	0.5	2.7	0.2	13.6	0.6
76	08:00	20:00	15.8	0.7	3.3	0.2	19.0	0.9
77	20:00	08:00	8.6	0.4	3.0	0.2	11.6	0.5
86	08:00	20:00	12.7	0.5	4.1	0.3	16.8	0.8
87	20:00	08:00	9.7	0.4	2.8	0.2	12.5	0.6
96	08:00	20:00	12.9	0.6	3.9	0.3	16.8	0.8
97	20:00	08:00	9.3	0.4	2.7	0.2	12.0	0.6
106	08:00	20:00	15.6	0.7	5.9	0.4	21.5	1.0
107	20:00	08:00	9.4	0.4	4.4	0.3	13.8	0.6

Table D.4. MEASURED CONCENTRATIONS FROM 40 cm/s FACE VELOCITY QQ FRONT FILTERS

SAMPLING PERIOD	START TIME PDT	STOP TIME PDT	MEASURED CONCENTRATIONS — ORGANIC CARBON $\mu gC/m^3$	error	ELEMENTAL CARBON $\mu gC/m^3$	error	TOTAL CARBON $\mu gC/m^3$	error
26	08:00	20:00	10.7	0.5	5.6	0.4	16.3	0.8
27	20:00	08:00	5.7	0.2	3.0	0.2	8.7	0.4
36	08:00	20:00	12.4	0.5	5.5	0.4	17.9	0.8
37	20:00	08:00	4.5	0.2	3.0	0.2	7.5	0.3
46	08:00	20:00	11.4	0.5	4.8	0.4	16.2	0.7
47	20:00	08:00	3.9	0.2	2.5	0.2	6.3	0.3
56	08:00	20:00	9.7	0.4	3.7	0.3	13.3	0.6
57	20:00	08:00						
66	08:00	20:00	12.3	0.5	2.3	0.2	14.6	0.7
67	20:00	08:00	8.6	0.4	2.3	0.2	11.0	0.5
76	08:00	20:00	14.0	0.6	2.9	0.2	16.9	0.8
77	20:00	08:00	6.7	0.3	2.7	0.2	9.5	0.4
86	08:00	20:00	9.7	0.4	4.4	0.3	14.0	0.6
87	20:00	08:00	5.9	0.3	2.3	0.2	8.2	0.4
96	08:00	20:00						
97	20:00	08:00	8.4	0.4	2.9	0.2	11.3	0.5
106	08:00	20:00	12.4	0.5	5.2	0.4	17.6	0.8
107	20:00	08:00	8.7	0.4	3.8	0.3	12.6	0.6

Table D.5. MEASURED TOTAL CARBON CONCENTRATIONS FROM TQ BACKUP FILTERS

SAMPLING PERIOD	START TIME PDT	STOP TIME PDT	MEASURED TC CONCENTRATIONS 20_3cm/s µgC/m³	error	40_3cm/s µgC/m³	error	80_3cm/s µgC/m³	error
26	08:00	20:00	6.2	0.4	3.4	0.2	2.0	0.1
27	20:00	08:00	3.7	0.2	1.9	0.1	1.3	0.1
36	08:00	20:00	5.2	0.3	3.3	0.2	2.2	0.1
37	20:00	08:00	3.0	0.2	1.8	0.1	1.2	0.1
46	08:00	20:00	5.8	0.4			2.0	0.1
47	20:00	08:00	2.5	0.2	1.6	0.1	1.4	0.1
56	08:00	20:00	4.9	0.3	3.7	0.2	1.9	0.1
57	20:00	08:00	2.8	0.2	1.7	0.1	1.2	0.1
66	08:00	20:00	5.7	0.4	4.1	0.3	2.0	0.1
67	20:00	08:00	3.6	0.2	2.3	0.2	1.2	0.1
76	08:00	20:00	5.6	0.4	3.8	0.3	2.2	0.1
77	20:00	08:00	3.7	0.3	2.5	0.2	2.1	0.1
86	08:00	20:00	6.5	0.4	3.2	0.2	2.9	0.2
87	20:00	08:00	4.2	0.3	2.7	0.2	1.7	0.1
96	08:00	20:00	5.4	0.4	3.5	0.2	2.0	0.1
97	20:00	08:00	3.8	0.3	2.4	0.2	1.5	0.1
106	08:00	20:00			3.5	0.2	2.2	0.1
107	20:00	08:00	3.9	0.3	2.4	0.2	1.6	0.1

Table D.6. MEASURED TOTAL CARBON CONCENTRATIONS FROM QQ BACKUP FILTERS

SAMPLING PERIOD	START TIME PDT	STOP TIME PDT	MEASURED TC CONCENTRATIONS 20_3cm/s µgC/m³	error	40_3cm/s µgC/m³	error
26	08:00	20:00	3.6	0.2	2.6	0.2
27	20:00	08:00	2.0	0.1	1.3	0.1
36	08:00	20:00	3.3	0.2	2.6	0.2
37	20:00	08:00	1.4	0.1	1.2	0.1
46	08:00	20:00	3.8	0.3	2.5	0.2
47	20:00	08:00	1.3	0.1	1.1	0.1
56	08:00	20:00	3.4	0.2	2.4	0.2
57	20:00	08:00	1.6	0.1	1.2	0.1
66	08:00	20:00	3.8	0.3	2.5	0.2
67	20:00	08:00	2.5	0.2	1.3	0.1
76	08:00	20:00	3.5	0.2	2.6	0.2
77	20:00	08:00	2.2	0.1	1.4	0.1
86	08:00	20:00	4.4	0.3	2.3	0.2
87	20:00	08:00	2.1	0.1	1.8	0.1
96	08:00	20:00	3.9	0.3	2.4	0.2
97	20:00	08:00	2.7	0.2	1.7	0.1
106	08:00	20:00	5.3	0.4	2.7	0.2
107	20:00	08:00	2.3	0.2	1.8	0.1

APPENDIX E: GC/MS RESULTS

Table E.1. GRAND AVERAGES (ng/m^3)

	QQF		QQB		TQB	
	mean	std dev	mean	std dev	mean	std dev
Carboxylic acids						
hexanoic	4.3	2.9	0.3	0.6	0.5	0.7
heptanoic	10.8	7.4	0.2	0.3	0.5	0.5
octanoic	6.9	3.6	0.7	0.8	1.1	1.0
nonanoic	4.9	2.4	0.1	0.3	0.3	0.6
decanoic	3.1	1.3	0.3	0.5	0.6	0.8
undecanoic	1.3	0.7	0.3	0.4	0.5	0.6
dodecanoic	6.2	3.2	4.3	2.3	4.1	2.7
tridecanoic	2.3	2.9	0.8	0.9	1.2	0.9
tetradecanoic	16.0	8.0	7.3	11.7	9.9	10.7
pentadecanoic	7.6	6.0	3.3	4.6	4.6	4.7
hexadecanoic	60.1	32.6	13.1	19.8	36.9	34.4
octadecanoic	53.1	28.3	5.8	9.9	21.6	44.8
PAHs and Alkyl PAH's						
naphthalene	0.9	1.0	0.2	0.6	0.8	2.0
2-methylnaphthalene	0.4	0.3	0.06	0.2	0.2	0.4
1-methylnaphthalene	0.3	0.2	0.03	0.1	0.07	0.2
biphenyl	0.5	0.6	0.0	0.0	0.1	0.5
2,6-dimethyl-naphthalene	0.1	0.07	0.03	0.03	0.04	0.07
1,3+1,6-dimethyl-naphthalene	0.1	0.08	0.03	0.07	0.1	0.2
acenaphthylene	0.09	0.04	0.00	0.01	0.02	0.03
fluorene	0.07	0.05	0.00	0.01	0.03	0.03
phenanthrene	0.6	0.4	0.2	0.1	0.3	0.3
anthracene	0.09	0.06	0.03	0.03	0.04	0.04
2-methylphenanthrene	0.09	0.04	0.00	0.01	0.02	0.03
1-methylphenanthrene	0.10	0.04	0.01	0.02	0.04	0.04
fluoranthene	0.3	0.1	0.08	0.04	0.11	0.07
pyrene	0.29	0.09	0.07	0.03	0.08	0.05
benz[a]anthracene + chrysene	0.4	0.1	0.05	0.03	0.10	0.07
benzo[b+j+k]fluoranthene	2.4	2.0	0.01	0.01	0.08	0.07
benzo[e]pyrene	0.9	0.6	0.00	0.00	0.01	0.02
benzo[a]pyrene	0.2	0.3	0.00	0.00	0.00	0.00

Table E.1. GRAND AVERAGES (ng/m^3; cont.)

	QQF		QQB		TQB	
	mean	std dev	mean	std dev	mean	std dev
Alkanes						
pentadecane	0.2	0.3	0.09	0.3	0.2	0.5
hexadecane	0.8	2.0	0.9	1.3	0.7	1.4
heptadecane	0.0	0.0	0.0	0.0	0.3	0.9
pristane	0.02	0.05	0.02	0.06	0.1	0.4
octadecane	0.4	0.4	0.7	0.7	1.1	1.9
nonadecane	1.3	1.6	0.8	0.9	1.3	2.1
eicosane	0.5	1.2	0.4	0.7	0.9	1.7
heneicosane	1.0	0.7	0.7	0.8	1.2	1.1
docosane	2.3	1.6	1.4	1.6	1.8	2.1
tricosane	5.5	5.1	1.9	1.4	1.5	1.2
tetracosane	10.1	9.2	2.8	2.5	2.5	2.3
pentacosane	11.0	8.4	1.6	1.1	1.8	1.8
hexacosane	7.7	7.0	0.8	0.6	0.7	0.7
heptacosane	6.7	4.5	0.5	0.5	0.5	0.6
octacosane	8.8	7.7	0.3	0.4	0.8	1.5
nonacosane	8.4	4.9	0.4	0.5	1.2	3.1
Heterocyclic Compounds						
dibenzofuran	0.2	0.2	0.04	0.06	0.1	0.2
dibenzothiophene	0.05	0.04	0.04	0.08	0.03	0.05
quinoline	1.6	1.4	0.9	1.7	0.7	1.2
methylquinolines	2.2	2.5	1.5	2.1	0.9	1.3
PAH Ketones and Quinones						
1-indanone	0.4	0.4	0.1	0.2	0.02	0.06
benzothiazole	0.04	0.08	0.2	0.4	0.3	0.8
2-coumaranone	0.5	0.5	0.02	0.04	0.01	0.04
1,3-indanedione	1.1	1.1	0.5	1.0	0.4	0.5
coumarin	0.3	0.2	0.2	0.1	0.2	0.2
9-fluorenone	0.6	0.6	0.1	0.2	0.3	0.5
xanthone	0.1	0.1	0.06	0.06	0.09	0.08
9,10-anthdione	0.7	0.4	0.4	0.6	0.3	0.3
benzanthrone	0.1	0.1	0.02	0.03	0.03	0.03
7,12-benz[a]adione	0.03	0.07	0.0	0.0	0.0	0.0
Phthalate Esters						
diethyl	0.7	1.3	4.4	5.5	6.3	11.4
dibutyl	16.3	12.4	14.5	8.1	21.4	10.1
butylbenzyl	6.3	3.0	1.1	1.5	5.1	3.4
2-ethylhexyl	106.8	50.5	4.0	9.4	51.6	38.6
dioctyl	1.7	0.9	0.3	0.3	0.6	0.3

Table E.1. GRAND AVERAGES (ng/m^3; cont.)

	QQF		QQB		TQB	
	mean	std dev	mean	std dev	mean	std dev
Methyl Alkanoic Esters						
dodecanoate	0.0	0.0	0.06	0.05	0.02	0.03
tetradecanoate	0.02	0.06	0.08	0.05	0.06	0.07
hexadecanoate	0.2	0.2	0.5	0.5	0.3	0.3
octadecanoate	0.6	0.6	0.3	0.3	0.5	0.4
eicosanoate	0.04	0.05	0.01	0.02	0.04	0.04
Alcohols						
dodecanol	3.0	3.5	1.7	2.5	1.1	1.6
tetradecanol	0.4	0.8	1.6	2.0	0.4	0.8
Miscellaneous						
tributylphosphate	7.5	11.4	1.3	0.9	3.6	1.6
dioctyl adipate	3.8	3.0	0.2	0.3	2.4	2.5
cholestane	0.3	0.4	0.05	0.1	0.02	0.06
dibutylcresol	0.4	0.8	1.6	1.6	0.6	1.4
pristanone	0.0	0.0	0.4	1.2	0.0	0.0

Table E.2. DAYTIME AVERAGES CSMCS GC/MS (ng/m^3)

	— QQF DAY —		— QQB DAY —	
	MEAN	STD DEV	MEAN	STD DEV
Carboxylic acids				
hexanoic	5.3	3.0	0.3	0.6
heptanoic	7.8	5.8	0.3	0.2
octanoic	6.4	4.0	0.3	0.7
nonanoic	4.4	2.3	0.0	0.0
decanoic	2.9	1.2	0.3	0.9
undecanoic	1.6	0.7	0.3	0.4
dodecanoic	10.6	13.4	18.4	46.2
tridecanoic	2.6	2.9	1.5	1.3
tetradecanoic	25.1	17.5	12.8	23.7
pentadecanoic	10.3	6.2	4.3	3.1
hexadecanoic	74.8	33.1	20.2	29.7
octadecanoic	66.1	42.9	1.9	2.7
PAHs and Alkyl PAHs				
naphthalene	1.3	1.3	0.0	0.0
2-methylnaphthalene	0.6	0.4	0.0	0.0
1-methylnaphthalene	0.3	0.3	0.0	0.0
biphenyl	0.6	0.7	0.0	0.0
2,6-dimethylnaphthalene	0.15	0.05	0.02	0.03
1,3+1,6-dimethyl-naphthalene	0.21	0.08	0.03	0.07
acenaphthylene	0.11	0.06	0.0	0.0
fluorene	0.08	0.05	0.00	0.01
phenanthrene	0.6	0.4	0.2	0.2
anthracene	0.10	0.05	0.03	0.03
2-methylphenanthrene	0.11	0.03	0.00	0.01
1-methylphenanthrene	0.11	0.03	0.01	0.02
fluoranthene	0.31	0.09	0.09	0.04
pyrene	0.31	0.09	0.07	0.03
benz[a]anthracene + chrysene	0.44	0.09	0.04	0.03
benzo[b+j+k]fluoranthene	1.7	2.0	0.01	0.01
benzo[e]pyrene	0.5	0.6	0.0	0.0
benzo[a]pyrene	0.05	0.08	0.0	0.0

Table E.2. DAYTIME AVERAGES CSMCS GC/MS. (ng/m^3; cont.)

	— QQF DAY —		— QQB DAY —	
	MEAN	STD DEV	MEAN	STD DEV
Alkanes				
pentadecane	0.4	0.5	0.09	0.3
hexadecane	0.5	1.9	0.6	1.3
heptadecane	0.0	0.0	0.0	0.0
pristane	0.0	0.0	0.0	0.0
octadecane	0.3	0.4	0.6	0.6
nonadecane	0.9	1.7	0.6	0.9
eicosane	0.5	1.2	0.3	0.6
heneicosane	0.8	0.9	0.6	0.8
docosane	1.6	1.2	1.2	1.6
tricosane	2.5	1.8	1.7	1.5
tetracosane	5.1	3.2	2.5	2.5
pentacosane	6.3	3.0	1.7	1.4
hexacosane	3.5	2.1	0.6	0.6
heptacosane	3.7	1.6	0.3	0.4
octacosane	4.3	3.6	0.2	0.2
nonacosane	5.4	2.9	0.2	0.3
Heterocyclic Compounds				
dibenzofuran	0.3	0.2	0.04	0.06
dibenzothiophene	0.05	0.05	0.04	0.08
quinoline	1.4	1.1	0.6	0.9
methylquinolines	1.3	0.8	1.2	1.5
PAH Ketones and Quinones				
1-indanone	0.7	0.9	0.0	0.0
benzothiazole	0.03	0.08	0.0	0.0
2-coumaranone	1.2	1.3	0.01	0.03
1,3-indanedione	2.1	1.7	0.3	0.7
coumarin	0.4	0.2	0.2	0.1
9-fluorenone	0.5	0.6	0.08	0.2
xanthone	0.1	0.1	0.06	0.04
9,10-anthdione	0.7	0.4	0.3	0.5
benzanthrone	0.05	0.07	0.0	0.0
7,12-benz[a]adione	0.0	0.0	0.0	0.0
Phthalate Esters				
diethyl	0.5	0.6	3.9	5.4
dibutyl	16.4	15.7	11.7	7.3
butylbenzyl	8.5	2.1	1.8	2.0
2-ethylhexyl	149.9	26.9	0.4	1.1
dioctyl	2.2	1.0	0.3	0.2

Table E.2. DAYTIME AVERAGES CSMCS GC/MS. (ng/m^3; cont.)

	— QQF DAY —		— QQB DAY —	
	MEAN	STD DEV	MEAN	STD DEV
Methyl Alkanoic Esters				
dodecanoate	0.0	0.0	0.07	0.05
tetradecanoate	0.02	0.06	0.06	0.05
hexadecanoate	0.2	0.2	0.5	0.5
octadecanoate	0.8	0.6	0.3	0.3
eicosanoate	0.04	0.05	0.02	0.02
Alcohols				
dodecanol	1.9	2.0	1.7	2.9
tetradecanol	0.3	0.8	1.0	2.1
Miscellaneous				
tributylphosphate	2.5	1.8	1.5	0.7
dioctyl adipate	4.0	3.0	0.06	0.1
cholestane	0.1	0.3	0.06	0.2
dibutylcresol	0.8	0.9	2.1	1.5
pristanone	0.0	0.0	0.0	0.0

Table E.3. NIGHTTIME AVERAGES CSMCS GC/MS (ng/m^3)

	— QQF NIGHT —		— QQB NIGHT—	
	MEAN	STD DEV	MEAN	STD DEV
Carboxylic acids				
hexanoic	2.9	1.2	0.2	0.4
heptanoic	9.3	7.6	0.1	0.2
octanoic	5.8	2.4	0.5	0.6
nonanoic	4.7	2.1	0.2	0.3
decanoic	2.6	1.7	0.4	0.6
undecanoic	1.1	0.6	0.2	0.3
dodecanoic	5.3	1.8	3.5	2.1
tridecanoic	1.3	0.5	0.5	0.3
tetradecanoic	14.9	4.8	9.5	12.5
pentadecanoic	6.0	3.0	2.3	4.9
hexadecanoic	54.9	30.3	10.4	21.3
octadecanoic	55.5	26.2	6.4	11.1
PAHs and Alkyl PAHs				
naphthalene	0.4	0.7	0.3	0.7
2-methylnaphthalene	0.3	0.3	0.08	0.2
1-methylnaphthalene	0.1	0.2	0.05	0.1
biphenyl	0.2	0.3	0.04	0.1
2,6-dimethylnaphthalene	0.06	0.05	0.02	0.02
1,3+1,6-dimethyl-naphthalene	0.2	0.2	0.01	0.02
acenaphthylene	0.07	0.03	0.01	0.01
fluorene	0.05	0.05	0.01	0.01
phenanthrene	0.4	0.2	0.2	0.1
anthracene	0.06	0.03	0.03	0.02
2-methylphenanthrene	0.07	0.04	0.01	0.01
1-methylphenanthrene	0.08	0.04	0.01	0.01
fluoranthene	0.2	0.08	0.06	0.03
pyrene	0.2	0.08	0.05	0.03
benz[a]anthracene + chrysene	0.4	0.2	0.04	0.02
benzo[b+j+k]fluoranthene	2.1	1.0	0.01	0.01
benzo[e]pyrene	1.0	0.5	0.0	0.0
benzo[a]pyrene	0.3	0.4	0.0	0.0

Table E.3. NIGHTTIME AVERAGES CSMCS GC/MS. (ng/m^3; cont.)

	— QQF NIGHT — MEAN	STD DEV	— QQB NIGHT— MEAN	STD DEV
Alkanes				
pentadecane	0.2	0.2	0.03	0.1
hexadecane	0.3	0.8	0.6	0.8
heptadecane	0.0	0.0	0.0	0.0
pristane	0.02	0.06	0.02	0.07
octadecane	0.3	0.2	0.5	0.4
nonadecane	0.8	0.7	0.6	0.5
eicosane	0.0	0.0	0.2	0.5
heneicosane	0.7	0.4	0.2	0.4
docosane	2.0	1.7	0.7	0.6
tricosane	5.8	5.6	1.3	0.9
tetracosane	10.9	10.1	1.8	1.4
pentacosane	11.9	9.4	1.0	0.8
hexacosane	8.9	7.5	0.6	0.6
heptacosane	7.7	5.1	0.3	0.5
octacosane	9.1	8.5	0.3	0.4
nonacosane	8.9	6.7	0.3	0.5
Heterocyclic Compounds				
dibenzofuran	0.1	0.07	0.04	0.06
dibenzothiophene	0.03	0.02	0.01	0.01
quinoline	1.8	1.6	0.6	1.7
methylquinolines	2.8	2.7	0.9	1.9
PAH Ketones and Quinones				
1-indanone	0.3	0.4	0.2	0.2
benzothiazole	0.06	0.09	0.2	0.5
2-coumaranone	0.3	0.3	0.03	0.04
1,3-indanedione	0.6	0.9	0.5	0.9
coumarin	0.2	0.1	0.1	0.09
9-fluorenone	0.3	0.2	0.1	0.2
xanthone	0.08	0.04	0.05	0.05
9,10-anthdione	0.6	0.4	0.3	0.5
benzanthrone	0.2	0.09	0.02	0.03
7,12-benz[a]adione	0.1	0.1	0.0	0.0
Phthalate Esters				
diethyl	0.7	1.4	3.6	4.4
dibutyl	15.2	7.1	15.6	7.7
butylbenzyl	4.5	1.5	0.3	0.4
2-ethylhexyl	66.5	15.1	5.2	10.4
dioctyl	1.6	0.8	0.3	0.4

Table E.3. NIGHTTIME AVERAGES CSMCS GC/MS. (ng/m^3; cont.)

	— QQF NIGHT —		— QQB NIGHT—	
	MEAN	STD DEV	MEAN	STD DEV
Methyl Alkanoic Esters				
dodecanoate	0.06	0.2	0.04	0.03
tetradecanoate	0.01	0.02	0.06	0.04
hexadecanoate	0.2	0.2	0.3	0.2
octadecanoate	0.2	0.2	0.2	0.09
eicosanoate	0.02	0.04	0.00	0.01
Alcohols				
dodecanol	2.9	3.9	1.6	2.6
tetradecanol	1.03	1.07	1.5	0.9
Miscellaneous				
tributylphosphate	10.6	12.0	0.8	0.8
dioctyl adipate	3.6	3.3	0.2	0.3
cholestane	0.4	0.4	0.0	0.0
dibutylcresol	0.0	0.0	1.3	0.9
pristanone	0.0	0.0	0.8	1.7

APPENDIX F: CSMCS SAMPLING CODES

EXAMPLE: 42HJHQQF

4	DAY (STUDY DAYS 1-10 CORRESPONDING TO DATES 8/11/86 - 8/20/86)
2	PERIOD
H	HUNTZICKER'S LAB
JH	SAMPLER
QQ/TQ	QQ OR TQ FILTER COMBINATION
F/B	FRONT OR BACKUP FILTER

SAMPLERS

JH	TWO-PORT SAMPLER
SM	FACE VELOCITY SAMPLER
INS	IN SITU CARBON ANALYZER

SAMPLING PERIODS

5 SAMPLES/DAY:	1	08:00 - 12:00
	2	12:00 - 16:00
	3	16:00 - 20:00
	4	20:00 - 24:00
	5	24:00 - 08:00
2 SAMPLES/DAY:	6	08:00 - 20:00
	7	20:00 - 08:00